

## N O T I C E

THIS DOCUMENT HAS BEEN REPRODUCED FROM  
MICROFICHE. ALTHOUGH IT IS RECOGNIZED THAT  
CERTAIN PORTIONS ARE ILLEGIBLE, IT IS BEING RELEASED  
IN THE INTEREST OF MAKING AVAILABLE AS MUCH  
INFORMATION AS POSSIBLE

DOSIMETRIC INVESTIGATIONS OF COSMIC RADIATION ABOARD THE  
KOSMOS-936 AES  
(JOINT SOVIET-AMERICAN EXPERIMENT K-206)

E. V. Benton, Ye. Ye. Kovalyev, V. Ye. Dudkin

(NASA-TM-75772) DOSIMETRIC INVESTIGATIONS  
OF COSMIC RADIATION ABOARD THE KOSMOS-936  
AES (JOINT SOVIET-AMERICAN EXPERIMENT K-206)  
(National Aeronautics and Space  
Administration) 90 p HC A05/MF A01 CSCL 06R G3/52 N81-16730  
Unclas  
41245

Translation of "Dozimetricheskiye issledovaniya kosmicheskikh iz-  
lucheniya na bortu ISZ 'Kosmos-936' (Sovmestnyy sovetsko-amerikanskiy  
eksperiment K-206) Report, INSTITUTE OF MEDICO-BIOLOGICAL PROBLEMS.  
MINISTRY OF HEALTH, USSR, Moscow, 1979



NATIONAL AERONAUTICS AND SPACE ADMINISTRATION  
WASHINGTON, D.C. 20546  
APRIL 1980

## STANDARD TITLE PAGE

1. Report No. NASA TM-75772	2. Government Accession No.	3. Recipient's Catalog No.	
4. Title and Subtitle DOSIMETRIC INVESTIGATIONS OF COSMIC RADIATION ABOARD THE KOSMOS- 936 AES (JOINT SOVIET-AMERICAN EXPERIMENT K-206)		5. Report Date April 1980	
		6. Performing Organization Code	
7. Author(s) E. V. Benton, Ye. Ye. Kovalyev, V. Ye. Dudkin		8. Performing Organization Report No.	
		10. Work Unit No.	
9. Performing Organization Name and Address Leo Kanner Associates Redwood City, California 94063		11. Contract or Grant No. NASW 3199	
		13. Type of Report and Period Covered Translation	
12. Sponsoring Agency Name and Address National Aeronautics and Space Adminis- tration, Washington, D.C. 20546		14. Sponsoring Agency Code	
		15. Supplementary Notes Translation of "Dozimetricheskiye issledovaniya kosmicheskikh izlucheniya na bortu ISZ 'Kosmos-936' (Sovmestnyy sovetско-amerikanskiy eksperiment K-206)," Report, INSTITUTE OF MEDICO-BIOLOGICAL PROBLEMS. MINISTRY OF HEALTH, USSR, Moscow, 1979	
16. Abstract The K-206 experiment made it possible to obtain new information on cosmic radiation and to understand preceding results from the Kosmos-782. This experiment was a joint Soviet-American project. Particular attention was given to the following: placement of detectors; unified methods of handling calibration of USSR and USA detectors; study of neutron radiation within the biosatellite; studies of fragmentation of heavy nuclei on accelerators.			
17. Key Words (Selected by Author(s))		18. Distribution Statement  Unclassified-Unlimited	
19. Security Classif. (of this report) Unclassified	20. Security Classif. (of this page) Unclassified	21. No. of Pages 90	22.

## Introduction

In 1975, the K-103 American dosimetric experiment was conducted on the Kosmos-782 artificial Earth satellite. A Soviet experiment on dosimetry and spectrometry of cosmic radiation was conducted on this same satellite at the same time. Part of the Soviet studies were conducted within the framework of the joint Soviet-French experiment, the Bioblock-2. American tracking detectors made of cellulose nitrate CNUSF (threshold of recording  $LET_{350}$  [lineynaya peredacha energii, linear energy transfer]  $\geq 80 \frac{\text{kev}}{\mu\text{m}}$ ) were used for recording the heavy nuclei of galactic cosmic radiation; Soviet detectors made of cellulose nitrate KNTs (recording threshold  $LET_{350} \geq 200 \frac{\text{kev}}{\mu\text{m}}$ ) and also Soviet nuclear emulsions of the PR-2 type, thermoluminescent dosimeters and spectrometers with S-1 telescope counters were used.

The results of the experiments were discussed in a symposium presenting the results of the biological studies on the Kosmos-782 AES held in September 1976 in Moscow. During the consideration of results of dosimetric studies, a considerable disparity was observed in the values of fluence of charged particles measured by the Soviet and American specialists (up to 10 times). These disparities can be explained by use of detectors with varying sensitivity, the absence of joint calibration, different locations for the detectors and correspondingly, different screening of them, etc. The results of studies on the Kosmos-782 AES also showed that fluence of particles depends strongly on the mass of substances surrounding the detector. For instance, in the K-103 experiment, a relatively large number of nuclei of Cr-24 and Ti-22 was recorded in comparison with Fe-26 which, apparently, is the result of fragmentation of the Fe-26 nuclei. Therefore, for correct interpretation of the results of measurements it is necessary to have quantitative data on thickness of the substance, equipment, etc. which surround the detectors.

It is nevertheless necessary that a comparatively large mass of substance and scientific equipment of the satellite are the source of secondary neutrons. For part of the scientific results obtained in the Kosmos-782 AES experiment, a joint publication was prepared.

For clarifying questions which arose in the experiments on the Kosmos-782 AES, a joint Soviet-American K-206 experiment was planned on radiation dosimetry on the Soviet biosatellite in 1979. The design of the experiment was judged at sessions of the Soviet-American working group on space biology and medicine in 1976 in Yerevan and in 1978 in Leningrad; also it was considered in the working sessions of Soviet and American specialists. During consideration of the K-206 experiment, the necessity to pay particular attention to the following was noted:

- placement of the detectors in a single position if possible;
- unification of methods for treating detectors;

-- the necessity for ground calibration of the detectors on accelerators in the USSR and USA;

-- study of the fields of neutron radiation within the biosatellite;

-- conduct of the gamma-thickness measurement of the biosatellite relative to the location of the detector;

-- the necessity for conducting investigations on accelerators in order to study fragmentation of heavy nuclei.

All these recommendations were taken into account when compiling a plan for the K-206 experiment which was accomplished in August 1977 on the Kosmos-936 biosatellite.

## TABLE OF CONTENTS

Introduction	1
Section 1. The Soviet Part of the K-206 Experiment	1
1. Introduction	1
2. Nuclear Photoemulsions	2
2.1. Materials	2
2.2. Flight Experiment	3
2.3. Calibration Experiment	3
2.4. Photographic Treatment of Nuclear Emulsion	4
2.5. Method of Examination of Nuclear Emulsions [missing in orig].	8
2.6. Results Obtained	8
2.7. Consideration of Results	9
3. Fissionable Foils	18
3.1. Materials and Methods for Processing	19
3.2. Results Obtained and Their Consideration	20
4. Dielectric Tracking Detectors	21
4.1. Materials	21
4.2. Flight Experiments	23
4.3. Calibration Experiment	23
4.4. Chemical Processing of the Dielectric Tracking Detectors	24
4.5. Method of Inspection of Dielectric Tracking Detectors	24
4.6. Results Obtained	26
4.7. Consideration of Results	29
References	32
Chapter 2. Dosimetric Investigations with a Telescope of Counters and TLS Dosimeters	34
1. Formulation and Method of the Experiment	34
2. Results of Measurement	34
Chapter 3. Gamma-thickness Measurement of the Kosmos-936 Biological Satellite	38
Section II. The American Part of the Kosmos-206 Experiment	43
1. Introduction	43
2. Heavy Nuclei--Fluence, Integral LET Spectrum and Spatial Distribution	44
2.1. Materials and Methods	45
2.2. Results	48
2.3. Discussion	49
3. Charge Spectrum of Heavy Nuclei	53
3.1. Material and Method	54
3.2. Results	56
3.3. Discussion	58

4. Neutrons	61
4.1. Material and Method	62
4.2. Results	64
5. Full Absorption of a Dose	75
6. Nuclear Emulsions	77
6.1. Material and Method	77
6.2. Results	78
6.3. Discussion	79
References	81
Conclusion	83

SECTION 1. THE SOVIET PART OF THE K-206 EXPERIMENT.  
DOSIMETRIC INVESTIGATION OF COSMIC RADIATION ON BOARD THE  
KOSMOS-936 APS

(Nuclear emulsions, fissionable foils, plastic detectors)

A.I. Vikhrev, S.A. Dashin, V. Ye. Dudkin, Ye. Ye. Kovalyev,  
A.M. Marchnyy, N.A. Nefedov, Yu. V. Potapov  
(Institute of Medical and Biological Problems of the Ministry of Public Health USSR, Moscow)

1. Introduction

/7\*

The present day stage of mastery of outer space is characterized by a significant increase in duration of orbital flights and more complexity in the operating programs of the crew who solve a broad circle of problems of scientific and applied value. This requires a careful study of different factors which interfere with completion of the program and have an effect on the work capability and health of the crew. It is necessary to isolate the radiation danger among these factors; it increases with an increase in the duration of flight. Therefore, a careful study of the radiation conditions in the craft, which besides other things is subject to a different time modulation, is an important and necessary stage in the mastery of near-Earth outer space using long-term orbital stations.

The study in near-Earth orbits of fluxes of protons, neutrons, heavy charged particles, the value of doses from the components listed, spectra of linear transmission of energy (LET), "cross linking" of readings of different detectors placed in a single location, unification of the methods of processing the detectors were part of the task of the joint Soviet-American K-206 experiment. A comprehensive ground experiment on calibration of the detectors used with a selection of different charged particles on accelerators in the USSR and USA was conducted for the order of preparation and for the check-out methods

The following were introduced into the composition of the flight dosimetric K-206 container in the Soviet and joint Soviet-American section:

-- nuclear photoemulsion (for measuring fluences and spectra of charged particles);

-- foils from materials fissionable under the effect of particles (for measuring fluences of neutrons with different thresholds beginning with 1 MeV);

-- thermoluminescent glass (TLG) (for measuring the integral dose);

-- plastic detectors (for measuring fluences and spectra of LET

/8

---

\*Numbers in the margin indicate pagination in the foreign text.

of heavy charged particles).

In the succeeding Sections we will present processing methods and the results obtained for all of the detectors used will be presented.

## 2. Nuclear Photoemulsions

Nuclear photoemulsions in the K-206 experiment were designed:

- for measuring the fluence of charged particles at different points on the container including points with different protective thickness;
- for studying the spectrum of linear loss of energy of charged particles in the  $LET_{ts}$  0.2--80 KeV/ $\mu$ m;
- for evaluating the value of the dose from charged particles in the indicated LET range.

### 2.1. Materials

In the experiment, nonbacked relativistic PR-2 photoemulsions were used for measuring the LET spectrum (density of the grain for the relativistic single charge particles  $20 \pm 2$  grains/100  $\mu$ m, brand G emulsion); the BR-2 was used for measuring fluxes of charged particles (density of the grains for relativistic single charge particles  $30 \pm 2$  grains/100  $\mu$ m, brand V emulsion) and R-2T-50 type photoemulsion on a triacetate base (density of the grains for the relativistic single charge particles  $30 \pm 2$  grains/100  $\mu$ m, brand A).

The collection of nuclear photoemulsions contained:

G1--G4 -- a 3 layer emulsion of the PR-2 type with thickness 215  $\mu$ m and area  $5.2 \times 3.4$  cm<sup>2</sup>, brand G1: G5, G6, G7; G2: G8, G9, G10; G3: G11, G12, G13; G4: G14, G15, G16;

V1--V4 -- a 3 layer emulsion of the BR-2 type with thickness 400  $\mu$ m and area  $5.2 \times 3.4$  cm<sup>2</sup>, brand V1: V5, V6, V7; V2: V8, V9, V10; V3: V11, V12, V13; V4: V14, V15, V16;

A1--A4 -- 4 layer emulsions of the R-2T-50 type with thickness 60  $\mu$ m and area  $7.5 \times 7.5$  cm<sup>2</sup>, brand A1: A40--A43; A2: A44--A47; A3: A48--A51; A4: A52--A55.

A5--A6 -- a 4 layer emulsion of the R-2T-50 type thickness 50  $\mu$ m and area  $6.0 \times 6.0$  cm<sup>2</sup>, brand A5: A57, A58, A59, A60; A6: A61, A62, A63, A64;

Three sets with indices Kr-200, Kr-400, Kr-2000 -- 2 layer emulsions of the PR-2 type with thickness 215  $\mu$ m and area  $5.2 \times 2.6$  cm<sup>2</sup>, brand Kr-200: G35, G36; Kr-400: G37, G38; Kr-2000: G39, G40.

All of the sets were wrapped in black paper and sealed in a packet made

of lavsan 20  $\mu$ m thick, the number of the set was inscribed at one corner of the packet; on this same corner, the appropriate indices of layers of the nuclear photoemulsion making up the set was marked.

## 2.2. Flight Experiment

The joint Soviet-American K-206 experiment was completed on the Kosmos-936 artificial Earth satellite. The satellite was launched on August 3, 1977 and was in orbit for 19.5 days. The parameters of the orbit were: apogee--419 km, perigee--224 km, angle of inclination of the plane of the orbit to the plane of the equator--62.8°, the period of rotation around Earth--90.7 minutes.

During flight, operative control was carried out of the radiation conditions according to astrophysical data and also direct control using radiometers on board the Prognoz satellite. Activity of the Sun was at an average level. There were no solar flares in the indicated period. An overall view of the container with detecting blocks is given in Figure 1. The assemblies of the nuclear photoemulsion were positioned in the following way:

A1--A6 -- along the face of the Soviet block A, then along the lateral face (orthogonal layers) assemblies A1--A4 (A1 is turned toward the joint block C, further in order clockwise if one looks from above), A5 and A6 -- along the upper and lower faces, respectively; /11

G1--G2 -- assemblies along the upper and lower faces, respectively, of the joint block B placed in a row with the Soviet block A;

G3--G4 -- assemblies along the upper and lower faces, respectively, of the joint block B placed in a row with the American block A;

Kr-200 and Kr-400 -- assemblies along the upper face of the Soviet block A under the assembly A5;

Kr-2000 -- assembly along the lower face of the Soviet block A under assembly A6.

The view from below of the container with marking of the faces is presented in Figure 2. All of the assemblies of the nuclear emulsion before installation on the satellite and after return from orbit to Earth were kept in a refrigerator at a temperature of +3--5°C before photographing treatment.

## 2.3. Calibration Experiment

In order to obtain a calibration curve before measurement of the LET spectrum, broad calibration irradiation was conducted by beams of accelerated charged particles. The problems of calibration were irradiation of the emulsion layers of a set of particles with different values of LET for determining the threshold of the phenomenon. A summary of the calibrated irradiations presented is given in Table 1.

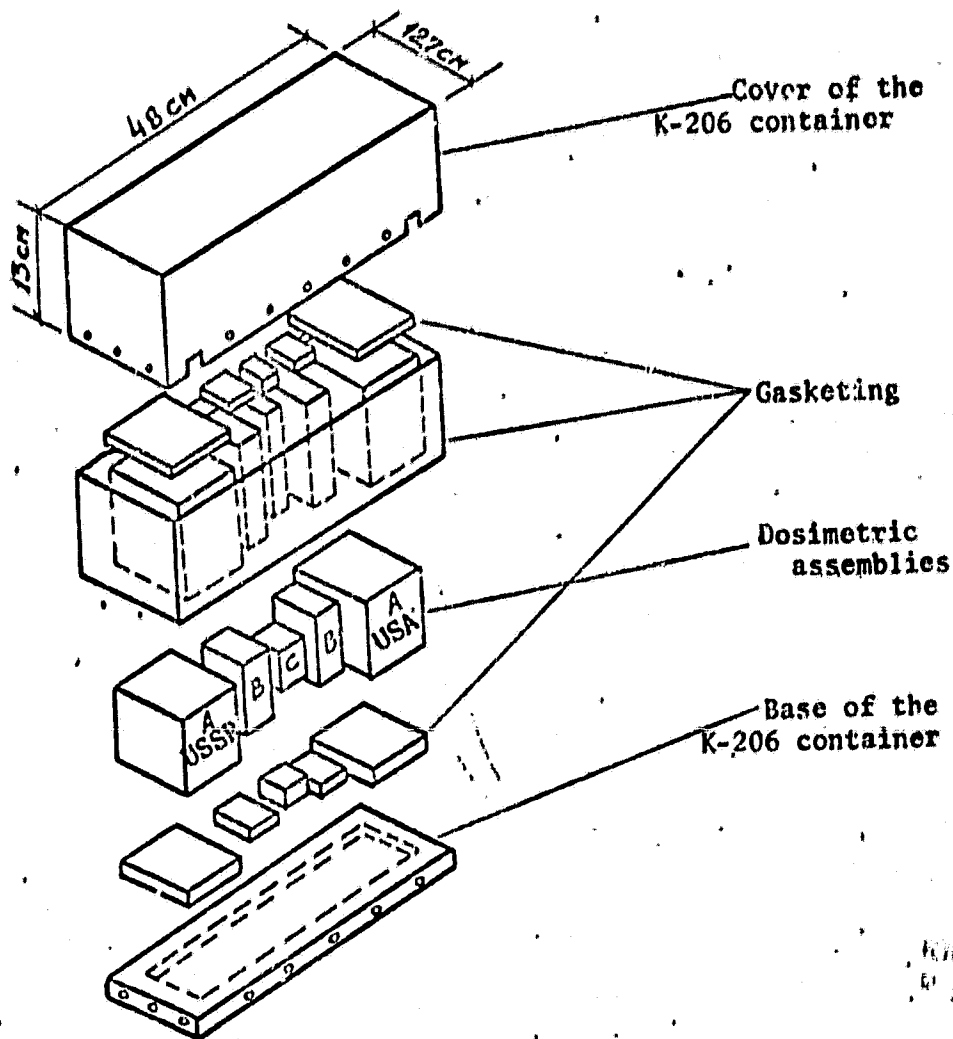


Figure 1. Overall view of the K-206 container with the dosimetric assemblies.

All the layers of nuclear emulsions before conducting irradiation and /11 then before the moment of photographic processing are kept in the refrigerator at a temperature of  $+3--5^{\circ}\text{C}$ .

#### 2.4. Photographic Treatment of Nuclear Emulsion

The appearance of a relativistic nuclear photoemulsion of the VR-2 and R-2T-50 type was conducted by the standard method in a methol-hydroquinone developer. At the same time, the flight calibration and control layers were put into a single solution. Development of

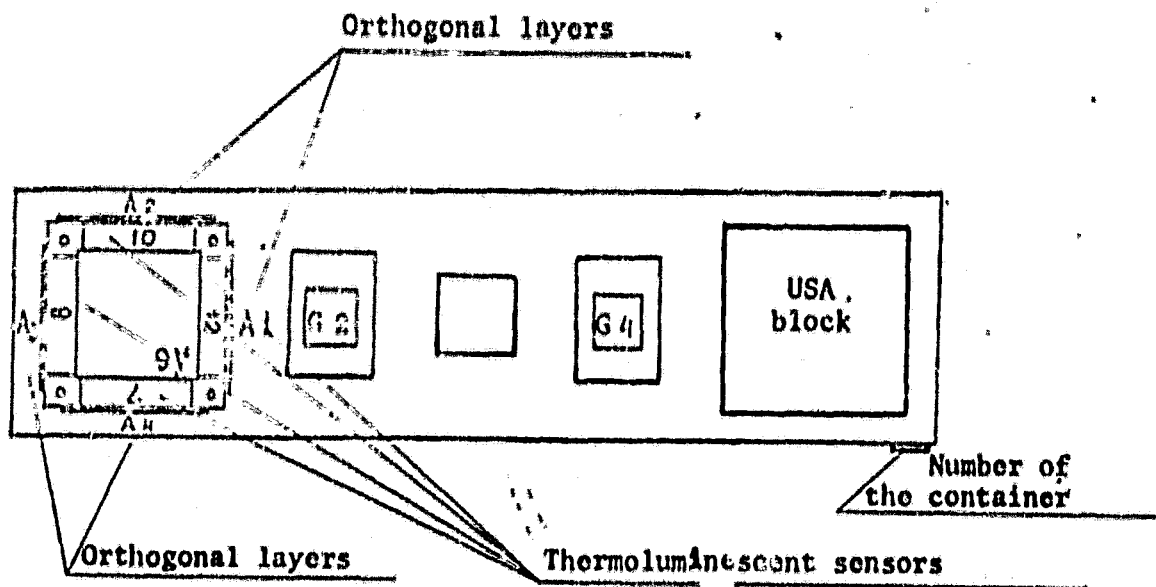


Figure 2. View from below into the container with dosimetric assemblies.

plates of the type

/11

[Translator's note: page missing in the original text including  
reference to Figure 3].

TABLE 1. CALIBRATING EXPOSURES

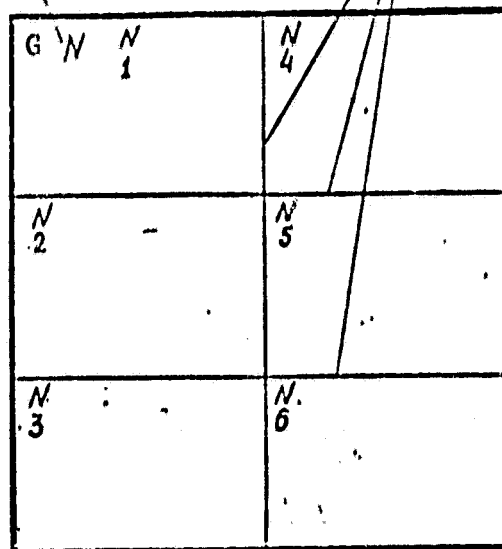
to. : - particle	Type of particle	Energy : Mev/nucleon	Mev/cm	Type of emulsion	Marking of the layers	Date of irradiation	Location of irradiation
1	Proton	55 ± 3	28,5 ± 1,3	PR -2 BR -2	G4 V3	I.07.77	ITEP
2	"	73 ± 2	23 ± 0,5	PR -2 BR -2	G3 V2	I.07.77	ITEP
3	"	92 ± 3	19,2 ± 0,5	PR -2	G2	I.07.77	ITEP
4	"	185 ± 3	12,5 ± 0,5	PR -2 BR -2	G1 V1	I.07.77	
5	"	645	7,0	PR -2 BR -2	G50-G53, G75 V50-V53 V39, V40, V85	I5.09.77	Dubna
6	α-particles from the PI- 239 source	1,29	1700	PR -2 BR -2	G70, G71 V80, V81	I2.09.77	ITEP
7	C12	200	396	PR -2 BR -2	G17, G18 V17, V18	28.07.77	Berkel
8	C12	77	792	PR -2 BR -2	G19, G20 V19, V20	28.07.77	Berkel
9	C12	9,1	4000	PR -2 BR -2	0,1 0,2, 03 V70-V72	29.08.77	Dubna
10	Ne <sup>20</sup>	200	1100	PR -2 BR -2	G23, G24 V23, V24	27.07.77	Berkel
11	Ne <sup>20</sup>	400	800	PR -2 BR -2	G25, G26 V25, V26	27.07.77	Berkel
12	Ne <sup>20</sup>	475	720	PR -2 BR -2	G27, G28 V27, V28	27.07.77	Berkel
13	Ne <sup>20</sup>	9,1	11000	PR -2 BR -2	07, G3, G9 V70-V73	29.08.77	Dubna

ORIGINAL PAGE IS  
OF POOR QUALITY

[Commas in tabulated material for this Table and all other Tables and Figures in the text are equivalent to decimal points].

Number of the emulsion layer

Line of the section



/15

Figure 3. Typical marking of a cross section layer of emulsion of the PR-2 type with a two-potential development.

Inspection of emulsion was made on MBI-3 and KSM microscopes with total magnification 900--1350 depending on the degree of load of the photolayer. As a rule, lenses with an immersion oil were used. Measurements were made at 5 different points on the plate in case of small differences which were always observed in all plates; the path for the entire length (or width) of the layer was inspected with fixing of the number of fields of vision and number of tracks (according to the surface and volume). The number of fields inspected varied from 50 to 200 depending on the load of the emulsion; this resulted in a statistical error no worse than 5% with standard development. /16

For a decrease in systematic error, repeated inspections were made of the plates and also intersecting measurements with different inspection instruments.

## 2.6. Results Obtained

The first stage for obtaining experimental results using nuclear photoemulsions included obtaining a calibrated relationship of the threshold of LET to the potential of development. For obtaining the value of the LET threshold with each potential, measurement was made

of the fluence of particles with different LET. Extrapolation of the fluence to a zero value gives an LET threshold value for each potential. Figure 4 shows also relationships for determining sensitivity of the PR-2 type emulsion as an example according to LET for potentials of development -165, -175, -180, -190 mV.

Determination of the threshold value of LET (scaling on the tissue) for each of the  $f$  values used of the oxidation-reduction potential made it possible to construct a calibration curve presented in Figure 5. The largest error in determining LET corresponds to the area of the plateau on the curve. In this field, small deviations in determining the OVP [oxidation-reduction potential, ORP] can result in a significant error in determining LET particles. The errors in Figure 5 include statistical error (less than 5%), error in measuring OVP (less than 2%), dispersion of the energy spread of calibrated particles (less than 10%). /19

On the basis of data from Figures 4 and 5, one obtained threshold values of LET for the values of the potentials used. These data are presented in Table 2.

Table 3 shows the measured planar fluences of charged particles. We will designate the planar fluence, according to [2] as the number of particles passing through the stationary surface for a unit of area. These measurements are made on a relativistic photoemulsion of the BR-2 and R-2T-50 type. Due to the large load of emulsion with tracking of particles (some emulsions were completely black and measurements were impossible to make) error in determining the planar fluence can reach an order of magnitude and the measured values can be considered only as low estimates.

Table 4 shows the results of measurement of the planar fluence and volumetric density of tracks in the PR-2 type emulsion with different threshold values of LET. The indicated errors were purely statistical. Usually it is considered that radiation in cosmic space is isotropic. The anisotropy of space radiation observed in a number of measurements usually is not large and can be ignored for practical computation of doses and dosimetric measurements. Due to varying shielding of the internal volume of the satellite, there is interest in measurement of angular distribution of incident radiation within the satellite. Such measurements were made on the upper and lower faces of the joint block B placed in a row with the Soviet block A. Figure 6 shows angular distribution of charged particles according to measurements on the G5, G6 (G1 assembly) and G9 (G2 assembly) layers. One should note the high degree of anisotropy for the G1 assembly in comparison with the G2 assembly. /21

## 2.7. Consideration of Results

The studies made and the results obtained make it possible to evaluate the radiation danger within a spacecraft, the contribution to the dose of particles with varying LET, and to make a comparison of results by different methods.

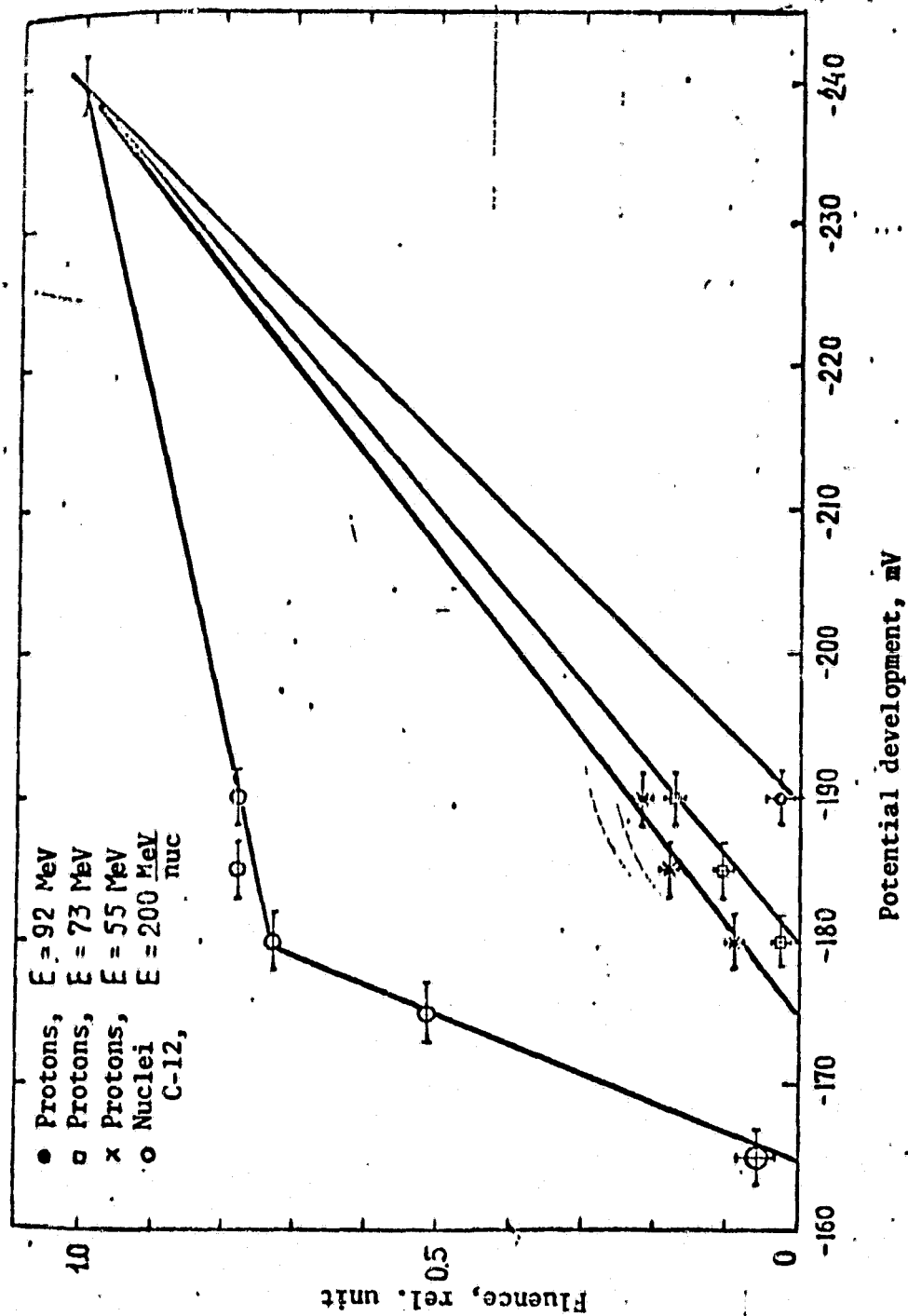


Figure 4. Determination of the sensitivity of type PR-2 emulsions according to LET for different potentials of development.

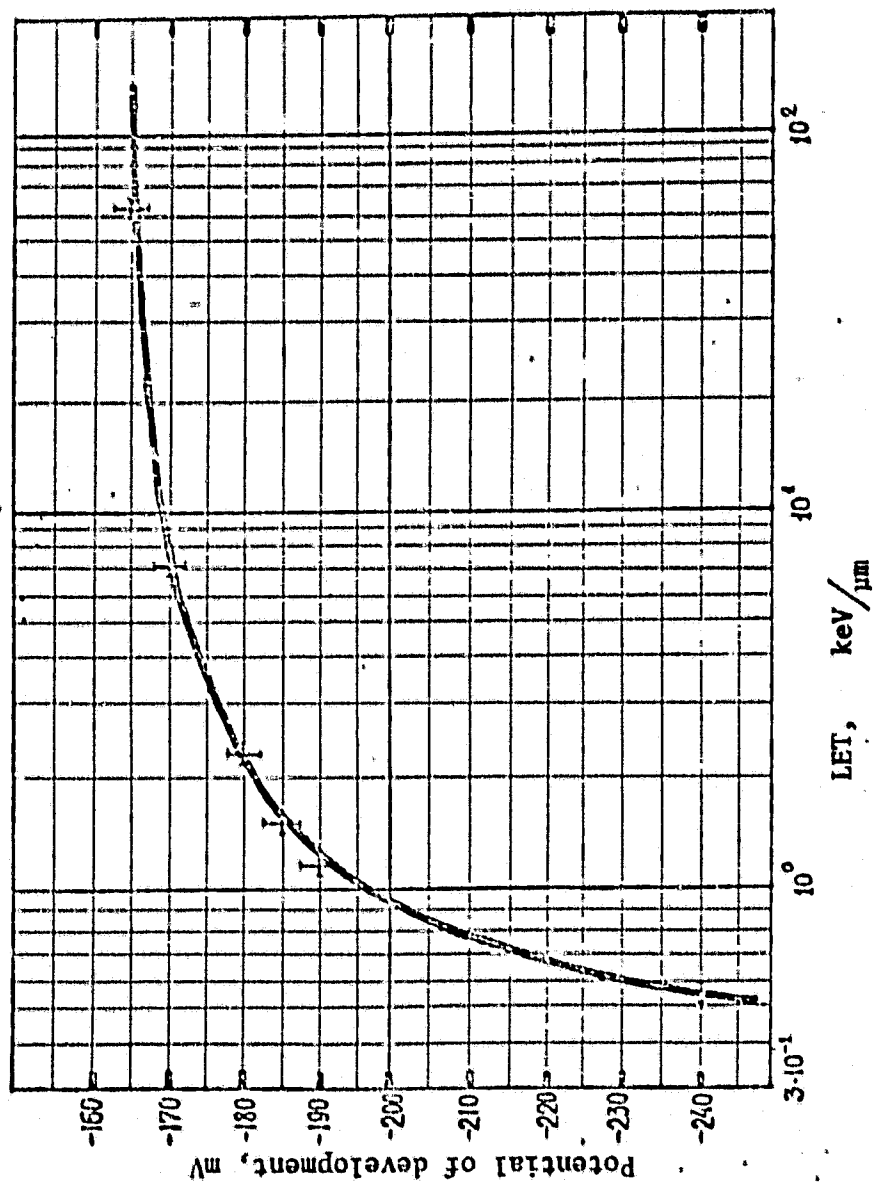


Figure 5. Calibrated relationship of  $LET_{ts}$  to the potential of development.

TABLE 2. THRESHOLD VALUES OF LET FOR THE VALUES OF POTENTIALS USED

/19

No. of plate, K	Potential of develop- ment, mV	Threshold value LET in the emulsion, MeV/cm	Equivalent threshold value LET in the tis- sue, MeV/cm
1	- 240 $\pm$ 2	5,5 $\pm$ 0,4	2,3 $\pm$ 0,4
2	- 190 $\pm$ 2	12,0 $\pm$ 0,5	4,6 $\pm$ 0,5
3	- 185 $\pm$ 2	16,0 $\pm$ 0,6	6,2 $\pm$ 0,6
4	- 180 $\pm$ 2	23,0 $\pm$ 0,8	9,1 $\pm$ 0,8
5	- 175 $\pm$ 2	33,0 $\pm$ 0,8	13,5 $\pm$ 0,8
6	- 165 $\pm$ 2	600 $\pm$ 20	300 $\pm$ 20

We note that for measuring the fluence of charged particles, nuclear photoemulsions for flights of this duration are not the best detectors. The maximum measured fluences in the emulsion do not exceed  $10^5$ -- $10^6$  particles/cm<sup>2</sup> (measurement of large fluences is practically impossible due to the excessive load of the nuclear photoemulsion). This contributes to the natural limitation for use of nuclear photoemulsions with the standard method of development as detectors for long-term flights.

/21

The use of nuclear photoemulsion as the detector for measuring the LET spectrum is more promising using a method of two-potential development. In combination with the plastic detector which makes it possible to measure the LET spectrum with a value  $> 100$  KeV/ $\mu$ m, this method makes it possible to obtain the full LET spectrum of radiation. The complexity of measurement of the fluence with small values of LET as a result of large load of emulsion can be avoided by measuring the full fluence by another detector, for example, fissionable foils or a spectrometer. A disadvantage of the method is its great difficulty and also the necessity for conducting fairly broad graduated irradiation by beams of particles with different LET values.

/23

On the basis of the LET spectra measured, one can calculate the absorbed and equivalent dose in the emulsion and also using transition ratios, in the tissue. A calculation of absorbed and equivalent doses is done according to the relationship:

TABLE 3. PLANAR FLUENCES OF CHARGED PARTICLES ACCORDING TO MEASUREMENTS IN THE BR-2 AND R-2T-50 TYPE EMULSIONS

/20

Location of the emulsion		Index of the emulsion layer	Planar fluence, $10^5$ part/cm <sup>2</sup>
Along the face of	A1	A40, A42	2,25
Along the face of	A2	A44, A45	1,7
Along the face of	A3	A48, A49	2,08
Along the face of	A4	A53, A54, A55	2,18
Along the face of	A5	A56 .. A59	2,15
Along the face of	A6	A60	2,64
On top of the combined block		VI2 - VI3	6,3
Below the combined block		VI4	7,0

/23

$$D_e = \sum_{k=2}^6 1,6 \cdot 10^{-8} \frac{\bar{\Phi}_v^k \cdot \bar{\ell}_e^k}{V_e \cdot \rho_e} \left( \frac{dE}{dx} \right)_e^k + 1,6 \cdot 10^{-8} (\Phi_{pr} - \Phi_p^2) \left( \frac{dE}{dx} \right)^1$$

$$H_e = \sum_{k=2}^6 1,6 \cdot 10^{-8} \frac{\bar{\Phi}_v^k \cdot \bar{\ell}_e^k}{V_e \cdot \rho_e} \left( \frac{dE}{dx} \right)_e^k Q^k \left( \frac{dE}{dx} \right) + 1,6 \cdot 10^{-8} (\Phi_{pr} - \Phi_p^2) \left( \frac{dE}{dx} \right)^1$$

Here  $D_e$  and  $H_e$ --are the absorbed and equivalent doses in the emulsion, rad or rem;

$\bar{\Phi}_v^k = \Phi_v^k - \Phi_v^{k+1}$ ---is the mean volumetric density of tracks from the LET in the interval from  $\left( \frac{dE}{dx} \right)^k$  to  $\left( \frac{dE}{dx} \right)^{k+1}$ ;

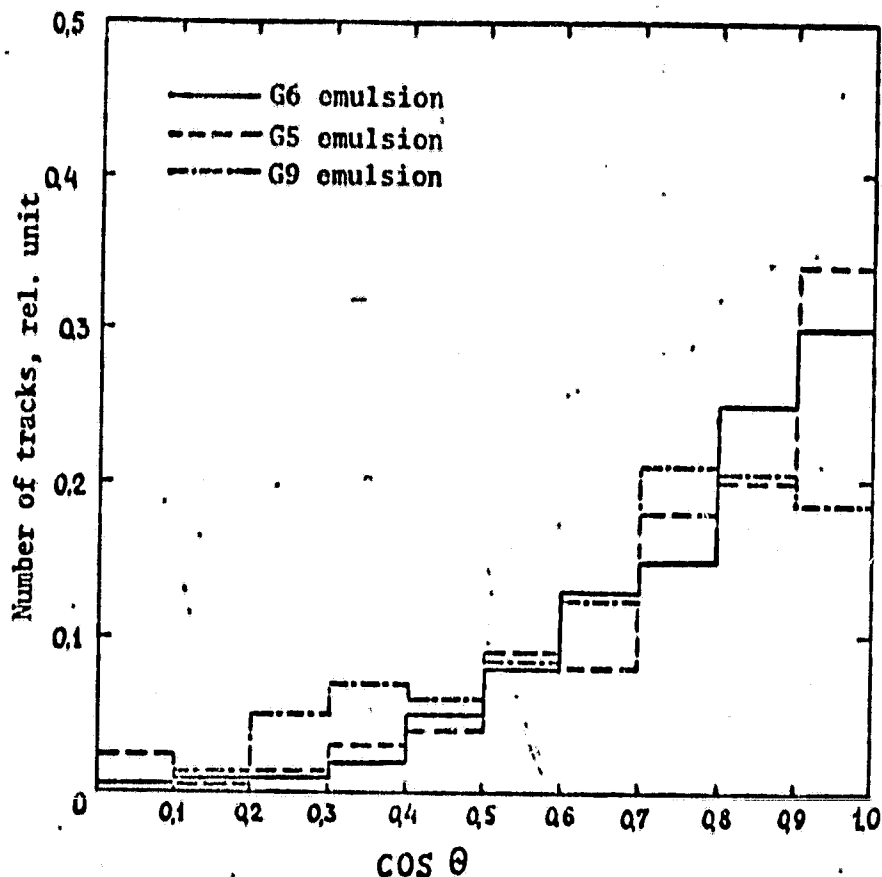
$\bar{\ell}_e^k$ --the average length of track in the elementary volume of the emulsion, cm;

TABLE 4. MEASUREMENTS IN THE PR-2 TYPE EMULSION WITH DIFFERENT THRES- /20  
HOLD VALUES OF LET

Emulsion	Potential of development, MV	Threshold value of LET in tis-suc	Planar fluence, cm <sup>-2</sup>	Density of flux, cm <sup>-2</sup> s <sup>-1</sup> sterad <sup>-1</sup>	Volumetric density of tracks in the emulsion part. cm [illegible]
$\frac{12}{1}$	-240±2	2,3 ± 0,4	(2,92±0,20) · 10 <sup>5</sup>	(1,38±0,1) · 10 <sup>-2</sup>	(7,8±0,1) · 10 <sup>7</sup>
$\frac{12}{2}$	-190±2	4,6 ± 0,5	(8,73±0,61) · 10 <sup>4</sup>	(4,12±0,3) · 10 <sup>-3</sup>	(1,08±0,05) · 10 <sup>7</sup>
$\frac{12}{3}$	-185±2	6,2 ± 0,6	(7,44±0,45) · 10 <sup>4</sup>	(3,5±0,5) · 10 <sup>-3</sup>	(7,99±0,1) · 10 <sup>6</sup>
$\frac{12}{4}$	-180±2	9,1 ± 0,8	(2,52 ± 0,25) · 10 <sup>4</sup>	(1,19±0,12) · 10 <sup>-3</sup>	(3,15±0,1) · 10 <sup>6</sup>
$\frac{12}{5}$	-175±2	13,5 ± 0,8	(2,04±0,61) · 10 <sup>3</sup>	(9,7±2,9) · 10 <sup>-5</sup>	(1,10±0,1) · 10 <sup>6</sup>
$\frac{12}{6}$	-165±2	300 ± 20	(5,1±2,6) · 10 <sup>2</sup>	(2,4±1,2) · 10 <sup>-5</sup>	(1,27±0,2) · 10 <sup>5</sup>

$(\frac{dE}{dx})^k$  -- is the mean value of LET which determines the k and k+1 /23  
threshold of development, MeV/cm;  $Q^k(\frac{dE}{dx})$  -- is the mean value of the co-  
efficient of quality for the two values of LET: k and k+1;  $V_e$  -- is the  
elementary volume in the emulsion (cylinder with base equal to the  
field of vision in the microscope and height equal to the thickness of  
the layer), cm<sup>3</sup>;  $\rho_e$  -- density of the emulsion, g/cm<sup>3</sup>;  $1.6 \cdot 10^{-8}$  -- the  
transfer coefficient from the absorbed energy to the dose;  $\phi_{pr}$  -- fluence  
of protons according to measurements with fissionable foil, prot/cm<sup>2</sup>; /24  
 $\phi_p^2$  -- the planar fluence of charged particles in the emulsion with a  
second potential (LET > 0.46 KeV/μm). The dose in the tissues was  
recalculated from the dose in the emulsion starting with the simple  
relationship:

$$D_{rs} = D_e \cdot \frac{\rho_e}{\rho_{rs}} \cdot \frac{(\frac{dE}{dx})_{rs}}{(\frac{dE}{dx})_e} \simeq 2 D_e$$



/22

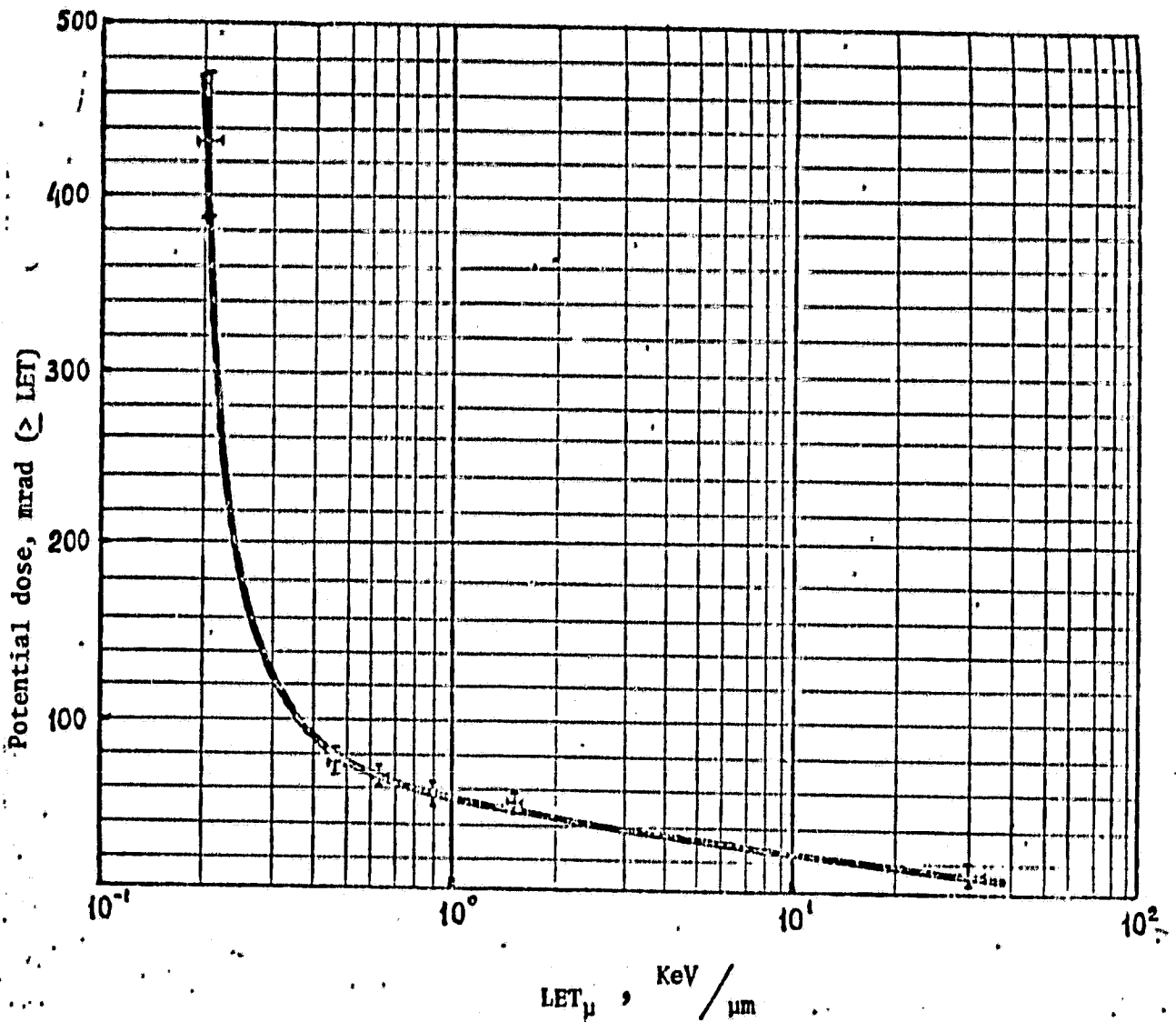
Figure 6. Angular distributions of charged particles according to measurements in the emulsion.

Figures 7 and 8 show the integral relationship of the dose in the tissue (according to the G12 plate) and the density of flow of particles (according to the G12 and G14 plates) from LET radiation. The total absorbed dose measured along the G12 plate is 433 mrad. With a calculation of the relationship of the coefficient of quality to LET, the value of the equivalent dose is 638 millirem ( $Q = 1.47$ ). This value of the dose from the charged particles is obtained with the following assumption:

/24

a) the contribution to the dose from stars formed during interaction of incident particles with nuclei of the medium is not considered;

b) the contribution to the dose of particles with small LET was evaluated according to the measured fluence of the protons using a uranium detector (see Section 3). According to this measurement the fluence of high energy protons is  $6.9 \cdot 10^6$  prot/cm<sup>2</sup>, which results in an addition of 298 mrad to the dose.



ORIGINAL PAGE IS  
OF POOR QUALITY

Figure 7. Integral relationship of absorbed dose from linear loss of energy in the tissue.

c) the contribution to the dose from neutrons of retarded and gamma radiation and electrons is not considered. /24

The contribution to the absorbed dose of stars can be evaluated according to measurements made by Schaefer during the joint Apollo-Soyuz flight [3]. During the 8-day mission, this contribution was 7.8 mrad or 45 millirem. Taking into account the fact that the Apollo-Soyuz flight and the Kosmos-936 flight occurred in orbits with fairly close parameters, one can make a correction for the contribution of stars to the dose due to the varying duration of the flight (9 and 19.5

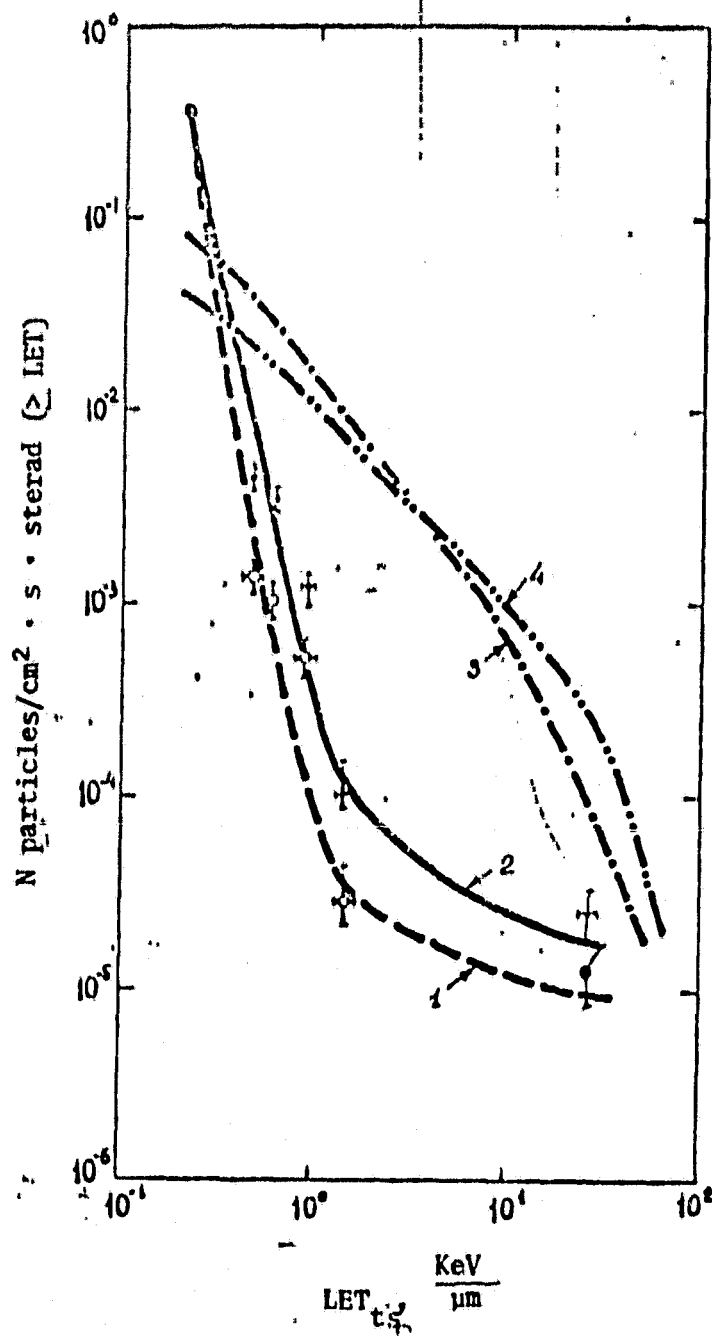


Figure 8. Integral density of the flux of charged particles in relation to linear lines of energy in tissue.

- 1---G14 plate, K-206 experiment
- 2---G12 plate, K-206 experiment
- 3---Kosmos-782 AES, spectrometer
- 4---Kosmos-782 AES, emulsion [8]

days, respectively). Then, this assumes a contribution to the dose from stars for the Kosmos-936 flight is 17 mrad or 96 millirem. Taking this contribution to the dose into account measured using emulsions and calculating for tissue, it amounts to 450 mrad or 734 millirem ( $Q = 1.62$ ). The values of doses obtained can be compared with values measured using TLS and TLD established at the same points. The values measured of doses in the TLS by volume  $1.3 \times 1.3 \times 0.4 \text{ cm}^3$  amounts in scaling on the tissue to  $680 \pm 40$  and  $570 \pm 60$  mrad (above and below, respectively). According to the measurements in the TLD, the absorbed dose is  $424 \pm 30$  and  $523 \pm 57$  mrad [4].

/27

American specialists in the K-206 experiment also measured doses in the K-2 type nuclear emulsion from protons with an energy of less than 10 MeV ( $\frac{dE}{dx} \text{ at } t_s \geq 4.5 \text{ KeV}/\mu\text{m}$ ). The values of the doses for two measurement points are 44.2 mrad or 130.2 millirem ( $Q = 2.95$ ) and 49.6 mrad or 145.9 millirem ( $Q = 2.95$ ) [4]. According to our measurements in the emulsion the dose from the particles with  $LET_{ts} \geq 4.5 \text{ KeV}/\mu\text{m}$  is 49.3 mrad or 243 millirem ( $Q = 4.9$ ). The question as to how noticeable the disparity is in values of the coefficient of quality and, correspondingly, in the shape of the spectrum of particles with LET above 4.6 KeV/ $\mu\text{m}$  requires further consideration.

The analysis of results of emulsion measurements made in the K-206 experiment indicates

- the necessity for further unification of all detectors used, the conduct of simultaneous calibration irradiations of different detectors on beams of ionizing particles;

- the necessity for conducting a detailed comparison of the LET spectra according to measurements in nuclear emulsion and with the S-1 spectrometer;

- the necessity for increasing the number of potentials of development for obtaining the LET spectrum with more frequent decomposition particularly in the field above 10 KeV/ $\mu\text{m}$ ;

- the necessity for measuring the characteristics of radiation incident on the spacecraft;

/28

- the necessity for measuring fluences and spectra of LET for different protective layers;

- the necessity for making the appropriate calculations according to passage of cosmic radiation through the protective spacecraft taking into account the experimentally measured spread of the mass.

### 3. Fissionable Foils

Fissionable foils under the effect of the neutrons of the materials are designed for measuring the fluence of neutrons with different

thresholds, beginning with  $\approx 1$  MeV and also for evaluating the fluence of protons with an energy above 17 MeV.

### 3.1. Materials and Methods for Processing

Fissionable foils were used in the experiment made of Bi-209 (thickness  $\approx 0.3$  mg/cm<sup>2</sup> and  $\approx 1$  g/cm<sup>2</sup>), U-238 (thickness  $\approx 1$  mg/cm<sup>2</sup> and 3.8 g/cm<sup>2</sup>), Np-237 (thickness  $\approx 0.03$  mg/cm<sup>2</sup>). Recording of the fragments of division due to the effect of neutrons (and protons) was accomplished by glass (bismuth and uranium foils) and mica (neptunium foils). The sets of these dosimeters were placed on the upper and lower faces of the Soviet A block. All of the foils before and after completion of the flight were kept separate from the detector (glass, mica). On September 15, 1977, chemical processing of the flight and control detectors was completed. The processing method was standard. The traces of fragments of separation which appear after treatment with fluorine acid on the glass are counted using a microscope with a magnification of 300.

Calculations of the fluences of neutrons were made according to the well known relationship:

$$\phi = \frac{J}{K \cdot N_0 \cdot \sigma_f};$$

where  $\phi$ --is the fluence of neutrons, neutron/cm<sup>2</sup>;

J--the number of fragments of division recorded, cm<sup>-2</sup>;

K--the effectiveness of recording the fragments of division, for glass  $K = 0.42$ ;

$N_0$ --the number of nuclei of the divided substances of the target, nuc/cm<sup>2</sup>;

$\sigma_f$ --cross section of division of the nuclei by neutrons.

We note that the cross section of division under the effect of neutrons has a threshold character. Figure 9 shows a cross section of division by neutrons of different energies [5].

The reactions of separation also occur under the effect of protons (method of calculating fluences of protons is completely similar). In a case of mixed irradiation (as in our case) it is difficult to isolate the recorded fragments caused separately by neutrons. For this division it is necessary to know the shape of the energy spectrum of neutrons and protons and also the full fluence of protons. Such data can be obtained by a twofold method. Firstly, using data on the shape of the spectrum and full fluence of protons with an energy greater than 17 MeV ( $LET_{ts} \leq 3$  KeV/ $\mu$ m) obtained using the S-1 spectrometer, it was established separately from the K-206 container as a rule. This circumstance can lead to difficulty in evaluating error as a result of different shields of the spectrometer and fissionable foils. Such work at the present time has not yet been completed. The shape of the spectrum of neutrons can be used according

/29

to the bibliographical data.

Secondly, division can occur on the basis of well known relationships from another flight. For purposes of unambiguity (also like American specialists [4]) we will use the relationship on fluence of neutrons and protons obtained on the Skylab [6]. According to the data, 24% of the recorded fragments are caused by neutrons.

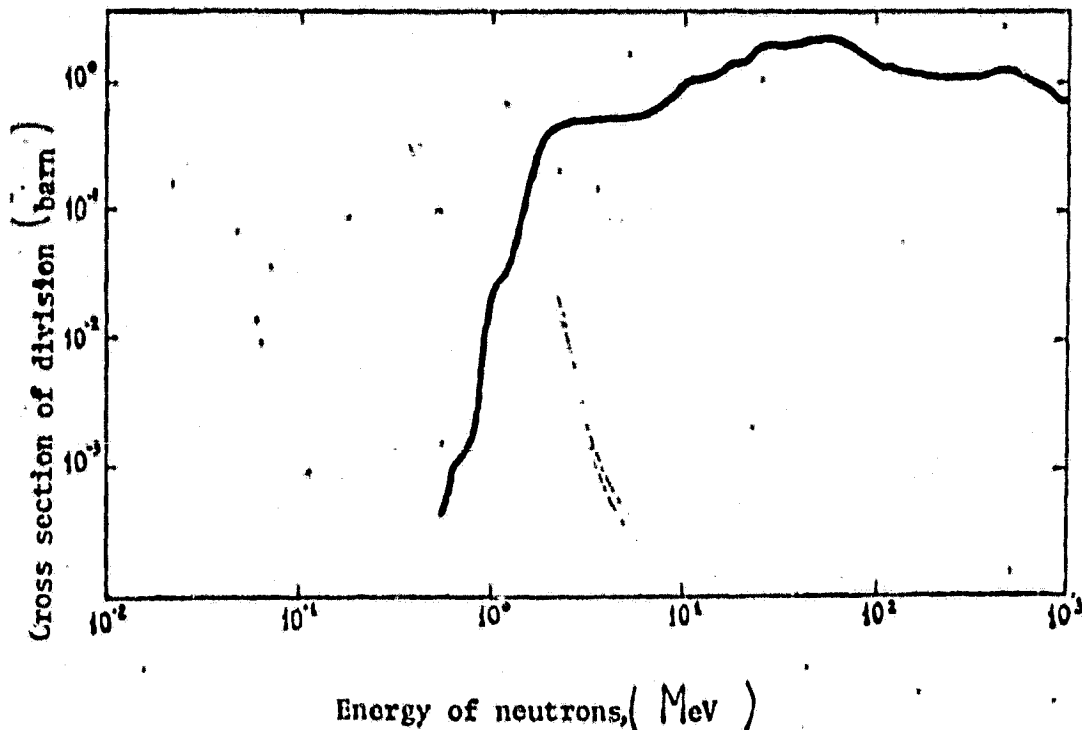


Figure 9. Cross section of division of U-238 by neutrons of different energies.

### 3.2. Results Obtained and Their Consideration

In the measurements made, the number of recorded fragments for 1 cm<sup>2</sup> is: on the Bi and Np foils--at the background level; on the U foil with thickness 1 mg/cm<sup>2</sup>--18 frag/cm<sup>2</sup> and thickness 5 g/cm<sup>2</sup>--154 frag/cm<sup>2</sup>. Taking into account the number of nuclei which participate in the recorded reactions, the fluences of particles which cause such density in the recorded fluxes, amount to, respectively,  $1.7 \cdot 10^7$  and  $1.2 \cdot 10^7$  part/cm<sup>2</sup>. Taking into consideration the contribution of the neutron components (24%), the fluences of neutrons with energy greater than 1 MeV amount to  $4.1 \cdot 10^6$  and  $2.0 \cdot 10^6$  neut/cm<sup>2</sup>. The corresponding measurements by our American colleagues give a value to the fluence of neutrons ( $E > 1\text{MeV}$ )  $2.1 \cdot 10^6$  neut/cm<sup>2</sup>

with an error somewhat below a magnitude [4]. The agreement of the values obtained is completely satisfactory. An evaluation of the specific dose [7] equivalent to the dose from neutrons gives the value of 140 millirems which agrees well with the evaluation of the American specialists of 125 millirem [4].

The evaluation presented of the fluence of protons ( $E_p > 17$  MeV) with a calculation of a 24% contribution of neutrons gives the value of (taking into account the difference in value of the cross section of division for protons and neutrons)  $7.9 \cdot 10^6$  and  $5.9 \cdot 10^6$  prot/cm<sup>2</sup>.

In subsequent experiments, one can continue measurements of fluences of neutrons having given attention both to the expansion of the range of recorded energy of neutrons (right up to thermal) and the increase in precision in the field of energy study (higher than 1 MeV).

### 3. Dielectric Tracking Detectors

Measurements of fluences and spectra of heavy particles of cosmic radiation were made by our group during recent years on a number of space objects [8, 9-12]. These works showed that polymer dielectric tracking detectors are very effective for this type of study thanks to their insensitivity to background radiation (electrons, protons, photons), tissue equivalency, and long retention of information. /32

Interest in this study is due to the capability of heavy particles to inactivate cells of the organism of man and other biological subjects and, in particular, the unique regenerating structures. The latter circumstance can be considered when planning long-term space flight only when there is broad physical data on this type of particle in outer space.

The dielectric tracking detectors in the K-206 experiment are designed for solving the following problems:

- measurement of the fluence of heavy charged particles at different points on the satellite;
- the study of attenuation of the fluence by different layers of the shield;
- obtaining charged and energy spectra of heavy charged particles where the container is installed. A method is presented below as well as results and consideration of the data obtained.

#### 4.1. Materials

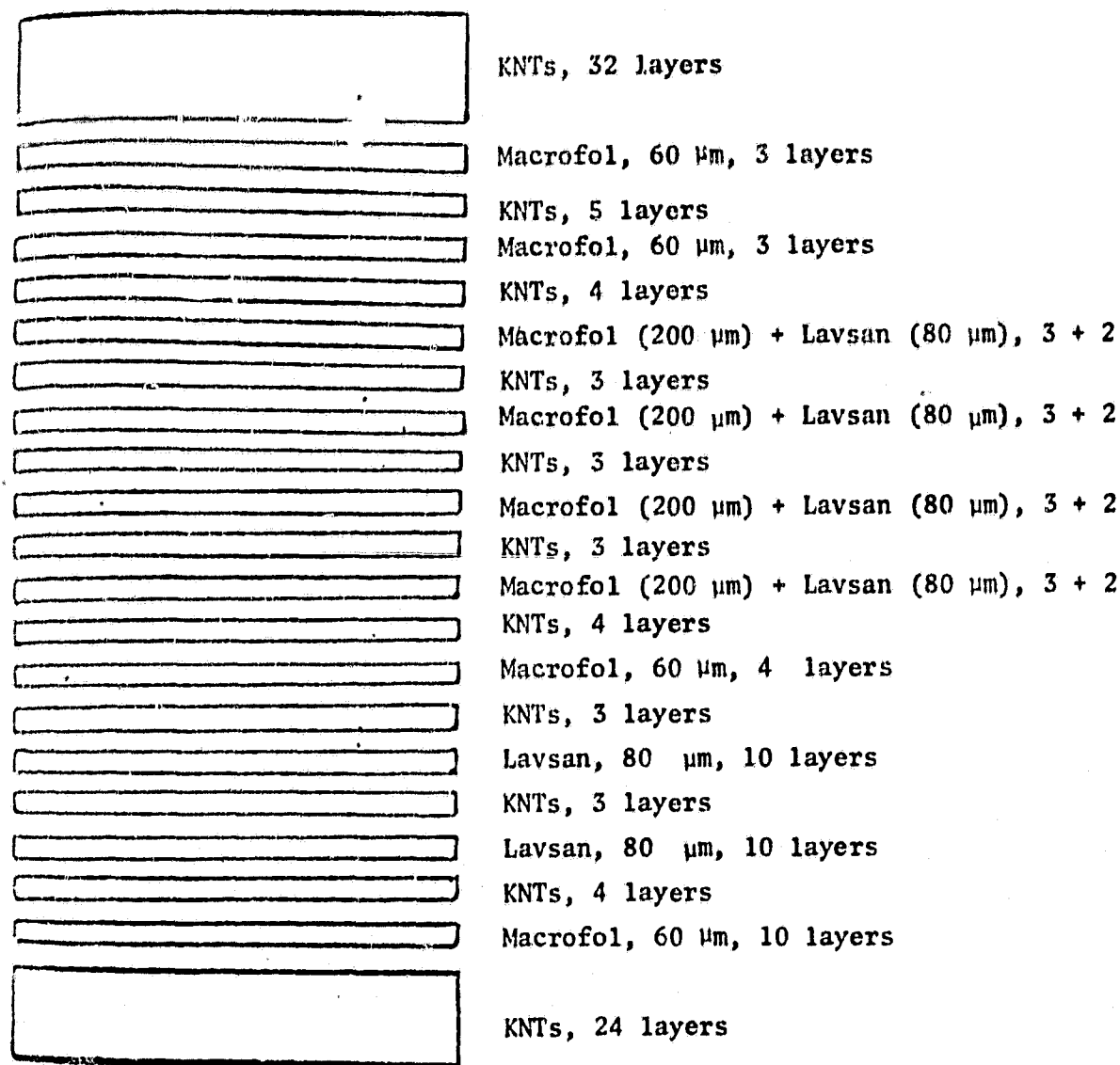
In the experiment, nitrocellulose detectors were used (Kodak-Pathe and KNTs), polycarbonate (Lexan, Macrofol) and lavsan. The detectors were combined in several assemblies and blocks located at different points in the container and the satellite.

The 7F--12F assemblies contained two layers of nitrocellulose

(Kodak) and polycarbonate (Lexan) detectors with dimensions 4.5 X 6.0 cm. The layers are marked A, B, C, D and A and B are polycarbonates. All of the assemblies were sealed in packets with black polyethylene.

The A and B blocks contained, respectively, 148 and 406 detecting layers assembled in a single aligning coordinate system. The system of alternating layers in the blocks is presented in Figures 10 and 11.

/33

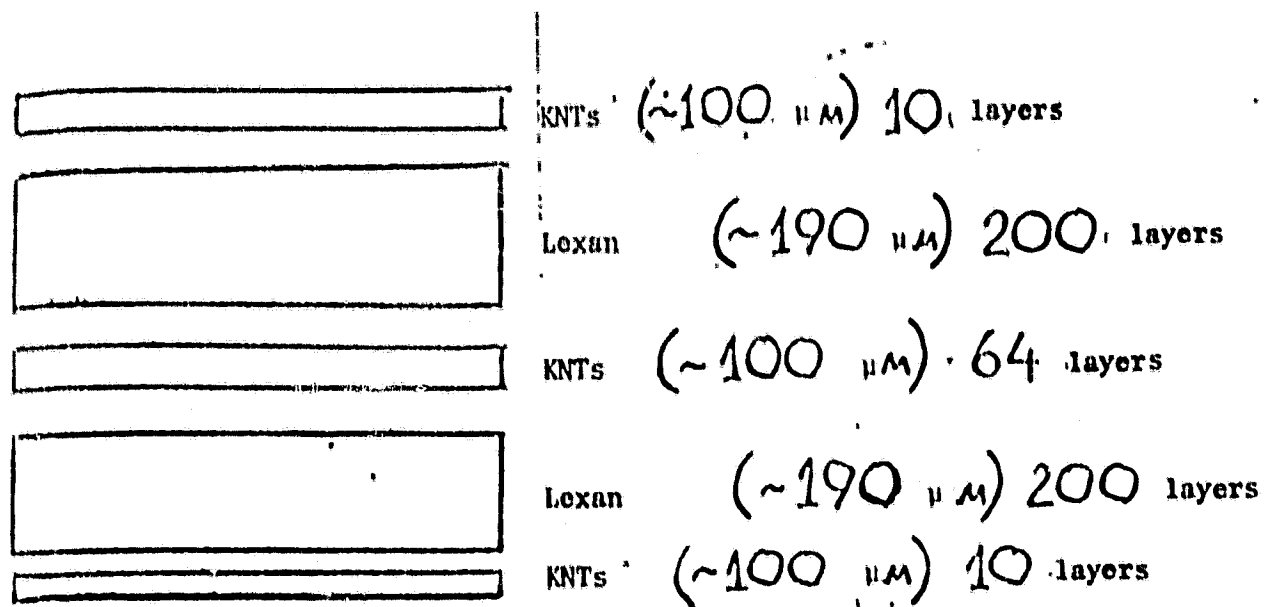


/34

Figure 10. Diagram of block A (USSR)

Besides the assemblies described, several others were used made up of three layers of KNTs which were placed at different points in the satellite.

/33



/35

Figure 11. Diagram of the B block (USSR)

#### 4.2. Flight Experiments

In the flight experiment the A, B, C blocks were placed in a single container (Figure 1) in such a way that the plane of the detector was turned toward the cover. Numbering of the layers goes from top to bottom.

The 7F--12F assemblies are placed along the faces of the joint block in the following way:

7F and 9F -- on the "top" and "bottom" faces,  
 8F, 12F, 19F, 11F -- counterclockwise around the face of the block with the 8F found on the face turned toward the American B block.  
 Three layer assemblies: the D port of the exterior S-1 instrument and the E container on the external surface of the satellite.

All of the assemblies and blocks of dielectric tracking detectors before installation in the satellite and after return to the laboratory before etching were kept in a refrigerator.

#### 4.3. Calibration Experiment

The problems of the calibration experiment are measurement of the threshold of recording of detectors and obtaining calibrated points on the calculated curve of the dependence of maximum etched length of the track from the charge of the particle. For this purpose, the samples of detectors from different batches of material were irradiated on different units with a set of heavy ions of varying energies. The data on the irradiations made are presented in Table 5. All of

the detectors before irradiation were stored in a dark cooled room and after irradiation before etching--in a refrigerator.

#### 4.4. Chemical Processing of the Dielectric Tracking Detectors

/37

After return of the flight blocks to the laboratory they were dismantled and the detectors were subjected to chemical treatment--etching.

Etching of the detectors was carried out in an aqueous solution of NaOH. For KNTs and Kodak-Pathe cellulose nitrate, the parameters of the process were, respectively, the following: concentration 6N and 2.5N; temperature 50°C and 40°C; duration--7 and 10 hours. Flight, calibration and control nonirradiated layers were immersed in a single solution simultaneously. Because the KNTs detector blocks irradiated in Berkeley were absent when processing was begun of flight detectors, their etching was carried out later in the same solution. The identical nature of the solution was controlled in concentration of products of etching, density, pH index and titration.

The thickness of the detectors after etching was 700  $\mu\text{m}$  (KNTs) and 90  $\mu\text{m}$  (Kodak-Pathe).

The surface of the KNTs detectors after etching became diffusely matte which made subsequent examination difficult. Due to this, the surface of the detectors of this type was treated with a colored solution of polyvinyl acetate (PVA) which, after drying, forms a thin transparent film.

#### 4.5. Method of Inspection of Dielectric Tracking Detectors

The Kodak-Pathe detectors from the 7F--12F assemblies were used for measuring planar fluence of charged particles, that is, the number of particles which pass through a stationary surface per area unit [2]. The procedure amounted to counting the number of tracks in two stages: first the tracks located on the 1.5 cm bandwidth along the length of the side of the detector; then a count was made of the entire area of the detector. At the same time, measurements were made of geometric characteristics of tracks, whose data are necessary for obtaining the LET spectra. The process of scanning and measurement was carried out on the MPE-1 microscopes with a volumetric magnification of 300X--600X. The statistics of observation provided a precision no worse than 4%. /38

The measurements of fluence of particles in the KNTs detectors were made using the MBS-2 stereomicroscopes with a magnification of 32X--80X. The KNTs detectors introduced into the A block were designed for measuring charged spectra of heavy nuclei for the maximum length of the track. A multilayer method was used for speeding of scanning, that is, etched and coated detectors were first made up into a set of 5--6 layers assembled for the same coordinate system as during exposure. In the scanning process, the coordinates were fixed at the beginning,

TABLE 5. CALIBRATED IRRADIATION OF DIELECTRIC TRACKING DETECTORS

/36

No.	Type of particles	Energy, MeV/nucleon	Type of detector	Angle	Location of irradiation
1	$\alpha$ - particles	0,5-1,3	KNTs	45°	IMBP
2	$B_{11}$	2 - 6	KNTs	19° 51°	LNR JINR <sup>1</sup>
3	$C_{12}$	3,7 - 9,1	KNTs Kodak Lexan Lavsan	30°	- " " -
4	$Ne^{20}$	2,4 - 9,1	KNTs  Lavsan	30°	- " -
5	$Ne^{22}$	3,25	KNTs Lavsan	10°, 30° 45°, 60°, 90°	- " -
6	$Ar^{40}$	0,25-3,75	KNTs Lavsan	20°, 45°, 90°	- " -
7	$Cr^{52}$	1,7-6,0	Lavsan	20°, 45°, 90°	- " -
8	$Ar^{40}$	199 98	KNTs (assembly) Lavsan (assembly)	30°, 45°, 60° 45°	Berkeley, USA - " -
9	$Fe^{56}$	509 114	KNTs (assembly) Lavsan (assembly)	45° 45°	- " - - " -

<sup>1</sup> [Laboratory of Nuclear Reactions, Joint Institute of Nuclear Research].

and at points of intersection of the tracks of the surface of the assembly. At the same time, the characteristic points of the track and direction of motion of the particles were indicated (in those cases where a tendency for change in the length of the cones along the track made this possible. Then, "cross linking" of the tracks was carried out, calculated taking into consideration the etched layer of the length of the visible part of the track and the run of the particles from the face of the block to the stopping point.

Treatment of the blocks of KNTs detectors irradiated in Berkeley was done using a semiautomatic coordinate meter, the Ascorecord. For this purpose, bandwidths of 1.5 mm were selected on the detectors calculating that in the sequential layers they lay along the direction of motion of the particles during irradiation and the coordinates of the points of input or output of all tracks were measured within limits of the band selected. Then this information retained on perforated tape was fed to a EVM [elektronnaya vychislitel'naya mashina, electronic computer] for joining of the tracks.

#### 4.6. Results Obtained

/39

Obtaining the threshold of recording and the relationship of the maximum etched length  $R_{\max}$  of the tracks of particles from their charge  $Z$  for detectors on the KNTs base was of significant importance for interpretation of the results of the flight experiment. In the first stage, according to the results of irradiation of alpha-particles and ions of boron ( $E < 9$  MeV/nuc) and carbon ( $E < 8$  MeV/nuc) the following threshold value was obtained  $LET_{100} = 196 \pm 7$  KeV/ $\mu$ m nb. These data were used for constructing the curve of  $R_{\max}(Z)$  (Figure 12, curve 1).

Further, after treatment of the blocks irradiated with ions of argon ( $E = 199$  MeV/nuc) and iron ( $E = 509$  MeV/nuc) calibrated points were obtained for the section of the relationship in the region of large charges. However, these points correspond to a higher threshold of recording of  $LET_{100} = 250$  KeV/ $\mu$ m.

The relationship calculated for this threshold value is presented in Figure 12 (curve 2).

The values of fluence measured, obtained using a system of orthogonal detectors placed on the face of the joint block C, are presented in Table 6.

In the first column of the Table the detector number is given and in the second the number of tracks found for 27 cm<sup>2</sup> of detector area, in the third column is the fluence of particles. One should note that the data are only for particles with a charge of  $Z > 3$  whose tracks pass through both layers of nitrocellulose detectors, that is, longer than 180  $\mu$ m. The values of fluence are presented without correction. The errors noted are purely statistical.

Moreover, the planar fluence of particles is measured with  $LET_{100} \geq 250$  KeV/ $\mu$ m using the KNTs detectors placed at different points on the

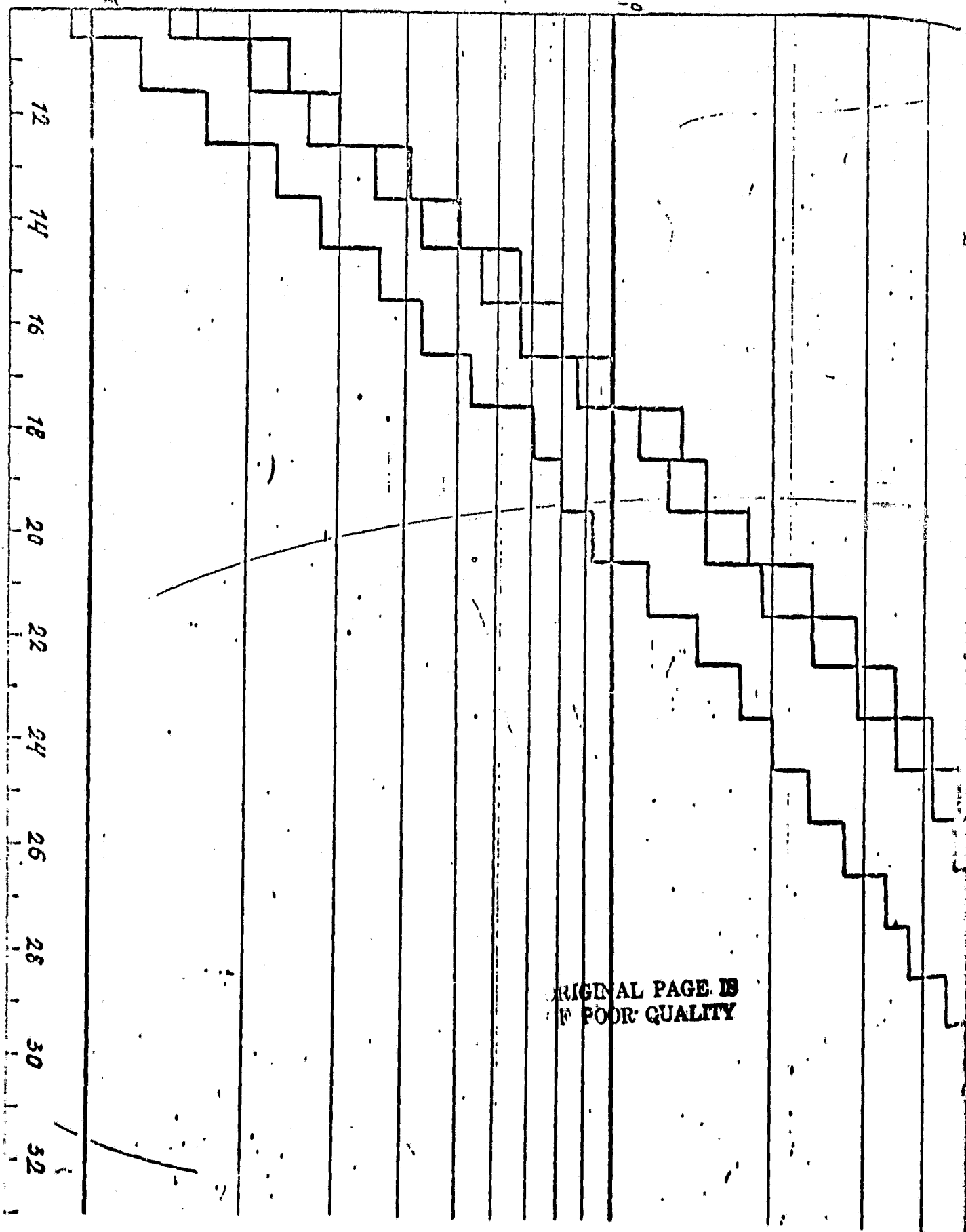


Figure 12. The maximum length of the track to the charge.

TABLE 6. MEASURED PLANAR FLUENCE OF HEAVY NUCLEI

Detector number	Number of tracks	Fluence, $\text{cm}^{-2}$
7 F	864	$32,0 \pm 1,1$
8 F	532	$19,7 \pm 0,9$
9 F	589	$21,8 \pm 0,9$
10 F	338	$12,5 \pm 0,7$
11 F	464	$17,2 \pm 0,8$
12 F	756	$28,0 \pm 1,0$

satellite. The results are presented in Table 7.

TABLE 7. PLANAR FLUENCE OF PARTICLES WITH  $\text{LET}_{1000} \geq 250 \text{ KeV}/\mu\text{m}$ 

Location for installing the detector	Number of tracks	Planar fluence, $\text{cm}^{-2}$
Block A, top (face A-5)	788	$7,9 \pm 0,3$
Block A, bottom (face A-6)	259	$2,60 \pm 0,15$
Bioblock container		$2,5 - 6,2$
For protection $\approx 2\text{G}/\text{cm}^2$	100	$10,0 \pm 1,0$
Outer surface of the satellite	737	$14,2 \pm 0,6$

The data apply to particles with  $Z > 7$  and length of the track more than  $\approx 200 \mu\text{m}$ .

Statistical error is always given.

/42

Figure 13 shows the charge distribution of particles whose tracks were measured in the "upper" section (thickness about  $4.3 \text{ g/cm}^2$ ) of the joint block A. 1203 tracks were observed in all; however, the histogram is presented for only 853 tracks which satisfy the criterion of sampling--the beginning and end of the track is within limits of the layer scanned. Identification was made in accordance with curve 2 (Figure 12).

#### 4.7. Consideration of Results

One of the most important results obtained is data on calibration of the KNTs detector irradiated in Berkeley with high energy ions of argon and iron; it follows from this that the threshold of recording with high energy particles is greater by approximately 20% than that obtained earlier on beams of ions with low energy. This result can be explained by the high transfer of energy from the zone of formation of the tracks by  $\delta$ -electrons which is characteristic for ionization of heavy high energy particles. If, in the process of further treatment of the blocks irradiated in Berkeley this result is confirmed with good statistical precision then, obviously, it will be necessary to make a new calculation on the relationship of the maximum etched length of the track to the charge of the particle based on a model of a radial distribution of absorption of energy [13, 14].

Table 6 shows data on the fluences of particles with a charge  $Z > 3$  and  $\text{LET}_{350} \geq 80 \text{ KeV}/\mu\text{m}$ , incident on different faces of block C. A comparison of data between them indicates significant anisotropy of the flux of particles in the area where the detectors are mounted. However, quantitative conclusions can be drawn after introducing a correction for the critical angles of the tracks of the particles with different values of  $\text{LET}_{350}$  and consideration of distribution of mass of the construction materials relative to the point of measurement. This becomes possible after completion of calculation for the  $\text{LET}_{350}$  spectra according to readings of these same detectors. A comparison of the values of fluence of particles with  $\text{LET}_{1000} \geq 250 \text{ KeV}/\mu\text{m}$  (Table 7). One did not detect significant divergencies from the results of similar measurements on the Kosmos-690, 872 AES [10-12].

/44

The charge distribution of particles presented in Figure 13 is not conclusive. Treatment of the A block continues. After discovering the length of all tracks which satisfy the criterion for sampling given above, the appropriate charges and energies of particles for them at the input of the block and the run of the particles in the block will be calculated. Then, the particles will be classified according to charge and energy distributions of the particles recorded will be constructed. These intermediate results will be transformed into a family of charge-energy spectra and the ratio of representation capability of heavy particles within the satellite (in identical energy range) using a method which we developed taking into account the effectiveness and recording of a section with different charges

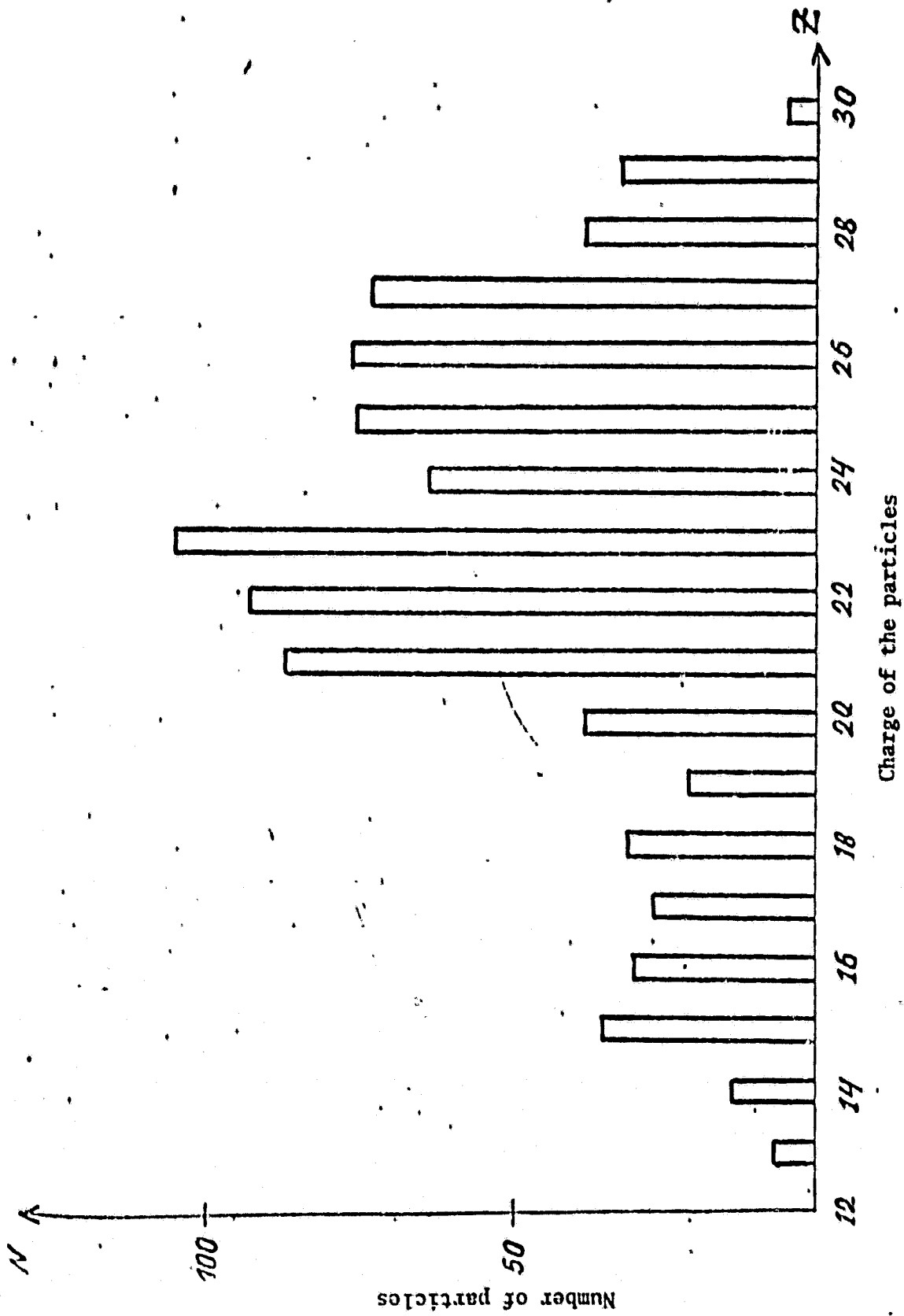


Figure 13. Charge distribution of tracks measured.

and energies in a block with the prescribed geometry (A.M. Marennyy, S.A. Dashin, unpublished data).

The authors wish to take this opportunity to express their thanks to their colleagues: V.A. Sakovich--for his useful comments, to N.A. Bardashev, G.P. Gertsen, S.A. Kamanin, L.L. Mironychev, and N.I. Churin for participation in conduct of experimental studies, to V.I. Popov for his irradiation work in the city of Dubna and to L.M. Yevsyukov for his assistance in formulating results of the work. The authors are very grateful to Dr. Ye. V. Benton and his colleagues in the University of California for irradiation of the detectors at Berkeley and assistance at other stages of the joint work.

# REFERENCES

/45

1. Kocherov, N.P. and N.R. Novikova, Zh. nauchn. i prikl. i kinematografi, 3, 183-190 (1971).
2. Attix, F.H. and W.C. Roesch, Radiation dosimetry, Vol. 1, Academic Press, New York and London, 1968, pp. 20-25.
3. Schaefer, H.J., "Nuclear emulsion measurements of the dose contribution from tissue disintegration stars on the Apollo-Soyuz mission," NR 105-860/2, Pensacola Fla., Faculty of Physics, University of West Florida, 1977.
4. Benton, E.V., R. Cassou, A. Frank, R.P. Henke and D. Peterson, "Space radiation dosimetry on board Kosmos 936," US portion of experiment K-206, 1978.
5. Kon'shin, V.A., Ye. S. Marusevich and V.I. Regushevskiy, Byulleten' informatsionnogo spektra po yadernym dannym Atomizdat [Bulletin of the information spectrum according to nuclear data], Issue 1, Atomizdat Press, 1965.
6. Fishman, G.J., "Neutron and proton activation measurements from Skylab," AIAA Paper, No. 74-1227, AIAA/A6U, Conference on Scientific Experiments of Skylab, Huntsville, Alabama, 1974.
7. Normy radiatsionnoy bezopasnosti, NRB-76 [Standards of radiation safety, NRB-76], Moscow, Atomizdat Publishers, 1978, p. 53.
8. Kovalyev, Ye. Ye. et al., "Measurement of spectra of linear energy loss on the Kosmos-782 AES," Kosmicheskiye issledovaniya [Space studies], at the Publishers.
9. Marrennyy, A.M., "Recording of heavy charged particles on the Kosmos-613 AES," VIII symposium on space biology and medicine, Interkosmos, Varna, Bulgaria, 1975.
10. Vinogradov, Yu. A., A.M. Marennyy and V.I. Popov, "Results of measurement of fluence of heavy GCR particles in the Spectrum experiment on the Kosmos-782 AES," X symposium on space biology and medicine, Interkosmos, Sukhum, USSR, 1977.
11. Marrennyy, A.M., V.I. Popov and B.I. Solyanov, "Experiment on the Bioblock-2. Design and make-up of the assemblies. Method of topologic recording and identification of heavy nuclei of Galactic Cosmic Radiation," Radiobiologiya 17/4, 559-561 (1977).
12. Benton, E.V., D.D. Peterson, A.M. Marennyy and V.I. Popov, "HZE particle radiation studies aboard Kosmos-782," (In press).
13. Kudrysashov, Ye. I., A.M. Marennyy, O.M. Meshcheryakova and V.I. Popov, "Microdistribution of absorbed energy in the track of heavy charged particles," Kosm. biol. i meditsina, 5, 35-39 (1970).

/46

14. Kudryashov, Ye. I., A.M. Marennyy, O.M. Meshcheryakova and V.I. Popov, "The effect of boundaries of two media on distribution of absorbed energy in the track of a charged particle," Kosm. biol. i meditsina, 3 (1973).

## CHAPTER 2. DOSIMETRIC INVESTIGATIONS WITH A TELESCOPE OF COUNTERS AND TLS DOSIMETERS /47

V.V. Markelov, Yu. A. Akatov, S.B. Kozlova, V.N. Bryksin  
(Institute of Medical and Biological Problems of the Ministry of Public Health USSR, Moscow)

### 1. Formulation and Method of the Experiment /48

One of the sections of the K-206 experiment was conduct of dosimetric studies with a telescope of counters and TLS dosimeters.

The purpose of our experiment was:

1. Measurement of integral doses for flight.
2. Study of the changes of power of doses according to the turns of flight.
3. Study of the contribution to dose of protons of the Brazilian Magnetic anomaly.
4. Measurement of particle fluxes.
5. Study of the LET-spectra.

A silicon surface-barrier continuous detector with thickness 500  $\mu\text{m}$  and area 1  $\text{cm}^2$  was used as the telescope of counters for S-1 instrument. In order to separate the direction of incoming particles close to normal incidence it was switched on in agreement with the second detector. The amplitude of the signal at the output of the semiconductor detector was proportional to the value of energy absorbed in it in the broad LET range.

The range of measured values of LET amounts to 2--1000  $\frac{\text{MeV}}{\text{cm}}$  tissue/cm. When measuring the power of doses, only a continuous detector was used whose amplitude of pulses was totalled by the electronic system. Information on the density of particle flux was also taken from this detector.

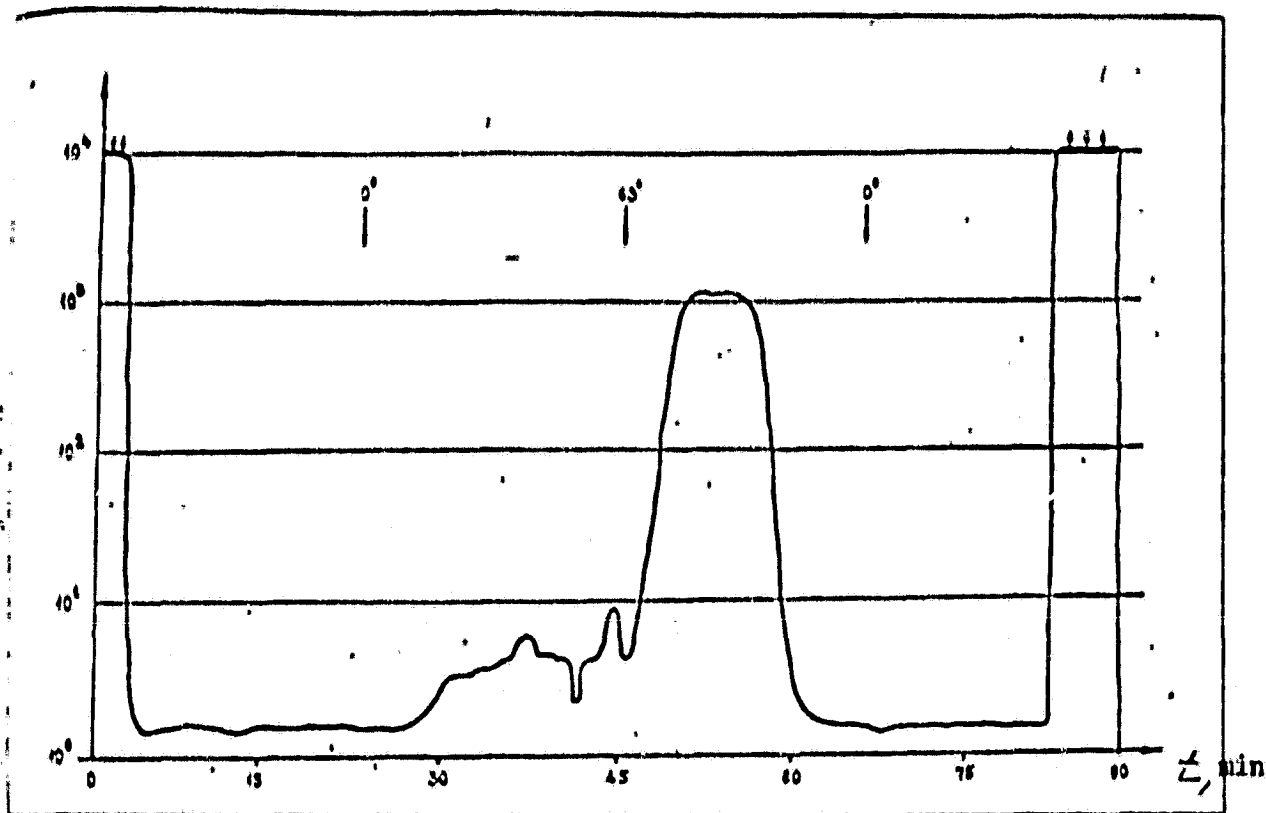
Two S-1 instruments with telescopes of counters were used in the experiment; they were mounted inside and outside the satellite in combination with the TLS dosimeters. The TLS dosimeters had dimensions of 14 X 14 X 4 mm.

### 2. Results of Measurement

The integral dose for flight in the area where the internal S-1 instrument was set up, according to the readings of the TLS dosimeters, amounted to 520 mrad. The same dosimeters were mounted on the exterior surface of the satellite showed a dose of 20 rads in flight.

The curves of change of power of doses and density of fluxes of particles within and outside the satellite along the turns of the flight are presented in Figures 14 and 15.

/49



/50

Figure 14. Change in flux of charged particles on the surface of the satellite for 1 turn.

In Figure 14 one can note three areas--the area close to the equator where, due to maximum screening effect of the magnetosphere, the power of the dose is on the order of 0.2 mr/hr; the field of northern and southern latitudes where the power of the dose is increased to 1.5 mr/hr due to less cutting off of the magnetosphere of Earth by GCR (GKI [galakticheskoye kosmicheskoye izlucheniya, galactic cosmic radiation, GCR]) particles and the field of the Brazilian magnetic anomaly where power can reach a value of 200 mrad/hr. This peak is apparent on the section of turns passing through this zone. The average daily dose without the contribution of the Brazilian anomaly is 10 mrad/24 hr with a flux of particles of 1 part/cm<sup>2</sup> · s. With average daily total dose 25 mrad/24 hr, it follows that the contribution of the dose of protons of the Brazilian anomaly is a value on the order of 60% for a given orbit of the satellite.

/49

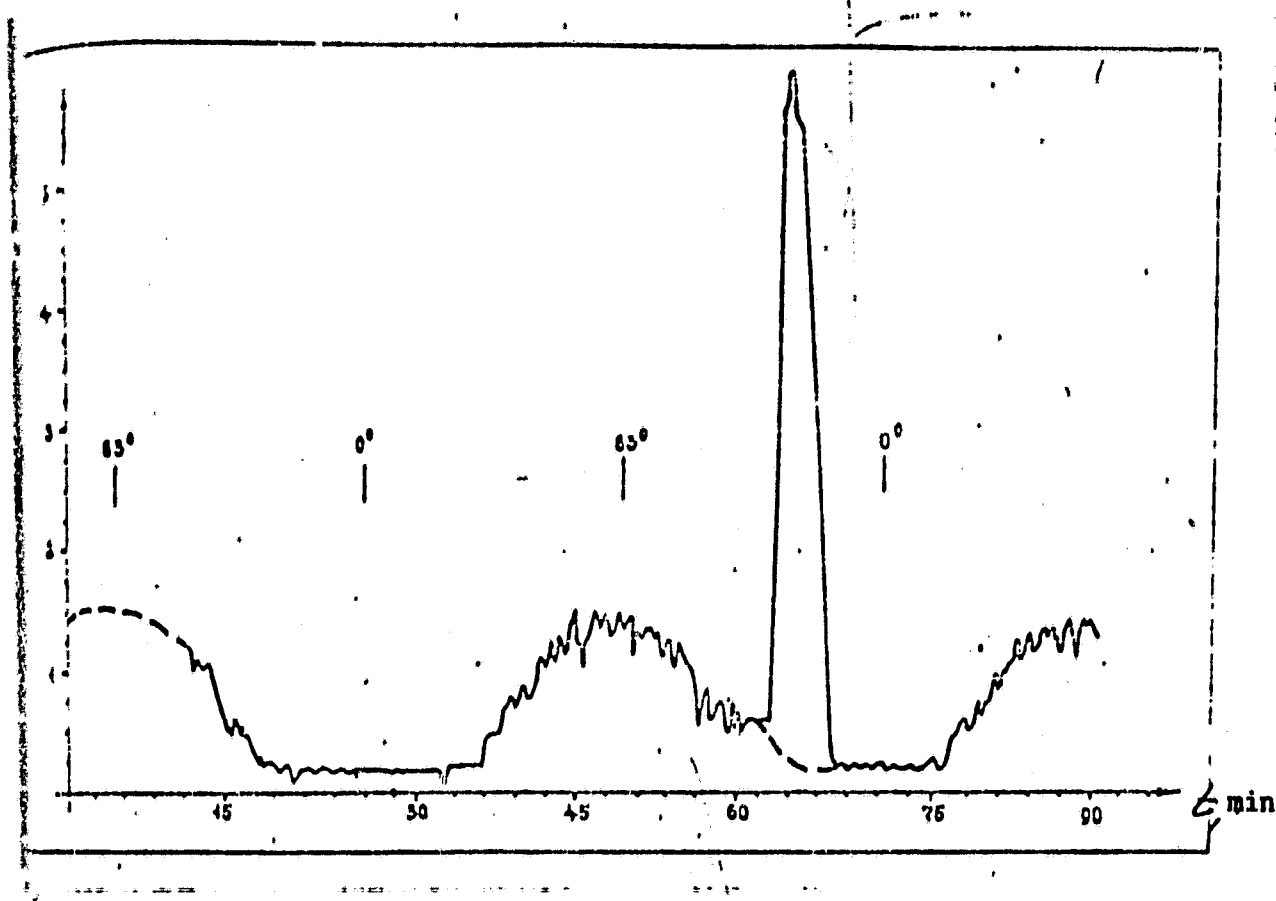


Figure 15. Change in power of the dose within the satellite for 1 turn.

From Figure 15 it is apparent that in the northern and southern latitudes on the exterior surface of the satellite one observes large surges of density of particle flux exceeding  $10^4$  part/cm<sup>2</sup> · s. This can be explained by passage of the satellite through a branch of the external electron band of Earth. /49

The large value of the recorded dose of 20 rads also confirms the presence of high intensity of radiation on the exterior surface. The absence of rises in power of the dose within the satellite in the period of these surges gives evidence of the low penetrating capability of this radiation.

In Figure 16 there are integral LET-spectra of GCR presented obtained by telescopes of counters within and outside the satellites. Here, for comparison, we present the LET spectra calculated and obtained by the American scientists on the Kosmos-872 AES.

The factor of quality calculated from the LET-spectra obtained on the Kosmos-936 gives a value of 1.4 inside the satellite and 2.5

ORIGINAL PAGE IS  
OF POOR QUALITY

outside. Processing of data of the experiment on the Kosmos-936 satellite will be continued.

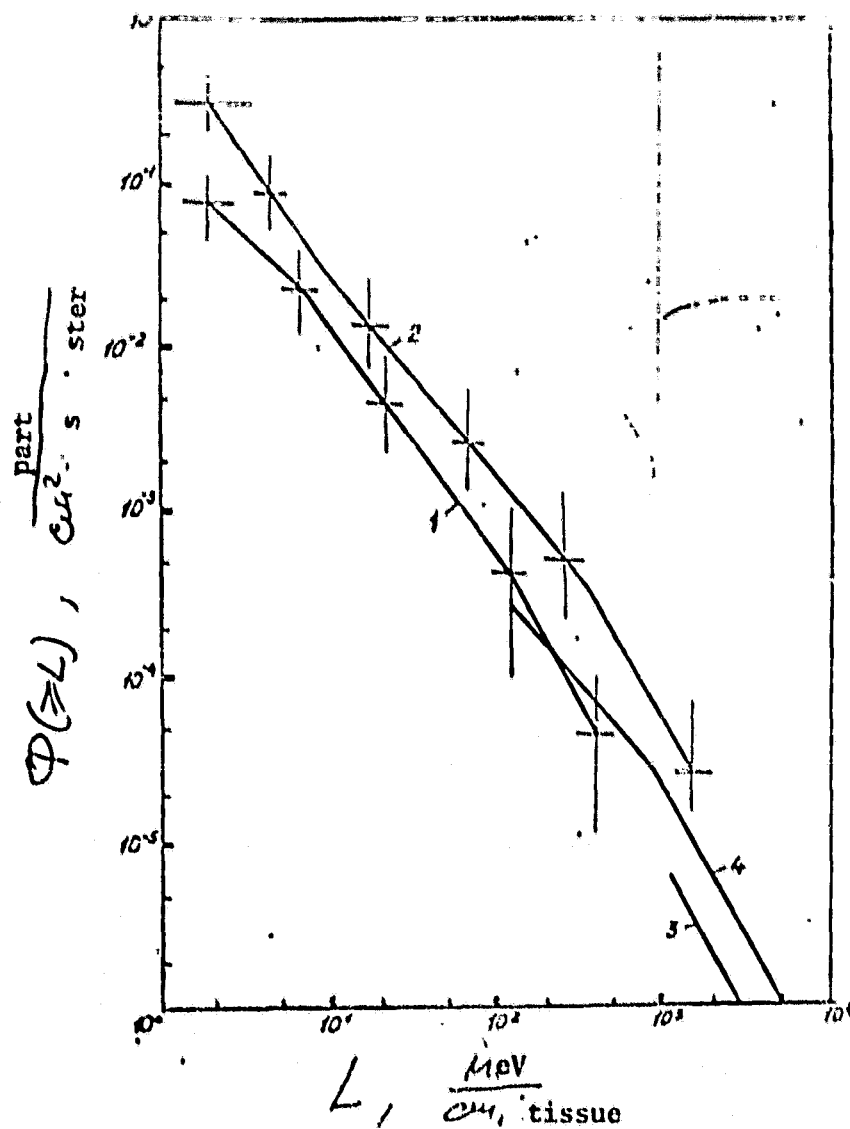


Figure 16. Integral flow spectra of LET

- 1--inside
- 2--outside
- 3--calculated
- 4--measurements on the Kosmos-782 made by Benton

ORIGINAL PAGE IS  
OF POOR QUALITY

N.N. Repin, V.A. Sakovich, V.M. Sakharov  
(Institute of Medical and Biological Problems of the Ministry of Public Health USSR, Moscow)

Distribution of thickness of the material for the dosimeter container located in the K-206 experiment on the Kosmos-936 AES was carried out by a method of gamma-illumination using a special unit. Determination of the thickness is based on a comparison of the intensity of gamma radiation of the point source of cesium-137 which passes through the equipment with intensity and without it. The principle of operation of the assembly involves a precise point within the apparatus where the isotropic gamma source is placed and unscattered radiation which passes through the equipment is recorded by a collimated scintillating BDEG2-23 detector which moves outside the apparatus by a coordinate system along the spherical surface from the center to the prescribed point. /54

Operation of the assembly involves period measurement of the number of pulses recorded by the detector in the photon unit for a fixed time  $\Delta\tau$  with continuous movement of the detector along the azimuthal angle  $\phi$  (within the prescribed limits from  $\phi_1$  to  $\phi_2$ ). The periodicity of single measurements was prescribed in such a way that for the time interval  $\Delta t$  between measurements, the detector moves at an angular dimension of the collimator  $\Delta\phi$ , relative to the numbered axis  $\Delta t \gg \Delta\tau$ . Upon achieving  $\phi_1$  or  $\phi_2$  with the detector, the measurements are continued and the detector is shifted on the numbered angle at an angular dimension of the collimator  $\Delta\theta$ , after which the measurement cycle is repeated. So that the results of the measurements will register sections of the surface lying next to each other and hold together different solid angles relative to a prescribed point  $\Delta\omega = \Delta\phi_0\Delta\theta$ , where  $\Delta\phi_0 = \Delta\phi/\theta = 90^\circ$ , an automatic change in the value of  $\Delta\phi$  was made in the assembly according to the principle  $\Delta\phi = \Delta\phi/\sin\theta$  which actually is realized in the change of the interval between single measurements.

Distribution of the number of single measurements of the number of pulses obtained in the frequency analyzer was converted to distribution of solid angles for the thickness of the material, on the basis of graduations of the detector using standard thickness samples made of aluminum. /55

Error in measurement of distribution of thickness involves the following factors: statistical error of single measurements; error involving recording of radiation scattered at small angles of sections of surface neighboring the section considered; error in the span and intervals between the sections considered and finally, the error caused by nonuniformity of thickness within limits of the section considered.

Statistical error of a single measurement is defined as activity of the source and duration of the measurements. The total duration of

the measurements at an angle  $\theta$  is proportional to  $\Delta\omega^{-2}$  and amounts to  $\approx 30$  hr. Therefore, with the radius of the spherical surface of the unit  $R = 3$  m, the value  $\Delta\omega = 0.7 \cdot 10^{-4}$  sterad, activity of the source is 50 mg-equiv  $\cdot R\alpha$  and when the condition  $\Delta t \gg \Delta \tau = 0.7$  s is observed, statistical error of a single measurement for effective thickness 1 g/cm<sup>2</sup> amounts to  $\approx 5\%$ . With an increase in thickness, this error increases proportionally to  $\exp(\mu\delta_{\text{eff}}/2)$ .

The contribution of radiation scattered by sections neighboring that considered, for the selected dimension of the collimator and discrimination of pulses from the detector at a minimum to the left of the photounit can reach 10%. For decreasing error involved with this effect, the relationship of the frequency of pulses to the calibrated standard for thickness obtained with a scattered layer of 5g/cm<sup>2</sup>Al is used as the graduation so that with minimum thickness 1 g/cm<sup>2</sup> one has an error  $\pm 0.25$  g/cm<sup>2</sup> in a range of thicknesses 1--10 g/cm<sup>2</sup>.

Distribution of thickness of the material of the biosatellite relative to placement of the dosimetric container was measured within a range of solid bodies presented in the Tables. The geometry of measurements relative to the container is presented in Figure 17. Distribution of solid angles according to thickness in g/cm<sup>2</sup>Al is presented in Tables 8--10. /57

The span and intervals between the sections considered amount to  $\approx 6\%$  for the unit used; however, in practice this does not cause distortion of distribution.

As a whole, the error in measurement of a single thickness amounts to  $\pm 0.3$  g/cm<sup>2</sup> with a thickness of 1 g/cm<sup>2</sup> and  $\pm 0.5$  g/cm<sup>2</sup> with thickness to 10 g/cm<sup>2</sup>.

TABLE 8. DISTRIBUTION OF THICKNESS RELATIVE TO THE FACES OF THE K-206

Face No.	$\theta^\circ$	$\varphi^\circ$	$\delta$ g/cm <sup>2</sup>
1	90	90	8,5
2	90	180	11,0
3	90	270	22,0
4	90	0	55,0
5	180	—	20,0
6	0	—	6,0

Face 1 is perpendicular to the cover of the hatch.

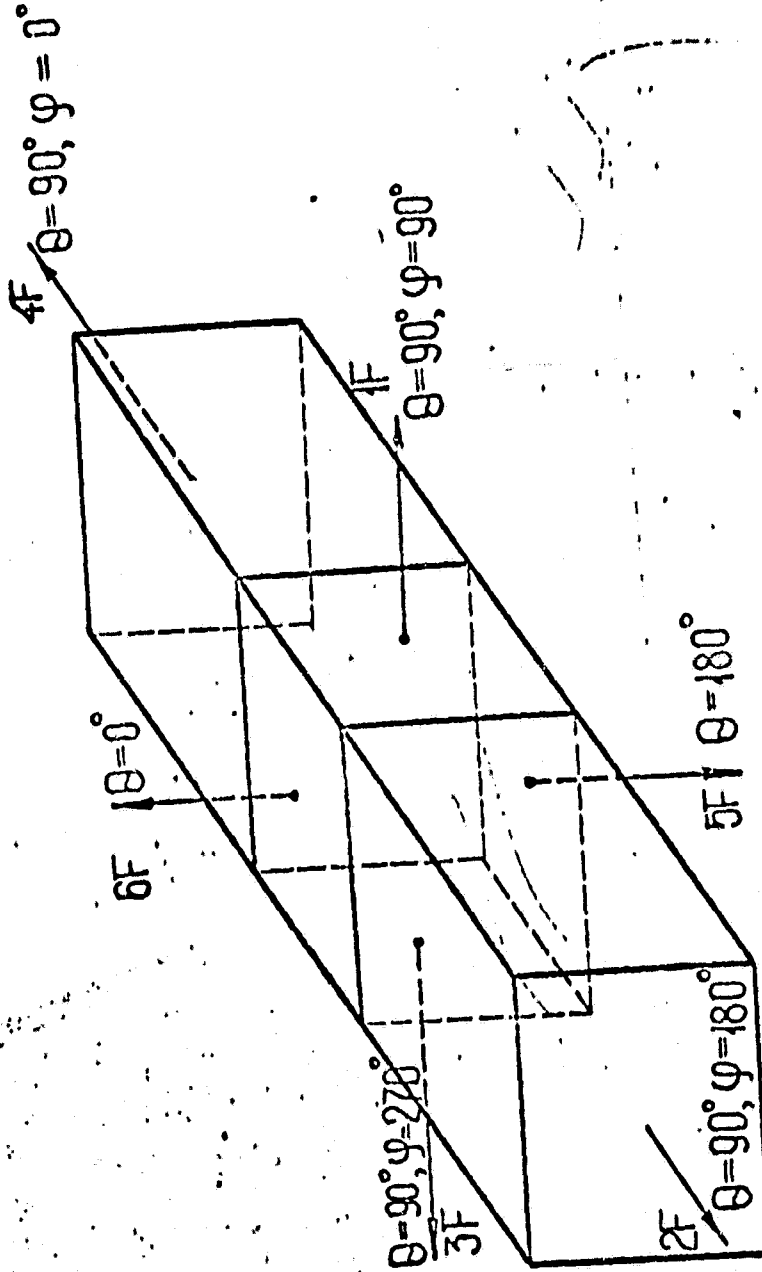


Figure 17. Geometry of measurements of distribution of thickness.

ORIGINAL PAGE IS  
OF POOR QUALITY

TABLE 9. DISTRIBUTION OF SOLID ANGLES ACCORDING TO THICKNESS FOR THE  
K-206 RELATIVE TO FACE 1

$\theta$	:	$\varphi^\circ$	:	$\delta \text{ g/cm}^2$	:	$\Delta \omega \text{ sterad}$	/57
0-40		0-360		5		1,57	
40-140		0-360		5-60		8,71	
140-180		0-360		20		2,28	

TABLE 10. DISTRIBUTION OF SOLID ANGLES ACCORDING TO THICKNESS IN A RANGE

/58

$$40^\circ \leq \theta \leq 140^\circ$$

$$0 \leq \varphi \leq 360^\circ$$

No. :	$\delta$ g/cm <sup>2</sup>	$\Delta\omega$ sterad	No. :	$\delta$ g/cm <sup>2</sup>	$\Delta\omega$ sterad
1.	5,0-5,5	0,073	19.	16,2-17,3	0,145
2.	5,5-6,0	0,143	20.	17,3-18,3	0,146
3.	6,0-6,5	0,187	21.	18,3-19,4	0,158
4.	6,5-7,0	0,279	22.	19,4-20,5	0,149
5.	7,0-7,5	0,387	23.	20,5-21,6	0,156
6.	7,5-8,0	0,387	24.	21,6-22,7	0,187
7.	8,0-8,6	0,370	25.	22,7-24,3	0,221
8.	8,6-9,2	0,337	26.	24,3-25,9	0,256
9.	9,2-9,8	0,286	27.	25,9-27,5	0,284
10.	9,8-10,4	0,266	28.	27,5-29,7	0,319
11.	10,4-11,0	0,253	29.	29,7-32,4	0,377
12.	11,0-11,6	0,228	30.	32,4-35,1	0,353
13.	11,6-12,2	0,190	31.	35,1-37,8	0,317
14.	12,2-13,0	0,167	32.	37,8-41,9	0,323
15.	13,0-13,8	0,157	33.	41,9-45,9	0,360
16.	13,8-14,6	0,168	34.	45,9-52,6	0,330
17.	14,6-15,4	0,169	35.	52,6-60,8	0,401
18.	15,4-16,2	0,156	36.	60	0,070

$$\Sigma = 8,710$$

## SECTION II. THE AMERICAN PART OF THE KOSMOS-206 EXPERIMENT. POSTMORTEM STUDIES OF SPACE RADIATION ON BOARD THE KOSMOS-936 AES /59

E.V. Benton, R. Kassar, A. Frank, R.P. Henke, D.D. Peterson

### I. Introduction /60

Living organisms in space are subjected to the effect of a complex and unique environment which includes radiation. The latter presents a danger for living organisms which can break down the normal physiological processes and interfere with their natural operation. The general interest in the effect of the space environment has increased due to the expansion of studies of man in outer space and has resulted in the expansion of all possible studies on Earth and in space. These studies have brought us valuable information on the effect of space for man and other organisms. Part of these studies were begun on the initiative of the USSR in 1974 as joint Soviet-American experiments on biosatellites. The first joint experiment was conducted at the end of 1975 on Kosmos-782 AES. It was directed at studying the effect of weightlessness on different physiological functions of animals and plants and also on measurement of physical parameters of particles with large charges of energy, that is, GCR [galactic cosmic radiation] nuclei.

The joint Soviet-American experiment K-206 on dosimetry of space radiation on board the Kosmos-936 AES was mainly conducted to determine the physical parameters of different components of radiation in space. It included a comparison of results obtained by the American and Soviet scientists in order to clarify the unintelligible divergence of results obtained on the Kosmos-782 AES on the fluence of heavy charged particles. The experiment also included ground calibrated studies and a measurement of the sensitivity of different detectors. These studies were conducted on accelerators at Berkeley and Dubna.

The K-206 experiment consisted of three separate parts: 25% of the volume was occupied by the USA assembly placed at one end of the container, 20% by the Soviet assembly at the opposite end and 50% by the joint assembly in the middle part of the container. The detectors from the joint 50% section were divided in equal parts between the Soviet and American scientists. The joint 50% assembly was intended for determining the fluence of LET spectra and the charged spectrum of heavy nuclei. It contained two thick stacks of plates with nuclear emulsions on top and below and 12 thin dosimetric packets attached in pairs to the six faces of a foam plastic cube at the center part of the 50% joint assembly. The 25% American assembly was designed for determining the physical parameters of heavy nuclei, the fluence and spectrum of neutrons, the fluence of protons and the total dose of radiation. Figure 1 gives a diagram of the K-206 experiment. /61

In subsequent sections, we will present in detail results obtained using detectors from the American side in the 50% joint assembly and

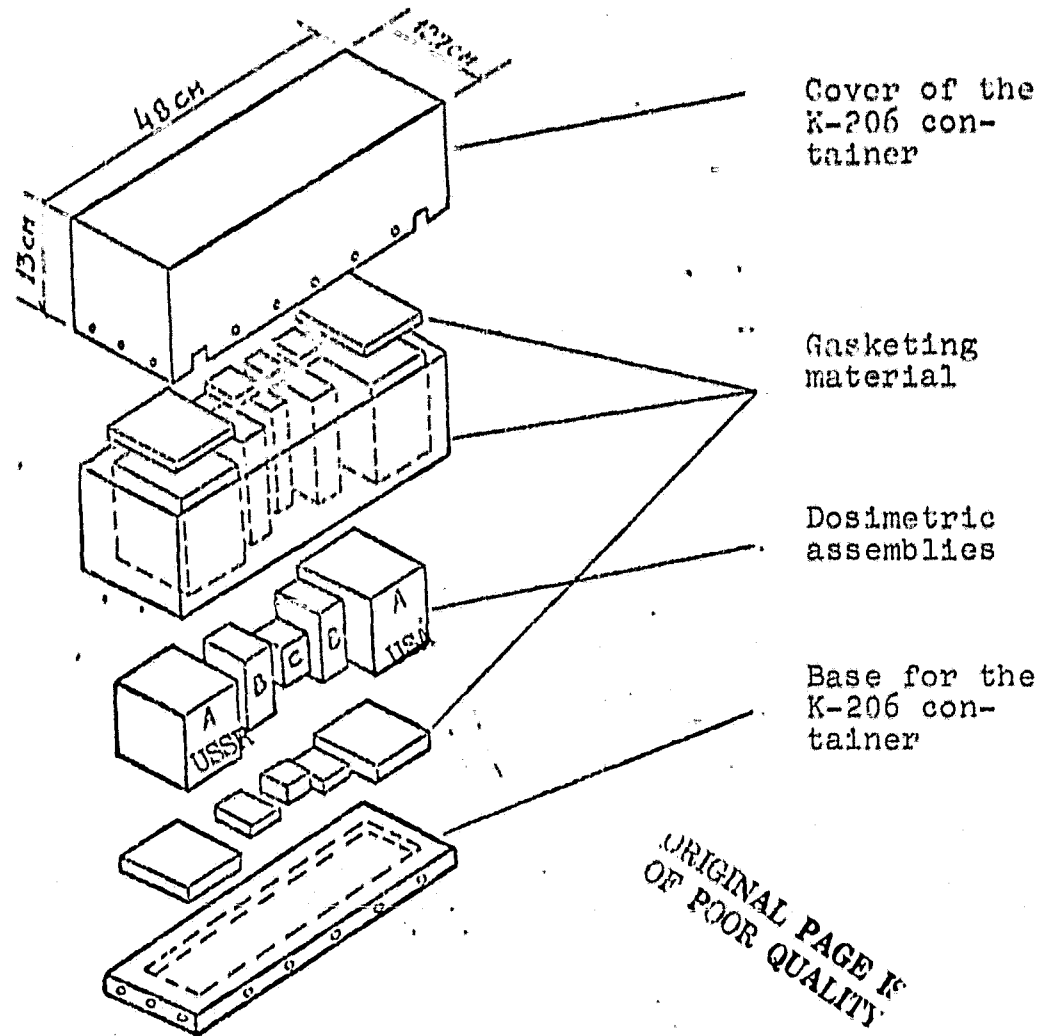


Figure 1. Diagrammatic image of the assembly of the K-206 experiment. Packing of the dosimetric experiment, showing the 25% American section (A) and the joint 50% section of the assembly of thick plates (B) and the orthogonal detectors (C).

in the 25% American assembly for the K-206 experiment for heavy nuclei of neutrons and protons on board the Kosmos-936 AES and also we will present analysis of the data obtained. /61

## 2. Heavy Nuclei -- Fluence, Integral LET Spectrum and Spatial Distribution.

During the last ten years, a research group at the University of San Francisco has conducted measurements of heavy nuclei on board spacecraft. The plastic tracking detectors which were put on board the Gemini-IV and VI spacecraft [1] recorded the tracks of densely ionizing particles. These measurements showed that the plastic detectors can be a simple and effective means for measuring integral fluences of

heavy nuclei within a spacecraft. Plastic films were particularly sensitive to these particles inasmuch as they did not record the more numerous, rapidly moving particles, for example, electrons and protons but recorded the tracks only of the relatively rare heavy nuclei of space radiation which exist in space. Recently, a summary was published of the work on heavy particles on the Apollo, Skylab and the SPS complex [3].

The aftereffects of the effect of heavy nuclei on a cosmonaut was considered in a report by the National Academy of Sciences of the USA with special recommendations for continuing and improving dosimetry of this type of radiation using plastic detectors. The interest in the effect of heavy nuclei has increased sharply since the cosmonauts on the Apollo-11 observed white flashes assumed to be caused by heavy nuclei.

The radiobiological effects of high energy heavy nuclei have recently begun to be studied in laboratories thanks to the possibility of irradiating objects on accelerated heavy ions with high energy, for example, on the Bevalac in Berkeley, California. Up until now, a complete concept has not been obtained of the effect of these particles on living organisms; the results of measurements of physical parameters of heavy nuclei in space will be an important part of studies in space.

In the following sections we will describe in detail our measurements of the physical parameters of heavy nuclei on board the Kosmos-936 AES.

## 2.1. Materials and Methods.

The fluence, the integral spectrum of LET and the spatial distribution of heavy particles were determined by analysis of the results of treating plastic tracking detectors placed in the 50% joint section of the K-206 experiment. The detector for heavy nuclei contained thin plates of cellulose nitrate (Kodak-Pathe, SA 80-15), polycarbonate (General Electric, Lexan) and nuclear emulsions. Each type of plate was put together in two films and hermetically sealed [rest of sentence missing the original text]. The area of plastic films amounted to  $4.5 \times 6 \text{ cm}^2$ . In all, 18 detectors were placed inside the K-206 flight container. 12 detectors in pairs were attached to each face of a plastic foam cube ( $7.7 \times 7.7 \times 7.7 \text{ cm}^3$ ) located at the center of the joint 50% section of the flight container. Six detectors were attached to each surface of the American 25% section of the container.

The flight plastic detectors were stored at  $5^\circ\text{C}$  in polyethylene bags.

A standard method was used for displaying the plastic detectors. Table 1 lists the etching details: composition of the etching agent, temperature and time for the procedure. In the first column are listed the designation of the samples. For example, 1 FB means flight (F), sample No. 1, layer (B). The four layers of plastic in the detector are designated with the letters A, B, C and D. The A and D layers are made of polycarbonate and the A layer is adjacent to the nuclear

TABLE 1

/65

## PARAMETERS OF PROCESSING THE AMERICAN PLASTIC DETECTORS

Sample	Plastic	Etching Agent	Time	$V_B$ , ( $\mu\text{m/hr}$ )
IFB - I2FB	CN*	a	10.0	$1.07 \pm 0.05$
IFC	CN	a	39.0	0.92
3FC - 6FC	CN	a	30.0	$1.01 \pm 0.02$
2FC, 7FC - I2FC	CN	a	29.0	1.19
IFA - 7FA, IIFA Lexan**		b	44.0	$0.15 \pm 0.02$
IFA - 7FA, IIFA*** Lexan		b	24.0	$0.55 \pm 0.01$

a) 2.5N NaOH, 40°C, solution is mixed.

b) 6.5N NaOH + 1 g/l polycarbonate monomer + 0.05% surface active substance (Dowfax 2A1), solution is mixed.

\* thickness 190 $\mu\text{m}$ , CN film.

\*\* thickness 190 $\mu\text{m}$ , Lexan film.

\*\*\* preliminary (before etching) treatment of samples.

emulsion. The B and C layers are made of cellulose nitrate. Orthogonal samples 1F-US-6F-US are in the joint 50% section of the flight block; 7F-US-12F-US -- in the American 25% section. /64

Inspection of the tracks of heavy nuclei in the etched plastic detectors was made with an optical microscope with a magnification of 200. The central part of each detector with dimensions 3 X 3 cm<sup>2</sup> was scanned. The scanning procedure of a given orthogonal detector consisted of attaching the C layer to the microscope stage and subsequent alignment and attachment of the B layer on top of the C layer. The C layer was etched until it was thinned by approximately 60% and in it many etched apertures penetrated it corresponding to the measured double cone or constricted cylinder in the B layer, the first measured layer. This method of scanning increases the effectiveness of search for small etched tracks which decreases the complexity and duration of the scanning procedure.

In the four plates of each orthogonal detector, before dismantling, two small adjustable apertures were drilled. the x and y coordinates of all tracks found during scanning are determined according to the ratio for the pierced aperture by means of mechanical nonius involving the guide screws x and y of the microscope stage. /66

Measurement of the parameters of the etched track was made with immersion lenses with a magnification of 1000 and with a precision of  $\pm 0.5 \mu\text{m}$ . The parameters measured included depth, projection and the small axis of depth of etching of the tracks, and also the depth and width of the narrowest part when the track was in the shape of a constricted cylinder. The etching rate for the entire mass of plastic was determined by measuring changes in thickness of the film. The etching rate of Kodak-Pathe cellulose nitrate depends greatly on the concentration of products of etching in the etching agent, 2.5 N NaOH at 40°C. The etching rate of the Pathe CN hardly depends on the concentration of etching products.

The etching rate for the track is calculated according to the parameter of the track measured using an analytical expression based on the geometry of the track and assuming that the etching rate of the track for the entire length traced is uniform.

For each type of plastic tracking detector there is an intrinsic ratio between the rate of etching of the track and the restricted losses of energy [2]. This relationship is the basis for evaluating the loss of energy restricted by the rate of etching of the track. Figure 2 shows preliminary calibration curves used for analysis of data obtained with the Kodak-Pathe plastics of cellulose nitrate and the Lexan polycarbonate (with sensitization to ultraviolet and without it). The graph in Figure 2 indicates the dependence of the etching rate of the track  $V_t$  on  $\text{LET}_{350}$ ; the index below indicates that when calculating a given value, [rest of sentence missing in the original text]. The curves in Figure 2 are constructed according to a method of least squares on the basis of calibration data obtained from ions of known energy and charged from the accelerator. /68

The condition for etching the track of particles is that the vertical component of the rate of etching of the track must be greater than the rate of etching of the mass of the plastic. From the curves in Figure 2 we find the minimum value of  $\text{LET}_{350}$  which depends on the type of plastic and on the development or preliminary processing before development. One also needs a determination of the critical value of the angle of immersion (measured from the surface of the film) for recording particles with a fixed value of  $\text{LET}_{350}$ . For obtaining an absolute value of the fluence, one uses corrected coefficients which depend on the angle of immersion and the value of  $\text{LET}_{350}$ . For example, the integral spectrum of  $\text{LET}_{350}$  was calculated by adding the product of each value of  $\text{LET}_{350}$  (appropriate to a given track) to the corrected coefficient for all tracks with a value of  $\text{LET}_{350}$  greater than the given value. The integral flux of particles for a given value of  $\text{LET}_{350}$  was calculated by dividing the total 217 At, where A and t are the area of the sample and the flight time.

The spatial distribution of incident heavy nuclei was determined according to the value of fluences of particles recorded by the six detectors attached to each face of a plastic foam cube in the central part of the joint 50% assembly in the experimental container. This mutually perpendicular placement of detectors made it possible to determine fluences in the direction of the three axes, xyz, in space.

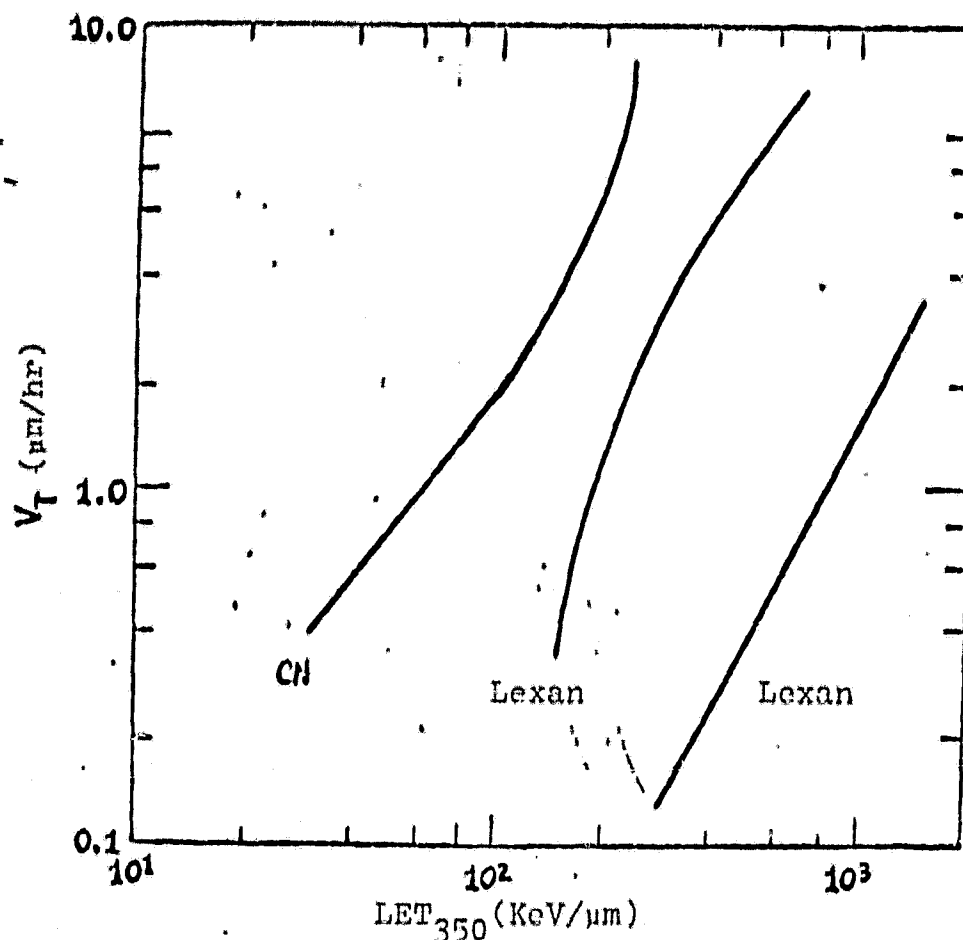


Figure 2. Calibrated relationships used for detectors made of Kodak-Pathé cellulose nitrate and Lexan polycarbonate.

## 2.2. Results

/68

The fluences observed and the fluxes of heavy nuclei recorded by the eight detectors of the joint 50% assembly and the American 25% are presented in Table 2. In the first column of this Table the detectors and their location are listed and in the second -- the number of tracks obtained for an area of 9 cm<sup>2</sup> of the detector. The numbers in the second column correspond to the number of heavy particles recorded on all four surfaces of two underlying layers of cellulose nitrate -- B and C. In the third and fourth columns, respectively, the fluences and fluxes are presented. The values of the fluxes are determined on the basis of duration of the flight of the Kosmos-936 AES -- 18.5 days.

/70

# DATA AT THE END\* TABLE 3: JOINT AND AMERICAN PLASTIC EXPOSURES

Detector Identification	Pressure	Fluence (Tracks/cm <sup>2</sup> )	Flux, (Tracks) cm <sup>2</sup> ·days
1FB-US/ joint section	561	40.1 ± 2.1	2.17 ± 0.11
2FB-US/ joint section	230	25.6 ± 1.7	1.53 ± 0.09
3FB-US/ joint section	319	55.4 ± 2.0	1.92 ± 0.11
4FB-US/ joint section	221	24.6 ± 1.7	1.53 ± 0.09
5FB-US/ joint section	279	51.0 ± 1.9	1.68 ± 0.10
6FB-US/ joint section	335	57.2 ± 2.0	2.01 ± 0.11
7FB-US/ American section	354	59.3 ± 2.1	2.13 ± 0.11
11FB-US/ American section	188	20.9 ± 1.6	1.13 ± 0.06

\*HZE particles with  $Z \geq 3$  and recorded runs  $\geq 180$   $\mu$ m.

Integral spectra are shown in Figure 2 [sic., 3]. The orthogonal /70 al detector 1F-US recorded the maximum fluences of heavy nuclei in six orthogonal detectors located in the joint 50% section.

## 2.3. Discussion

Flux of heavy nuclei. Table 3 compares the results obtained on the Kosmos-936, Kosmos-782 [5] and the Skylab [4] AES. The maximum, minimum and average values of flux presented in Table 3 were obtained from six orthogonal detectors from the joint 50% section of the container on the Kosmos-936 AES, the 12 detectors which were in the Kosmos-782 AES and the nine individual dosimeters of astronauts who flew on the SL-2, SL3 and SL4 Skylabs.

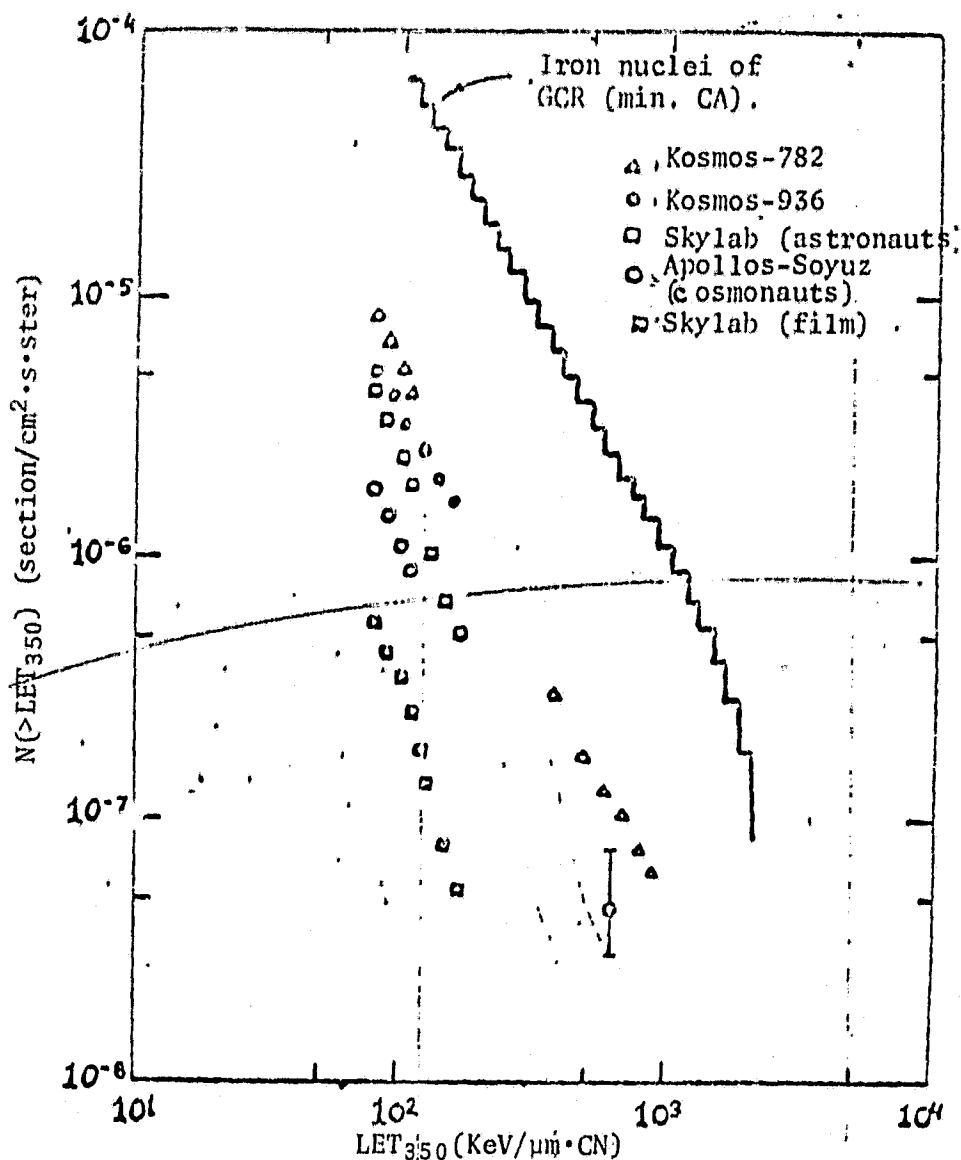


Figure 3. Integral spectra of LET for HZE particles measured with the plastic detectors during different space flights.

The average value of flux during flight on the Kosmos-936 AES was 2 to 3 times smaller than during flight on the Kosmos-782 AES. The consideration of factors which can affect the flux of heavy nuclei, for example, parameters of the orbit, distribution of protection of the spacecraft, solar modulations, the types of plastic detectors, indicates that the most probable causes for differences in fluxes during these flights involves differences in protection and type of detectors. The results of measurements during flight of the Skylab indicate the effects of the protection [4]. The flux of heavy nuclei inside the strongly protected storage area for films was ten times weaker than the flux recorded for the astronauts. The equivalent thicknesses enumerated of spherical protection of the

TABLE 3

/71

FLUXES OF HZE PARTICLES ON THE KOSMOS-936, KOSMOS-782 AND SKYLAB

Flight	Flux of Particles*		Particles cm <sup>2</sup> days
	Max.	Min.	Average
Kosmos-782	5.15	3.28	4.05 <sup>+</sup>
Kosmos-936	2.17	1.13	1.75 <sup>++</sup>
Skylab	3.75	1.9	2.71 <sup>+++</sup>

\*HZE particles with  $Z \geq 3$  and recorded run  $\geq 180$   $\mu$ m.

+Average for F1-F12 detectors.

++Average for orthogonal detectors from 1F-US to 6F-US in the joint 50% section.

+++Average from readings of individual dosimeters of the nine astronauts during flights on the SL-2, SL-3, and SL-4 Skylabs.

sleeping module for the astronauts and storage for the film amounted respectively to approximately 6 g/cm<sup>2</sup> and approximately 50 g/cm<sup>2</sup>. /72

At the present time, on the accelerator in Berkeley, the effect of the type of detector is being studied on the effectiveness of recording particles. The purpose of these studies is to determine the effectiveness of different types of plastics made of cellulose nitrate used in flights of the Kosmos-936 and Kosmos-782 AES.

The effect of solar modulation can be expressed as exceeding by 10% intensity of cosmic radiation during flight of the Kosmos-782 AES over that during the flight of the Kosmos-936 AES. The intensity of cosmic radiation was measured indirectly by ground neutron monitors which recorded continuously the rate of formation of secondary neutrons in the atmosphere. The neutron monitor installed at Mount Washington recorded only a 1% smaller rate of count for the Kosmos-936 AES (August 3-August 22, 1977) in comparison with the flight of the Kosmos-782 AES (November 25-December 15, 1975).

The parameters of the orbit (that is, the period, inclination, perigee and apogee) were essentially the same for the Kosmos-782 and Kosmos-936 AES. Therefore, these factors could not be the cause for differences in fluxes of particles. Also, the Vostok type satellite was used for each flight.

Integral spectrum of LET. The integral LET spectrum defined as the number of particles from the LET larger than the given is an important dosimetric parameter necessary for evaluating the potential biological danger for living organisms in space. For example, it is possible to use it for calculating the coefficient of the quality of radiation.

An example of the integral LET spectrum for heavy nuclei during flight of the Kosmos-936 is presented in Figure 3. The data were obtained from the 1F-US detector located in the joint 50% section of the K-206 container. For comparison, Figure 3 shows other spectra measured on the Kosmos-782 AES [4], on astronauts in the film storage unit on the Skylab [4] and astronauts on the Apollo-Soyuz (EPAS), complex [4]. Figure 4 also shows the calculated integral spectrum for model of space radiation during a solar minimum [4]. /74

The integral spectrum of heavy nuclei on board the Kosmos-936 AES dropped sharply with an increase in the value of  $LET_{350}$  as was observed in past flights. The maximum flux of heavy nuclei from the  $LET_{350} > 20 \text{ KeV/men}$  (that is,  $LET_m \geq 1.06 \text{ KeV/m tissue}$ ) amounted to  $5.1 \cdot 10^{-6} / \text{cm}^2 \cdot \text{s} \cdot \text{ster}$  for flight of the Kosmos-936 AES. This value lies between the flux on the Kosmos-782 AES ( $8.7 \cdot 10^{-6} / \text{cm}^2 \cdot \text{s} \cdot \text{ster}$ ) and the flux recorded in dosimeters on astronauts in the Skylab ( $4.5 \cdot 10^{-6} / \text{cm}^2 \cdot \text{s} \cdot \text{ster}$ ).

### Space Distribution.

The data obtained from six detectors in the joint 50% assembly indicated that the target found at the center of the plastic foam cube (to which the detectors were attached) had to obtain an approximately isotropic fluence of heavy nuclei.

The value of the fluence of heavy nuclei within limits of the statistical spread was uniform on top, below and to the sides of the plastic foam cube as indicated by the 1F-US, 3F-US, 5F-US and 6F-US detectors (see Table 2). The fluence in the 5F-US detector was somewhat lower than that permitted by statistical deviation. Attachment of the detectors to the cube was such that the 1F-US and 3F-US detectors looked from above and from below in relation to the container, the 2F-US and 4F-US -- to the Soviet and American sides, respectively, and the 5F-US and 6F-US -- to the lateral walls of the container.

The 2F-US and 4F-US detectors turned toward the ends of the container were protected by thick stacks of plates from the 50% joint section and also blocks of the 25% assemblies of the K-206 container. The equivalent thickness at approximately  $22 \text{ g}^2 / \text{cm}^2$  of aluminum protected the 2F-US and 4F-US detectors in the direction perpendicular to the surface of the detector. As measurement results showed, in the film storage unit on the Skylab [4], the flux of heavy nuclei beyond the protection approximately  $20 \text{ g/cm}^2 \text{ Al}$  is decreased by approximately two times. /75

As a result of the fact that the 2F-US and 4F-US detectors were protected by a thick stack of plates both in the joint 50% and in the end 25% sections, the fluence recorded in the detectors should be multiplied by approximately 2 in order to correct for the readings of the other four detectors. The "absolute" fluence of incident particles (that is, standardized for a uniform thickness of protection) must then be, approximately, uniform for each face of the cube.

## 1. Charge Spectrum of Heavy Metal.

The traditional approach to analysis of charges of particles is that the stacks of plastic tracking detectors are treated by etching them with hot solutions of alkali which gradually remove the material of the detector from its surface and preferably affected the trace of damage remaining from each densely ionizing particle. The rate of this etch effect was determined for the LET particles so that the final length of a conical track formed along the trajectory of the particle was the measurement of LET. Usually, in the etching process 5-20% of the initial thickness of the plastic was removed.

At inspection of the detector and measurement usually was conducted in two ways. 1) One of several layers was examined with fairly low magnification. Also several possibilities for scanning existed, for example, using the passage of sparks or a pair through the etched pierced aperture which would determine the position of the tracks. 2) The tracks found with low magnification were measured under high magnification and traced in layers not subjected to scanning. In the measurement process, the lengths of the cones were determined from two surfaces of the detector. The measurements made it possible to establish the trajectory of the particles and values of the LET along the trajectory. The process of treating the data consisted of two completely different phases. In the first phase, the parameters of each separate particle were determined on the basis of positions measured, the values of LET and, preferable, the x, y and z coordinates of the ends of the tracks which indicate the point at which the particles stop. Seven parameters were required in total complexity for determining the characteristics of the stopped particles. One set of parameters amounted to 3 coordinates of the point the particle stops, 2 spatial angles of the trajectory of the particle, the atomic number Z, the identified type of particle and the mass number A. In practice, usually it is impossible to fulfill separation of isotopes and therefore each Z number described the mass of the isotope represented in a small quantity and only Z of particles or the effective number was determined which assumes a continuously variable value and determines the varying value of Z and A. Therefore, the number of parameters for the particle was decreased to six. /76

In the second phase of the analysis of data, a statistical treatment of results was made. It consisted of studying the distribution of particles for one or several variables. Most often this charge spectrum shows distribution of the values of Z and one or several other parameters used for the characteristics of separate particles. The logical form in which the statistical results are obtained is the number of stopped particles with defined Z per unit of volume (or mass) and the solid angle  $\frac{dSZ}{d\Omega}$ . The integral  $\frac{dSZ}{d\Omega}$  for the solid angle  $4\pi$  steradians is the density of the ends of the tracks of the SZ charged spectrum. This distribution somewhat contradicted the charge-energy spectrum obtained usually from detectors which record high energy unstopped particles. The charge spectrum of stopped particles agrees with the reactions of plastic tracking detectors inasmuch as they record only particles relatively close to stopping. /77

if  $\frac{dS}{dR}$  is expressed in the form of a function from the position in space of a particle, then it is completely equivalent to the spectrum of energy expressed as the function of energy in the interval of all possible energies except the effects of nuclear fragmentation. Practically, for small  $z$ 's, the concept that  $\frac{dS}{dR}$  does not depend on position is allowable. With such an allowance, a connection was found for other values of interest to us and distributions, for example, of the LET spectrum.

The traditional methods for measurement of charges has been used frequently in different contexts. A large bibliography can be found in the book by Fleischer et al., [7]. Most often the values of  $Z$  are found by using the so-called relationship  $L-R$ . In this method, the length of the tracks measured  $L$  are applied on a graph as a function of the residual run of the  $R$  particle. The points obtained separately for each or all are jointly compared with theoretical curves for different possible values of  $Z$ . The approaches which Henke and Benton used (unpublished data) for results obtained on the Apollo-14 and 17 differ somewhat in that the comparison of measured and theoretical points was made by a completely analytical method using a method of least squares. With this approach, the measured tracks of particles are involved for which no stopping points have been defined.

The results presented in this section were obtained by a method which differs considerably from the traditional in that the measurement of the position of tracks and the rate of etching were carried out automatically using an analyzed image of the 720 Quantimet system. The detectors were etched for removing a large part of their initial thickness. This resulted in the formation of large apertures which penetrated through the layer of the plastic. The etching rate of the tracks was obtained by measuring the projection of areas of these apertures. This method was used earlier for measuring the Lexan detector assemblies located in the joint Apollo-Soyuz flight (EPAS) [Benton and Henke, nonpublished data].

### 3.1. Material and Method.

The charge spectra presented here were obtained for the joint dosimetric assembly (LF-US assembly). The assembly comprised layers of cellulose nitrate CN, Kodak-Pathe thickness 97  $\mu\text{m}$ , and layers of Lexan-GE polycarbonate with thickness 188  $\mu\text{m}$ . The sequence of the layers was the following: 10 CN layers, 200 Lexan layers, 65 CN layers, 200 Lexan layers and 10 CN layers. All of the layers of cellulose nitrate were etched with 2.5 N solution of NaOH at a temperature of 40°C. This solution was saturated with camphor for improving and stabilizing its etching capability. Etching for 112 hours decreased the thickness to 27  $\mu\text{m}$ , that is, to 28% of the initial thickness. After removing a large part of the thickness of layers, it was found that the majority of the particles recorded retained through holes in the layers of plastic. The input and output apertures of most of them reached approximately 4000  $\mu\text{m}^2$ .

The Lexan layers were etched in a 6.25 N solution of NaOH at 70°C. The solution contained 0.5% Bonax surfaktant and 1 g/l 4.4 -- isopropylidene diphenol for simulating the effects of the etching products of Lexan in the solution. Etching for 43.67 hr decreased the thickness of the layers to 36.6  $\mu\text{m}$ , that is, to 20% of the initial thickness.

9.75  $\text{cm}^2$  of each treated layer of cellulose nitrate was inspected and the results were processed semiautomatically with the Quantimet Image analyser. For each etched hole formed by particles intersecting the layer of plastic, the position and area of the aperture was determined.

The measured coordinates of the tracks were analyzed using an appropriate program on a computer in order to determine the trajectory of the particles which had three or more measured tracks on the /79 particle. The trajectories were used to construct linear regressions for the x and y coordinates measured as a function of Z. The parameters of the particle trajectories defined from the line of regression are shown as points of intersection of the trajectory with the surface  $Z=0$  ( $x_0$ ,  $y_0$ ) and angles of the azimuthal and immersion  $\alpha$  and  $\delta$  given by the equations (1):

$$\begin{aligned}\frac{dx}{dz} &= \cot \delta \cdot \cos \alpha \\ \frac{dy}{dz} &= \cot \delta \cdot \sin \alpha\end{aligned}\quad (1)$$

The parameters of the program for processing the tracks were selected so that they would be representative in it for all tracks from  $\delta > 30^\circ$ . The tracks with the smallest angles of immersion changed position so rapidly from layer to layer that including them could result in ambiguity of the results in view of the relatively high fluence of the tracks equal to 54 tracks/ $\text{cm}^2$ .

Then, the particles were identified and their stopping points were analyzed on a computer using a second program with a method of least squares.

Inasmuch as the tracks were measured automatically, the true points for stopping for each particle could not be determined. Therefore, measured values of the area of the track were used as a function of the position along each trajectory and for evaluating the atomic number Z of the particle and for determining its stopping place. This was done by minimizing the expression

$$m = \sum_{i=1}^n \left[ \frac{A_i - A}{\sigma A} \right]^2 \quad (2)$$

in relation to Z and at the stopping point of the particle. Here  $A_0$  -- is the value of the area calculated on a base of Z which measures the relationship between rate of etching of the track and LET of the

particle, the trajectory of the particle found according to the program for determining the tracks.  $A$  is the "measured" area of the particle as was described above and the weighted multiplier  $\frac{1}{\sigma_A}$  is obtained from deviations from the line presented. Inasmuch as one assumes [illegible /8 in the original text] value, this multiplier can be introduced as the sign totaled in equation (2). In this way,  $\sigma_A$  is determined by substitution of the minimum value  $m = 1^2 =$  number of degrees of freedom (number of measured tracks over particles  $-2$ ). Inasmuch as  $A$  is not a linear function of the  $Z$  particle and the stopping point in the equation (2), it is converted to a linear function by expansion in the Taylor series in corrections for  $Z$  and the stopping point. Then the solution for the correction to the initial approximation is obtained by means of normal linear substitution of least squares in two variables. The final solution is obtained by repeating the process until obtaining exemplary small values of corrections. Using the [word illegible] system one can obtain indeterminacy of  $Z$  and the stopping points and also corrections for these errors by normal methods of a linear method of least squares. During analysis of  $Z$ , the relationship to  $Z$  and  $A$  is converted to a relationship only of  $Z$  by substituting  $A$  in the approximate expression for the most widely distributed isotope,  $A = 1.776Z^{1.059}$ .

A statistical analysis of the calculated values of  $Z$  gives  $\frac{dp}{d\Omega}$  in the approximate expression  $\frac{\Delta N}{\Delta Z \Delta V \Delta \Omega}$  where  $\Delta N$  -- is the number of events occurring in the intervals  $\Delta Z$ ,  $\Delta V$  and  $\Delta \Omega$ . The intervals of the solid angles  $\Delta \Omega$  is selected so that the field of solid angles is divided from  $\delta = 30^\circ$  to  $\delta = 90^\circ$  and  $\delta = -30^\circ$  to  $\delta = -90^\circ$  for four equal parts. Equation (1) can satisfy only one positive value of  $\delta$ , however, negative values are used for designating a single direction of motion in the assembly (from on top to below) and the positive for designating the opposite direction (from below to above). The acting sections which are used for processing are listed in the section on results. For each segment  $\Delta \Omega$ , the exemplary volume in which the particle can stop,  $\Delta V$  (in equivalents of water inasmuch as the detector has a larger retarding capability than water) is defined using the criteria: 1) effectiveness must be /81 about 100% and 2) the stopping location must be fairly close to the segment measured in order to provide an exemplary small value of  $Z$ ,  $\Delta Z$ . The values  $\frac{dp}{d\Omega}$  are obtained by dividing the number of particles which adequately well satisfy the criteria described above into the appropriate values  $\Delta \Omega$  and  $\Delta V$ . The  $\Delta Z$  interval in the spectrum obtained is the variable and will be considered in the section on results.

### 3.2. Results

Figure 4 shows all of the measured positions of the tracks on 85 layers of cellulose nitrate. The points indicate each of 45.072 apertures. The area indicated amounts to  $4.14 \times 2.35 \text{ cm}^2$ . One can see many isolated points which form particles with the lower  $Z$  which were recorded only in a single layer and also many long small chains made up of points which form heavier particles recorded in the subsequent layers. Of these measured positions, 1834 particles with four or more tracks were obtained using the program for determining the

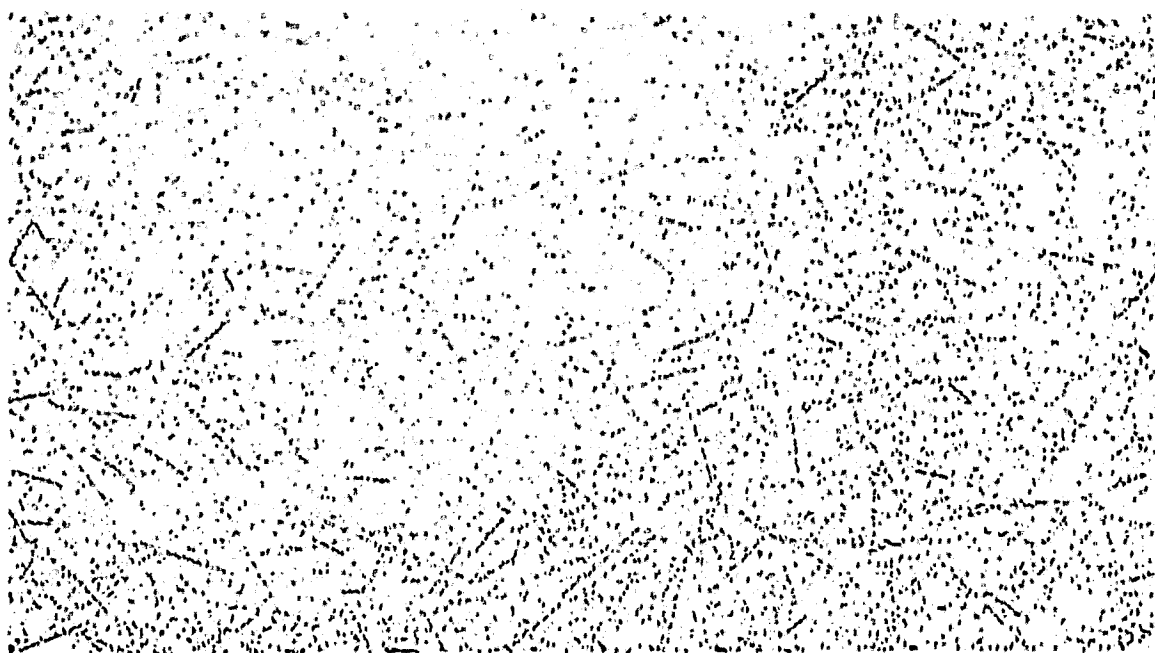


Figure 4. The position of all measured tracks in the layer of cellulose nitrate from the assembly for particles.

tracks. The criteria for selection in this program excluded most particles with  $\delta < 30^\circ$ . The precision of determining the position of the track was evaluated according to the mean square deviation of points from the trajectories constructed theoretically. The mean value found of this error amounted to 0.0023 cm or 23  $\mu$ m. From errors in determining the position, also error was found in measurement of the angle of immersion for the trajectory of each particle. It was proposed that approximately 50% of the trajectories were smaller than seven segments of tracks per particle and one can consider that the trajectory of the particles was defined completely correctly inasmuch as the median of  $\sigma_\delta = 0.92^\circ$ .

The measured charge spectrum is presented in Table 4 and in Figures 5 and 6. In Table 4 the angular dependence of the charge spectrum is given. The particles with all values of Z were combined in order to obtain adequate statistics for discovering angular distribution. Even with division of the solid angles found into ten equal segments of  $0.2\pi$  steradian, with adequate statistics, anisotropy of the flux of heavy nuclei was detected. From the initial 1834 particles with definite tracks, after selection according to all criteria, 625 remained in all.

Figure 5 shows a differential charge spectrum for Z considered as continuously variable. In this spectrum, each particle selected is presented in accordance with Gaussian distribution around the measured value of Z with an area  $\frac{1}{\Delta V \Delta \Omega}$  and with standard deviation 0.15 units of atomic number. The total of these Gaussian distributions form a spectrum. The integral form of the charge spectrum is presented in Figure 6.

ORIGINAL PAGE IS  
OF POOR QUALITY

ANGULAR RELATIONSHIP OF DENSITY OF STOPPED PARTICLES

Angle of Immersion (Interval of Degrees)	Angular Angle (Interval of Degrees)	Density of Stopped Particles (all selected particles) Particle/cm <sup>3</sup> . ster with $Z \geq 7$
-90 → -64,16	0 → 360	10.6 ± 1.3
-64,16 → -50	0 → 90	8.3 ± 1.2
	90 → 180	3.9 ± 0.8
	180 → 270	5.9 ± 1.0
	270 → 360	4.6 ± 0.9
3 → 64,16	0 → 90	14.1 ± 1.5
	90 → 180	9.6 ± 1.3
	180 → 270	8.8 ± 1.2
	270 → 360	11.8 ± 1.4
64,16 → 90	0 → 360	24.5 ± 2.0
		AVERAGE 10.2 ± 0.4

Although precision of determining certain values of  $Z$  is worse than  $\pm 1$ , an adequate number of particles have  $Z$  determined with adequate precision to permit definite peaks in the charge spectrum. The part of the charge spectrum which corresponds to the value  $Z < \sim 7$ , was not subject to determination with 100% effectiveness due to the insensitivity of detectors and requirements for tracks traced for four layers.

### 3.3. Discussion

The automatic method of obtaining points for constructing a charge spectrum has large advantages but has certain disadvantages in comparison with nonautomated methods of past years. The main advantage is the tremendous savings in labor and time and the possibilities of obtaining a huge volume of data. This advantage is reflected in the large number of particles included in analysis of the charge spectrum.

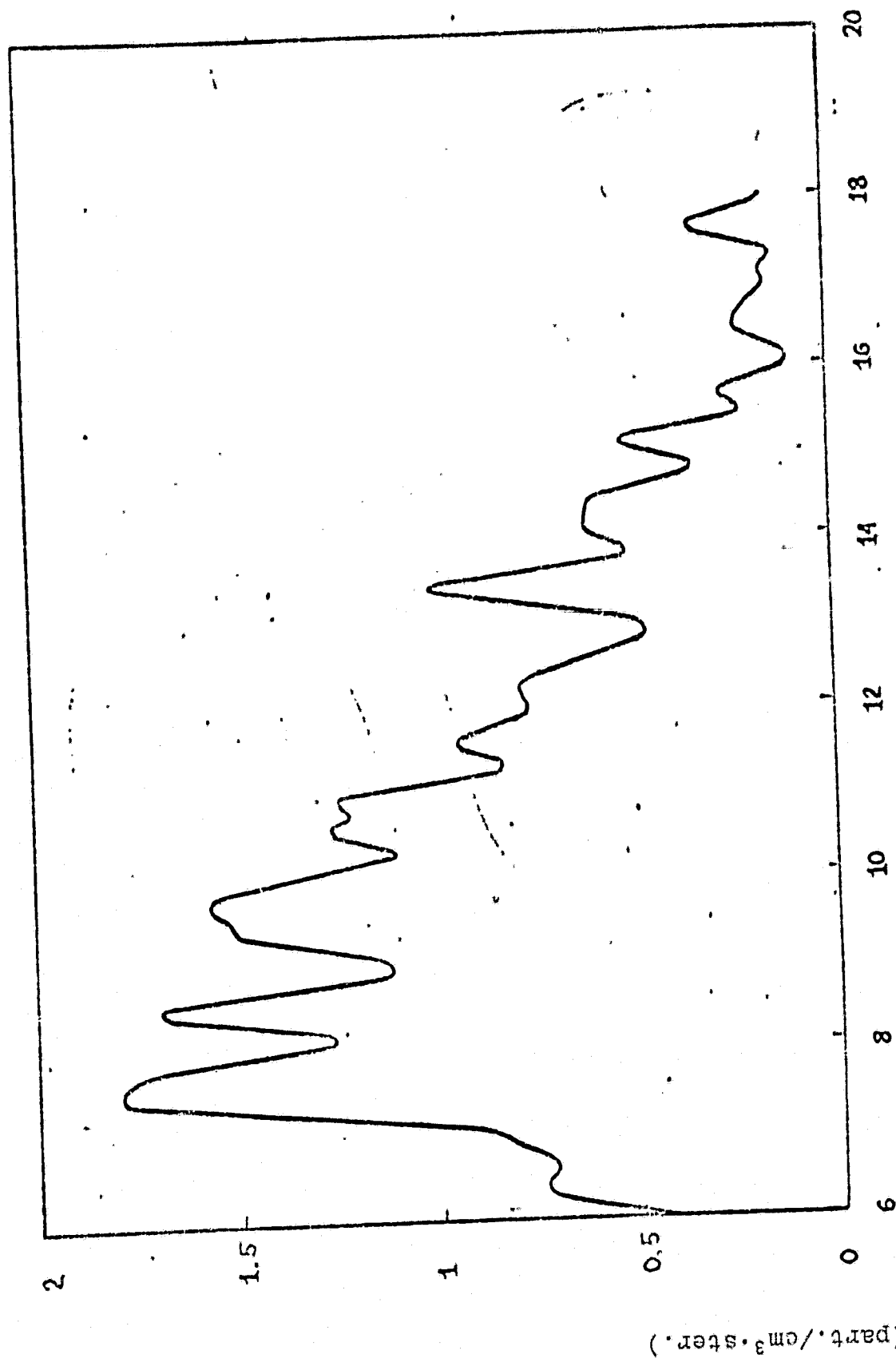


Figure 5. Differential  $\frac{d^2P}{dzde}$  of the charge spectrum

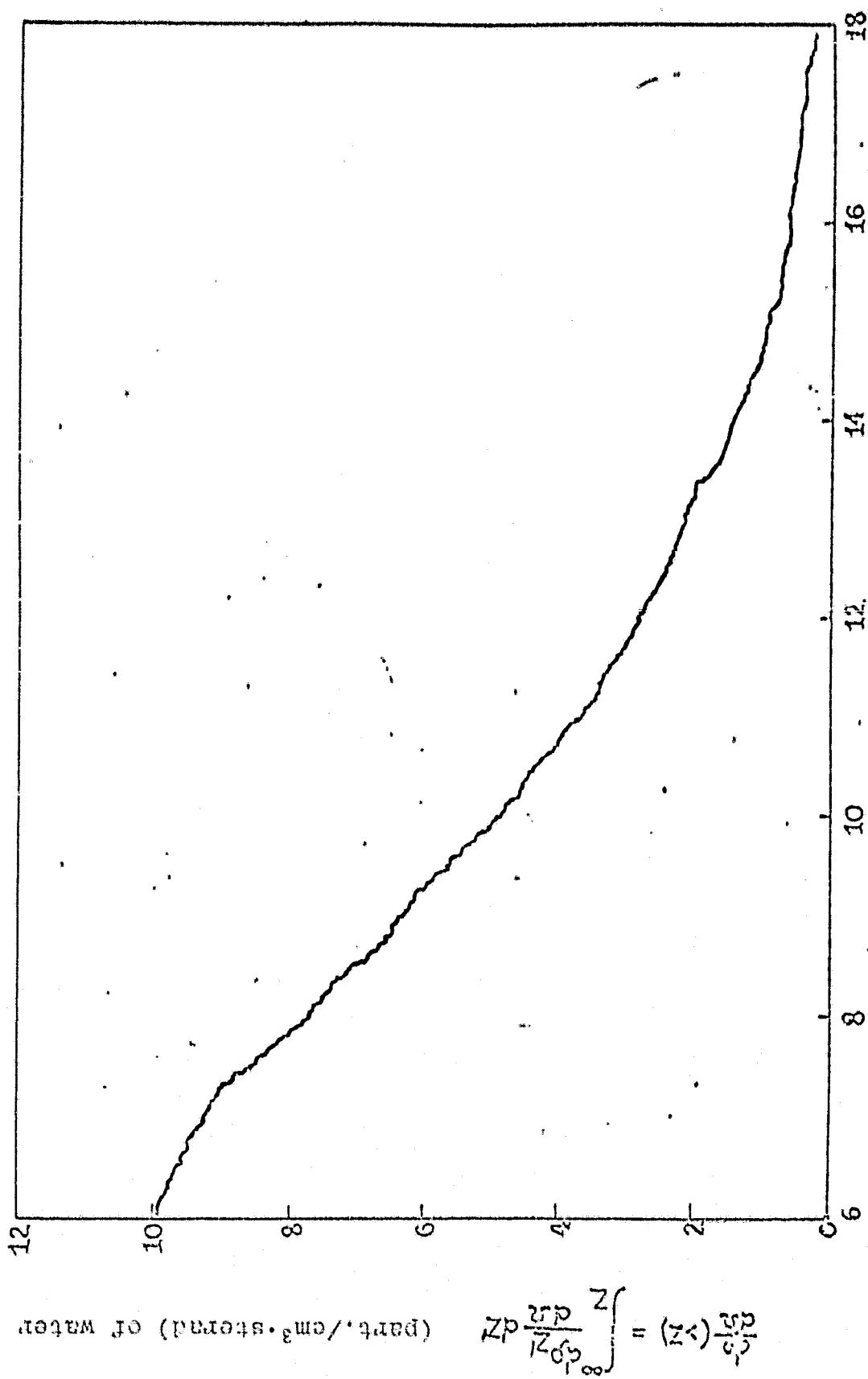


Figure 6. Integral charge spectrum

Most of the existing disadvantages of automated analysis of the assemblies come from lack of precision in the method in its present form. Many of these imprecisions can be overcome by improving the shape of the assemblies, methods of processing and measurement. The main limitations in the data obtained in this work involve the inadequately high resolution of  $Z$  and the obvious incapability of resolving particles with  $Z > \sim 18$ . Both these disadvantages apply to cellulose nitrate and can be avoided by reading the Lexan polycarbonate part of the assembly. The limitation in this experiment which can be avoided in the future is separation of high and low sensitive material into two separate sections in the total assembly of the detectors. Alternating layers of Lexan and cellulose nitrate can create a more uniform assembly which makes it possible to avoid large runs in trajectories of particles which intersect the low sensitivity layer with low LET. This significantly simplifies tracing the particles and causes less ambiguity. /87

#### 4. Neutrons.

During orbital flight in a spacecraft there are neutrons with a broad range of energies from thermal to hundreds of MeV. The spectrum of neutrons can be divided into three parts: thermal (less than 0.3 eV), resonance ( $0.3 \text{ eV} < E < 1 \text{ MeV}$ ) and high energy ( $> 1 \text{ MeV}$ ). This division involves reactions which are used for detecting them. One must make an assumption concerning the neutron spectra in these ranges of energy. The fluences of neutrons calculated on the basis of measurement of activity observed can vary significantly depending on the more "rigid" or the "softer" spectra in the incident flux. Sensitivity to a shift in the spectrum depends on the value of different cross sections of reaction in the given field of energy. In the field of high energies, the measurements are more complicated as a result of the fact that the nuclei of measured foils used for detecting neutrons in a reaction of the type  $(n, f)$  have a similar value to the cross section for the reaction  $(p, g)$ . The high fluences of protons with large energy which exist in the Earth orbits create fairly large background density of tracks in the mica detectors. /88  
Nondeterminancy of proton spectra and fluences create imprecision when calculating from the results of tracks from fragments of division into protons. The proton spectra were measured in previous orbital flights so that there was a good basis for approximation of the shape of the spectra on the Kosmos-936. Less is known of spectra of neutrons in space but one can assume that the neutrons are formed as a result of a division reaction of nuclei of atoms within the spacecraft and in the upper layers of atmosphere on charged particles with high energy, mainly, into protons. This makes it possible to draw certain thoughtful conclusions as to the shape of the spectra.

There were several types of detectors in the 25% American section for measurement of fluxes of neutrons within the spacecraft in the packing of the detectors. They all were passive integrating systems using thermoluminescent (TLD) for etched plastic detectors as the sensitive recording means. In the first case, the reaction  ${}^6\text{Li}(n, t){}^4\text{He}$  with highly effective cross section in the TLD for LiF. In the second case, radiator sheets alternating with cellulose nitrate

or with mica (muscovite) was required; one of these records the tracks of the He particles, the other the fragments of division.

#### 4.1. Material and Method.

Particle radiators were used in the assembly of detectors consisting of  ${}^6\text{LiF}$ , Ta-181, Bi-209, Th-323 and U-238. The first of these was used with cellulose nitrate for recording He-4 particles from their reaction  $\text{Li}(n,T){}^4\text{He}$ . The others were used with mica which records fragments of division formed during the reaction  $(n, f)$ . The other detectors of this type were designed for flight but were not obtained in time. Thickness of the sheets  ${}^6\text{LiF}$  with  $4.5 \text{ mg/cm}^2$ . The thickness of the divided films varied but they all were thicker than the runs of fragments of division formed. This provided more effective detectors, that is, the neutrons were hardly attenuated when passing through the sheets. The detectors made of  $\text{LiF}$  require correction for selfabsorption. /89

The TLD were of the  ${}^6\text{LiF}$  and  ${}^7\text{LiF}$  type; the dimensions of the plates were  $0.635 \times 0.635 \times 0.089 \text{ cm}^3$ . They consisted of pure pressed  $\text{LiF}$ . Discrimination on the basis of high quality alternating cross sections of  ${}^6\text{Li}$  for neutrons was accomplished by measuring the difference of the two materials. With this method, one can measure neutrons in the presence of relatively large absorbed doses from other particles.

The corresponding cross sections in the thermal range of energy are presented in Figure 7. When screening with a plate of cadmium 1 mm thick, the neutrons with energy less than 0.3 eV are absorbed in it, not reaching the detector. Therefore, if one uses pairs of detectors one of which is screened with cadmium and the other not, one can separate the readings measured into two fractions: those caused by neutrons of thermal energies and those higher than thermal. This method was used for measuring the contribution of thermal neutrons in the density of tracks measured by a combination of  ${}^6\text{LiF}$  detectors of cellulose nitrate. Half of these detectors were screened with cadmium during flight.

The gamma rays from the reaction  $\text{Cd}(\gamma)\text{Cd}$  separate this material as unsuitable for TLD screening from thermal neutrons. Besides this, protection was used made of  $0.3 \text{ g/cm}^2$   ${}^6\text{LiF}$ . This construction did not provide cutting off energy of the above listed detectors but effective cutting at approximately 1.5 eV was then achieved. On this basis, reactions were divided into neutrons with thermal and super-thermal energies. Half of each type of TLD found in flight was screened in this way.

The neutron detectors were set up in packets for flight. The packets had a thickness of 0.9 cm and consisted of two Lucite plates. A hole was cut in the thicker (0.6 cm) plate for placing the detectors. The USF assembly on the Kosmos-936 on two sides, from on top and below was bounded by packets of neutron detectors #1 and #2. /91

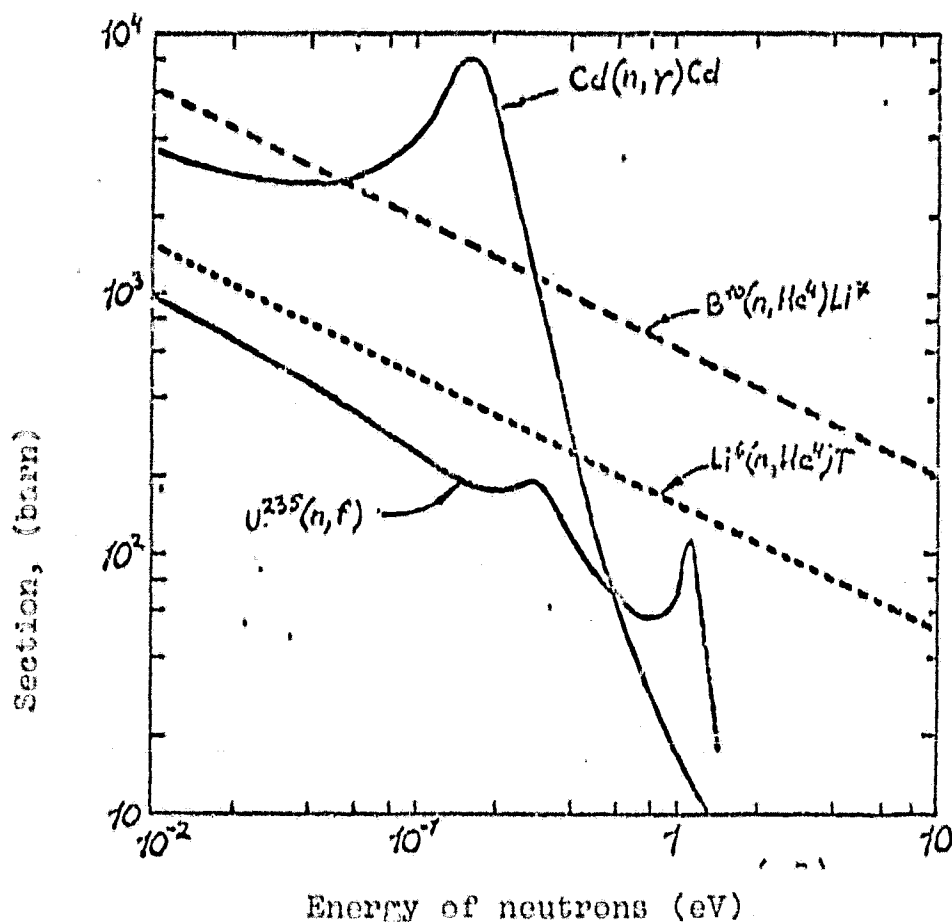


Figure 7. Certain sections of nuclear reactions in the field of thermal energies of neutrons used in the detectors.

Packet #1 was turned toward the outside and had a thinner protective covering for cosmic radiation than did packet #2. In packet #1 there were 3 Bi-209 and 4  $^6\text{LiF}$  radiators and also 9  $^6\text{LiF}$  TLD. Also background samples of mica and the plate of cellulose nitrate were used. In packet #2 there were 2 Bi-209, 2 Ta-182, 3 Th-232 and 3 U-238 radiator detectors and 12 TLD  $^6\text{LiF}$  and  $^7\text{LiF}$ . The Bi-209 radiators had dimensions 1.27 X 1.27 cm<sup>2</sup>. The Ta-181 and  $^6\text{LiF}$  radiators had dimensions of 1.8 cm in the diameter and the Th-232 and U-238 -- 1.27 cm in the diameter. The  $^6\text{LiF}$  material was placed on a sublayer and therefore only one cellulose nitrate detector was used for the active side of the sheet. The other sheets were not required in the sublayer and the mica detectors were placed on both sides. /91

Before assembly, the small scales were cleaned off the mica disks in order to create an undamaged surface and then they were etched for 16 hours in a 50% solution of hydrofluoric acid at room temperature. With such processing, the relict tracks of fragments of division on the surface of the mica were etched to significant dimensions. After processing the disks again they were etched for 50 minutes under the

same conditions. The tracks recorded during flight of the Kosmos-936 were etched to such a dimension that with a magnification of 350 times they could be distinguished from relicts by their much smaller dimensions. The exposed surfaces of the mica disks were examined as a whole to detect flight tracks. For each detector, the density of tracks was calculated and for the set of measurements of each type of detector the standard deviation was found. In certain measurements a correction was introduced for background tracks not caused by fresh products of division, by calculating the tracks on the surface of the mica which was not in contact with the fissioned foils during flight. Moreover, it was necessary to take into account the background from the U-238/mica detectors caused by spontaneous division of the U-238 nuclei. After dismantling the packet No. 2 it was again assembled with fresh sheets of mica. After 92 and 78 days the detectors were removed and etched for determining the contribution of spontaneous divisions in the entire density of the tracks. The rate of accumulation of tracks found amounted to  $1.710 \pm 0.85$  tracks/cm<sup>2</sup>·days. Cellulose nitrate used for the detectors was Kodak-Pathe Ca-80-15. During preparation for calculation the samples were cleaned with water at room temperature and then etched for 1 hr 40 min in a 6.25 N solution of NaOH at 40°C. The tracks of He-4 particles with low energy ( $\leq 2.05$  MeV) were viewed with a magnification of 430 times as short cylinders. For determining density of tracks, the detectors and flight control were checked. The TLD plates before measurement were washed with ethyl alcohol. After this, readings were taken on the standard instrument for TLD. In this instrument, the plates at a given rate were heated to a maximum temperature of 240°C. This caused a flare of light due to scintillation from radiation by the dosimetric plates. The quantity of light emitted is proportional to the absorbed dose of radiation obtained by the dosimetric plates. Emission of light is recorded by means of a photomultiplier and an integrating picoammeter. The dosimetric plates were each calibrated with gamma radiation of CS-187 from a source with known intensity. The integral output of current from the instrument was converted in this way to the equivalent of gamma irradiation. /92

A correction was also introduced into the TLD readings from the #2 packet for false background during postflight assembly again. The U-238 and Th-232 foils were radiated with gamma rays which make a small contribution to the power of the dose, the measured TLD in the period of assembling the packet. After taking the readings upon completion of flight, the foils were punctured and again assembled in a packet for measurement of this background. In the poorest case, the contribution of this background was smaller than 8% of the total measured absorbed dose. For most of the TLD it was smaller than 3%. Between the two packets with TLD, was the assembly with plastic detectors for HZE particles and 0.32 cm of brass so that the background dose in packet #1 was negligibly small. /93

#### 4.2. Results.

The results of counting the tracks and measurements with TLD are presented in Tables 5, 6 and 7. Measurements are presented in Table 5

TABLE 5

/94

DEENSITY OF TRACKS IN PLASTIC LIP/CELLULOSE NITRATE  
DETECTORS FROM DETECTOR PACKET #1

Detector #	Track/cm <sup>2</sup>	Protection
I	2172 $\pm$ 66	Absent
2	2268 $\pm$ 68	- " -
3	444 $\pm$ 22	1 mm Cd
4	431 $\pm$ 22	- " -
Background	167 $\pm$ 16	Absent
$E_h < 0,3$ eV	1788 $\pm$ 62	- " -
$E_h > 0,3$ eV	271 $\pm$ 31	- " -

TABLE 6

/95

## TLD READINGS

Packet of Detectors	Type of Detectors	Equivalent Gamma- Irradiation (mR)
#1	<sup>6</sup> LiF - Nonscreened	628 $\pm$ 8
	<sup>6</sup> LiF - Screened	569 $\pm$ 12
#2	<sup>6</sup> LiF - Nonscreened	485 $\pm$ 7
	<sup>6</sup> LiF - Screened	462 $\pm$ 6
	<sup>7</sup> LiF - Nonscreened	439 $\pm$ 10
	<sup>7</sup> LiF - Screened	418 $\pm$ 4

TABLE 7

/96

## RESULTS OF COUNTING TRACKS IN DETECTORS WITH FISSIONABLE/FOIL MICA

Packet of Detectors	Radiator	Recording of Tracks	Tracks cm <sup>2</sup>
1	2	3	4
# 1	Bi-209	Top	5.3 ± 2.3
		Bottom	—
	Bi-209	Top	7.2 ± 2.6
		Bottom	9.5 ± 2.3
	Bi-209	Top	5.9 ± 2.4
		Bottom	11.7 ± 3.1
	Background		0,8 (2tracks)
	Bi-209	Top	11.3 ± 3.0
		Bottom	6.0 ± 2.4
	Bi-209	Top	10.6 ± 3.0
# 2		Bottom	12.2 ± 3.2
	Ta-181	Top	0,4 (1Track)
		Bottom	0,4 (1Track)
	Ta-181	Top	0,8 (2Tracks)
		Bottom	0,4 (1Track)
	Th-232	Top	62.9 ± 8.1
		Bottom	60.2 ± 7.6
	-Th-232	Top	55.4 ± 7.4
		Bottom	79.7 ± 8.9
	~Th-232	Top	56.7 ± 7.4
		Bottom	71.6 ± 8.3
	~U-238	Top	221 ± 14
		Bottom	251 ± 15
	U-238	Top	271 ± 16
		Bottom	243 ± 15

ORIGINAL PAGE IS  
OF POOR QUALITY

		3	4
$^{238}\text{U}$		Top	$256 \pm 15$
		Bottom	$238 \pm 15$
Backgr and			0
Reassembly	Background of		$176 \pm 12$
$^{238}\text{U} - 238$	Spontaneous Division		$165 \pm 12$
All	Bi-209		$8,9 \pm 2,6$
All	Ta-181		Don't
All	Th-232		$64,4 \pm 8,6$
All	$^{238}\text{U}$		$77 \pm 24$

from plastic detectors made of cellulose nitrate for tracks per  $\text{cm}^2$ . 193  
 The errors involved in them are standard deviations calculated on the basis of statistical counts. The TLD readings are shown in Table 6. All of the errors are calculated on the basis of the spread of readings for certain plates. Table 7 shows the results of measurements from detectors on a base of fissionable foil. Here, also standard deviations are given on the basis of a statistical computation. The computation of errors for the U-238 measurement was many times higher due to the high background of spontaneous division. Due to the requirements of [illegible] it was necessary that the detector packets should be assembled for 87 days so that the tracks caused by spontaneous division accumulated in a significant quantity. The fluences of neutrons were calculated on the basis of measurements described and the appropriate reactions of the detectors.

#### Thermal Neutrons

According to the density of tracks measured with the  $^6\text{LiF}$ /cellulose nitrate detectors which are shown in Table 5, one can see that the component of thermal neutrons was  $1783 \pm 62$  tracks/ $\text{cm}^2$  which equals 80% of the total density of the tracks. Inasmuch as the thickness of the films of  $^6\text{LiF}$  was  $4.5 \text{ mg}/\text{cm}^2$ , which is more than three times greater

from the sum of the He-4 particles with energy 20.5 MeV, the high sensitivity of the detectors to thermal neutrons incident at a solid angle  $4\pi$ , belonged to the cellulose nitrate plastic. For thermal neutrons incident from the opposite side, as a result of selfscreening in  $^6\text{LiF}$ , the sensitivity was decreased. Calculation of selfscreening gives a coefficient of decrease of density of thermal neutrons equal to 0.74. For calculating the full fluence of neutrons for flight, it is necessary to assume that their incidence is isotropic. A fully corrected coefficient for  $4\pi$  of selfscreening which is necessary was therefore used for evaluating density of tracks and amounted to 1.43. The reaction of a similar detector with a thick layer of  $^6\text{LiF}$  for a solid angle  $4\pi$  according to measurement equals  $5.6 \times 10^{-3}$  tracks/thermal neutron [16]. On the basis of these coefficients, the calculated fluence of the thermal neutrons amounts to  $3.64 \cdot 10^5$  thermal neutrons/cm<sup>2</sup>. /98

The fluence of thermal neutrons can be found according to measurements from TLD. In Table 6 the equivalent dose caused by neutrons with energy 1.5 V showed the difference between readings of screened and nonscreened TLD  $^6\text{LiF}$ . It is apparent that they are equal, respectively, to  $59 \pm 20$  and  $23 \pm 13$  of equalivents per packets #1 and #2. Large errors are due to calculation of large numbers. In measurements with TLD, absorbed doses from charged particles are dominant. It is impossible to consider that these two figures differed widely and therefore an averaged value was used of 41 MR equivalent. The coefficient of transition from the fluence of thermal neutrons to gamma irradiation was reported earlier for the  $^6\text{LiF}$  plates [17]. It was found that  $10^{10}$ /cm<sup>2</sup> thermal neutrons give a thermoluminescent output equivalent to  $900 \pm R$  of gamma radiation of Cs-137. The fluences of thermal neutrons were calculated using this coefficient. A value of  $4.56 \cdot 10^5$ /cm<sup>2</sup> of thermal neutrons was found. This was 25% higher than the value found from  $^6\text{LiF}$ /cellulose nitrates by the plastic detectors. Probably the reason is covered in measurement error of this component /99 with the TLD. The value and higher cutoff of energy from 1.5 eV to 0.3 eV can occur.

Errors involving these two methods are due to the statistical spread of readings from the TLD instrument, absolute calibration, the transition coefficients for neutrons, unknown shape of the spectrum and the degree of isotropicity of the neutrons. It is doubtful that the low energy neutrons are well thermolyzed. During ruggedization of the spectrum, the fluences of thermal neutrons increase. If the neutrons are not isotropic, effectiveness can be significantly varied. It is difficult to evaluate subsequent nondeterminancy but the method of obtaining the neutrons, reactions of division in the spacecraft and in Earth's atmosphere must not relate to sharp deviations from  $4\pi$  to  $2\pi$  in geometry. Skillful evaluation of error gives  $\pm 20\%$  for plastic  $^6\text{LiF}$ /cellulose nitrate detectors and  $-50$  to  $+100\%$  for TLD.

Resonance neutrons. Resonance neutrons (0.3 eV-1 MeV) were measured by these detectors as were the thermal. The section of reaction  $^6\text{Li}(nT)\text{He-4}$  [?] is decreased with an increase in energy and therefore the contribution of neutrons with energies greater than 1 MeV is small. That is, measurements from detectors screened from thermal neutrons are caused mainly by resonance neutrons. The reactions of detectors

varies strongly in a broad range of neutrons of energies presented. The reactions of  ${}^6\text{Li}(n, \alpha){}^3\text{He}$  has a cross section of 950 barns for thermal neutrons and follows the relationship

$$\sigma = \frac{150.2}{E_n^{1/2}}$$

in an energy range of neutrons lower than 1 KeV. For an energy of 1 MeV, the section drops to 0.3 barns. In order to obtain a fluence on the basis of measurement of density of tracks it is necessary to make an assumption as to the shape of the neutron spectrum. A "soft" spectrum gives a smaller value of fluence than a "rigid" spectrum. The spectrum proportional to  $1/E_n$  can give a thoughtful estimate in this /100 field inasmuch as this approximately corresponds to the shape of the proposed spectrum for neutrons with average energies. One should take into account also an increase in energy in runs of particles of He-4 which forms during reaction of  ${}^6\text{Li}(n, \alpha){}^3\text{He}$  in this range of its energy. This results in an increase in effectiveness of the detector in calculating the reaction. In the case of thermal neutrons, the He-4 particles carry 2.05 MeV. With energy of the neutrons 1 MeV they carry 2.48 MeV. This approximately amounts to an increase in the run of particles by 22% in the LiF radiator and an increase in effectiveness of the count of tracks by approximately 30%. A corrected coefficient  $(1 \times 0.3 \times 10^{-6} E_n)^{-1}$  was used for the effectiveness of plastic  ${}^6\text{LiF}$ /cellulose nitrate detectors and  $(1 + 0.21 \times E^{-6})^{-1}$  for calculation of effectiveness of TLD.

For the  ${}^6\text{LiF}$ /cellulose nitrate detectors, the reaction in the function from energy of neutrons has the form:

$$R(E_n) = R_{Th} (1 + 0.3 \times 10^{-6} E_n)^{-1} \left( \frac{\sigma_{En}}{\sigma_{Th}} \right), \text{ where}$$

$R_{Th}$  -- is the reaction of thermoneutrons and  $\sigma_{En}$  and  $\sigma_{Th}$  -- the sections of interaction of neutrons with  ${}^6\text{Li}$ . For simplification of calculations, the section of reaction  ${}^6\text{Li}(n, \alpha){}^3\text{He}$  was approximated by the expression

$$\sigma_{En} = 0.25 + \frac{150}{E_n^{1/2}}$$

then the relationship becomes

$$\frac{\sigma_{En}}{\sigma_{Th}} = \frac{0.25 \times 10^{-4}}{0.158} + \frac{0.158}{E_n^{1/2}}, \text{ but}$$

the reaction of the detectors to resonance neutrons becomes

$$R_{Re} = R_{Th} \frac{\int_{0.3}^{100} \left( \frac{0.25 \times 10^{-4} + 0.158}{E^{1/2}} \right) (1 + 0.3 \cdot 10^{-6} E)^{-1} E^{-1} dE}{\int_{0.3}^{100} E^{-1} dE}$$

Numerical integration of this expression gives us  $R_{Re} = 2.86 \cdot 10^{-4}$  neutrons/cm<sup>2</sup>. It is apparent from Table 5 that above the cutoff, the maximum was measured at  $271 \pm 31$  tracks/cm<sup>2</sup>. This is converted into neutron fluence of  $9.5 \cdot 10^5$ /cm<sup>2</sup> in the field of resonance energies.

/101

Calculation of resonance neutrons on a basis of measurements with TLD involves larger errors than in the preceding case. One should use the difference of two large numbers as when calculating for thermal neutrons. Besides, the characteristics of cutoff of energy of neutrons by the <sup>6</sup>LiF screen with thickness 0.3 g/cm<sup>2</sup> results in large error in determining the reaction. For finding reactions of detectors in the 1/E spectrum of resonance neutrons, a numerical integration was made similar to that described above. For neutrons with energies between 1.5 eV and 1 MeV, a calibration coefficient was found equal to  $5.8 \cdot 10^8$  neutrons/cm<sup>2</sup> -- the R equivalent. In Table 6, the difference between the screened TLD <sup>7</sup>LiF and the screened TLD <sup>6</sup>LiF is the equivalent of a dose caused by these neutrons. In packet #2 this equals  $44 \pm 10$  mR equivalents. This gives a fluence of  $2.5 \cdot 10^7$  neutron/layer. This value exceeds that measured by the plastic detectors made of cellulose nitrate by 26 times. Measurements with the TLD must be considered the main source of error in spite of the better agreement of measurements of the separate plates as is apparent from the low statistical fluctuations. When comparing measurements from the TLD it is apparent that the difference between the nonscreened <sup>6</sup>LiF and <sup>7</sup>LiF detectors is  $47 \pm 17$  mR equivalents. This must be the measurement of full fluence of neutrons according to the <sup>6</sup>Li(n,T)He-4 reaction, however, it is almost the same as the measurement for the resonance neutrons. One can suspect that here there is a system error. Different types of TLD plates were placed in a not precisely uniform geometry in relation to the total dosimetric assembly. The differences between measurements in packets #1 and #2, and also a certain increase in the TLD readings in the front section of packet #2 indicate that considerable attenuation of fluences of incident charged particles occurs in the dosimetric assembly itself. One can assume that varying attenuation tested by different types of TLD creates a fluctuation which is almost the same size as the small difference corresponding to interaction of resonance neutrons.

/102

Errors in measurement with the plastic <sup>6</sup>LiF/cellulose nitrate dosimeters are considerably smaller. Most of the error is due to assumptions as to the shape of the spectrum of neutrons and the statistical spread in the counts of the tracks. The error limits in these measurements are estimated from -30% to +50%.

High energy neutrons. The fluences of high energy neutrons were determined by measurements with detectors from fissionable foils in combination with mica. The appropriate cross sections for Ta-181, Bi-209, Th-232 and U-238 are presented in drawings 8 and 9. In the former, the cross sections are given for reactions of the neutrons and protons with Th-232 and U-238 with energies less than 40 MeV. For Th-232, the section of reaction with both types of particles was compared with energies higher than 32 MeV but for U-238, the section of

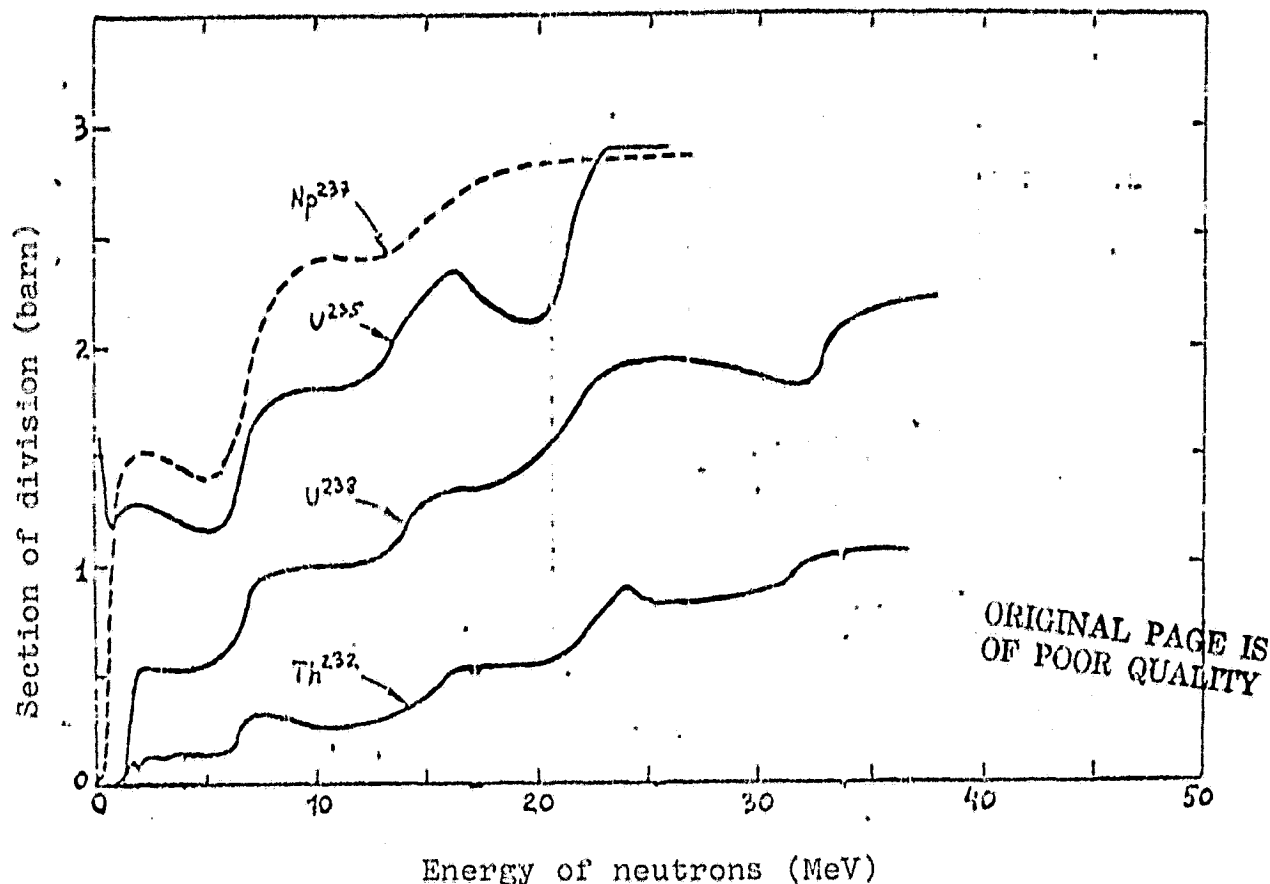


Figure 8. Cross section of the reactions (n,f) and (p, f) for Th-232 and U-238 in a field of energy of neutrons less than 40 MeV.

neutrons is considerably higher. The cross section for protons with energies between  $10^1$  and  $10^4$  MeV is presented in Table 9 for four radiator isotopes. On both drawings, the cross sections are taken from published data [11, 12, 20, 21, 22]. Certain gaps in the data are filled by interpolation. Cross sections for protons and neutrons are similar with an increase in energy of nucleons at least in that the effective charge of the proton becomes relatively less significant. Somewhere higher than 100 MeV, the curves of the cross sections become approximately uniform. For Bi-209 and Ta-181, the cross sections of reaction (n, f) and (p, f) are assumed to be identical. /102

The sensitivity of thick fissionable foils in measurement is equal to  $1.16 \cdot 10^{-5}$  tracks/neutron-barn [14]. Therefore, sensitivity to the spectrum of nucleons depends on the effective cross section of the detector for the spectrum which is given by the expression. /105

$$G_e = \int_0^{\infty} \sigma(E) N(E) dE, \text{ where}$$

$\sigma(E)$  -- the spectrum dependent on the energy of the section  $N(E)$  -- is the normalized spectrum of nucleons. The precise shape of the spectra of protons and neutrons on the Kosmos-936 is unknown. However,

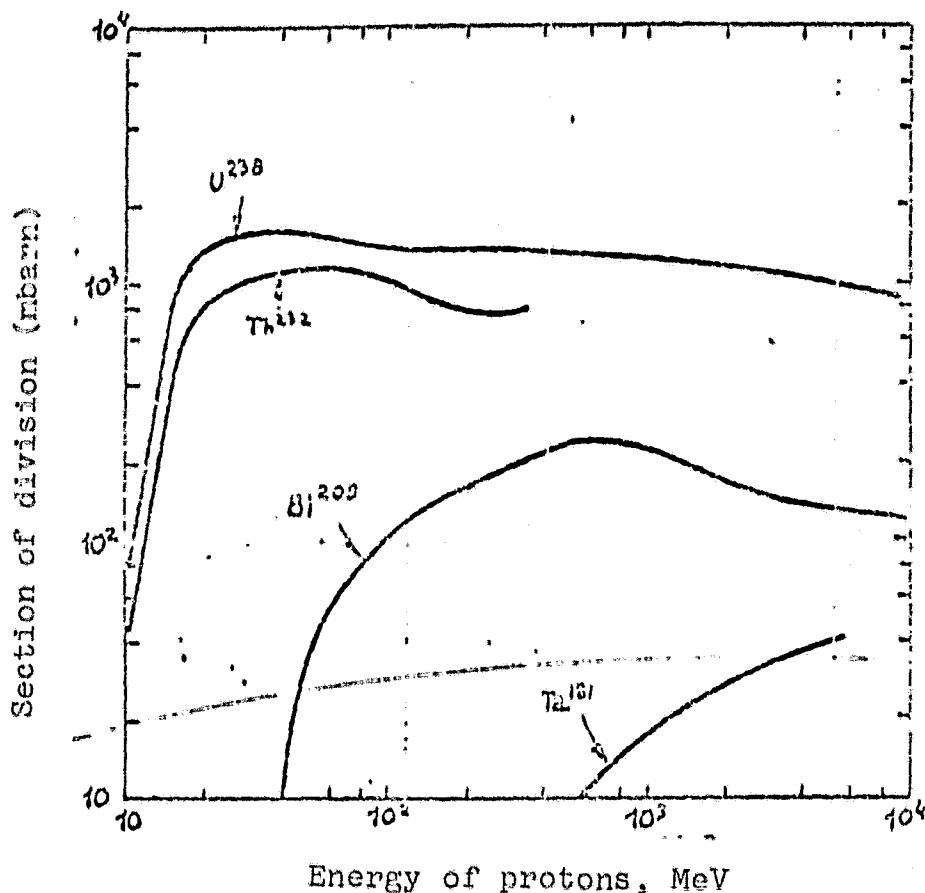


Figure 9. Cross section of reactions ( $p, f$ ) for Ta-181, Bi-209, Th-232 and U-238 in the field of energy from 10 to  $10^4$  MeV.

the proton spectra were measured in another orbital flight using nuclear emulsions. A typical example can be measurements on the Biosatellite III described in the references [8]. A numerical differential spectrum of neutrons was used as the representative spectrum of neutrons; it was created in an atmosphere of cosmic radiation [13]. The spectra for a number of atmospheric pressures were calculated at an altitude from 0 to 700 g/cm<sup>2</sup>. A case of 0 g/cm<sup>2</sup> which gives the most rigid spectrum was used. This calculation must give the best approximation for conditions on board the spacecraft. The methods of forming the neutrons are the same in both cases. The relative spectra of protons and neutrons are constructed in Figure 10. /105

For determining the effectiveness of detectors with Bi-209, Th-232, U-238, for the spectra of neutrons presented above with energies greater than 1 MeV, a numerical integration was made. For the detectors with Ta-181 this was not done. The density of tracks on these detectors was at a background level or about 0.5 tracks/cm<sup>2</sup>. The cross section of Ta-181 can be represented as being approximately constant equal to 30 mb with energies exceeding the threshold of activation of the nucleon 1000 MeV. Therefore, the sensitivity of the detector equals  $3.5 \cdot 10^{-7}$  tracks/nucleon. The background was equivalent to  $1.5 \cdot 10^6$

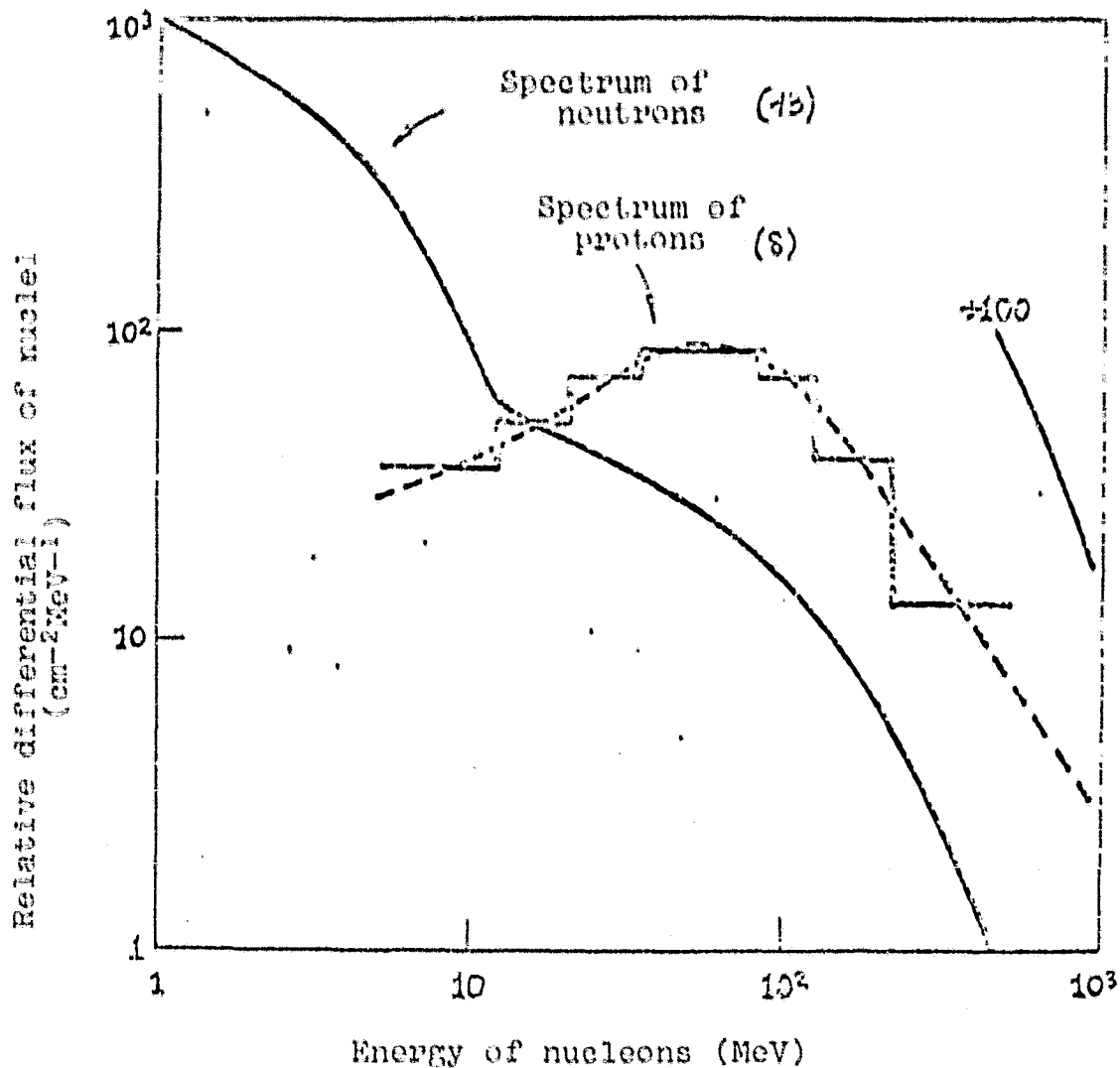


Figure 10. Representative relative spectra of neutrons and protons for satellites in near-Earth orbit.

$\frac{\text{nucleon}}{\text{cm}^2}$  with energy greater than 1 GeV. On the Kosmos-936, the flu- 2107  
ences in this energy field were considerably lower.

Calculation of the effectiveness for the proton spectrum was also made for the three most sensitive detectors. The effective threshold was placed at 17 MeV for detectors with Th-232 and U-238, and the spectrum of protons below this energy was cut off. The results of calculations are presented in Table 8. An attempt was made to determine the fluences of protons and neutrons primarily by calculating density of tracks expected with different percentages of their total number explained by neutrons and then by comparing the numerical values with the experimental densities of the tracks for obtaining the "best" approximation. The results are presented in Table 9. The number of detectors was much smaller and the error much larger so that this approach was useful. The errors corresponding to the experimental values

TABLE 8

/108

COEFFICIENTS OF EFFECTIVENESS FOR FISSIONABLE FOILS OF Th-232 AND U-238  
IN RELATION TO THE SPECTRA OF NEUTRONS SELECTED ( $E_n > 1$  MeV AND PROTONS  
( $E_p > 17$  MeV) -- TRACKS/NUCLEONS<sup>n</sup>

Foil	Spectrum of Neutrons	Spectrum of Protons
B1-209	$6.95 \times 10^{-7}$	$1.56 \times 10^{-6}$
Th-232	$7.24 \times 10^{-6}$	$1.04 \times 10^{-5}$
U-238	$1.50 \times 10^{-5}$	$1.57 \times 10^{-5}$

TABLE 9

/109

CALCULATION OF DENSITIES OF TRACKS IN FISSIONABLE FOILS FOR DIFFERENT  
CONTRIBUTIONS (%) TRACKS CAUSED BY NEUTRONS

Detector	0%	10%	20%	30%	40%	50%	100%	Experim- mental Results
B1-209	8.8	8.5	8.3	8.0	7.7	7.5	6.2	$8.9 \pm 2.6$
Th-232	57.9	58.6	59.3	59.9	60.5	61.2	64.5	$64.4 \pm 0.5$
U-238	87.4	92.0	96.7	101.3	105.6	110.5	133.7	$77 \pm 15$

involved statistical computation. Also large errors exist caused by assumptions made for calculating effectiveness. The best approximation is obtained in a case where the composition of nucleons is close to 100% of the protons but this is only an idea. /107

For clever calculation of the fluence of neutrons it was necessary to determine the relative content of protons and neutrons in them by some different method. There are reports [6] on certain measurements of fluence of protons and neutrons on the Skylab. These measurements were made simultaneously by an activation method during orbital flight in conditions similar to that on Kosmos-936. Flows were measured with two and three protons/cm<sup>2</sup>s with energy 30-100 MeV and 0.96 protons/cm<sup>2</sup>s with energy 3-15 MeV. With the shape of the spectra assumed for nucleons in this calculation, these values are converted in the flux to 7.85 protons/cm<sup>2</sup>s with energy greater than 17 MeV and 3.94 neutrons/cm<sup>2</sup>s with energies greater than 1 MeV. Starting from this relationship of nucleons, it was found that a 24% weighed density of tracks was due to neutrons. This gives us a fluence of neutrons with energy greater than 1 MeV on Kosmos-936 equal to  $2.1 \cdot 10^6$  neutrons/cm<sup>2</sup>. The corresponding fluence of protons with energy greater than 17 MeV /110

approx.  $5 \times 10^6$  per cm<sup>2</sup>. The reliability of assumptions made when error is small. However, probably they do not exceed an order of magnitude.

4. Full Absorption of a Dose. Besides measurement of neutrons, the TLD were used for measurement of full absorption of a dose caused by charged particles and gamma radiation. The unscreened detectors with <sup>7</sup>LiF make it possible to measure this value with a relatively small error. The large part of the dose during orbital near-Earth flight is due to protons. The thermoluminescent reaction to protons of <sup>7</sup>LiF in comparison with gamma radiation Co-60 was measured by the [illegible] [9]. These data are presented in Figure 11. These measurements presented in

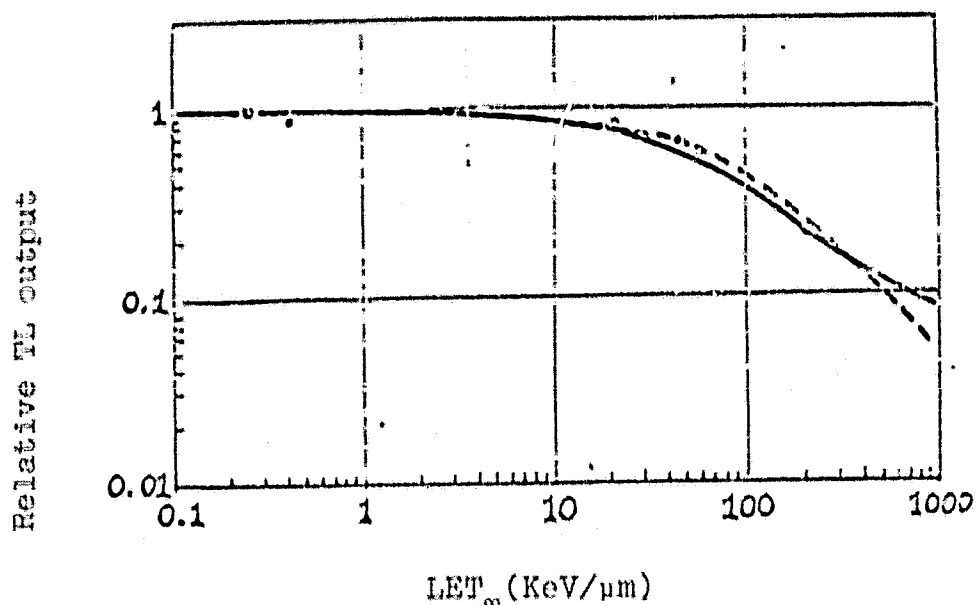


Figure 11. Thermoluminescent reaction as a function of the average retardant capability (LET) for LiF ----- theoretical with one type of capture, \_\_\_\_\_ theoretical with two types of capture, o - α-rays Po-210, • -- protons, □ - γ-rays of Co-60, ■ - electrons [9].

in the form of a function of  $LET_{\infty}$  of protons, can be compared with representatives of the spectrum of protons during orbital flight or an evaluation of the total thermoluminescent effectiveness. The curves of dose and flux obtained by Shaefer and Sullivan [18] and represented in Figure 12 can be used for this purpose. One can see that about 25% of the total dose from this spectrum is due to protons with  $LET > 10$  keV/m when a noticeable loss in sensitivity occurs. With maximum LET for protons, 85 keV/m, the sensitivity drops to almost 0.5. The full dose for this spectrum must be increased by approximately 7%. Assuming that 90% of the dose measured by 700 TLD plates is due to protons, the correction is 6%. The errors in measurement in absorbed dose is due to statistical computation shown in Table 5, the

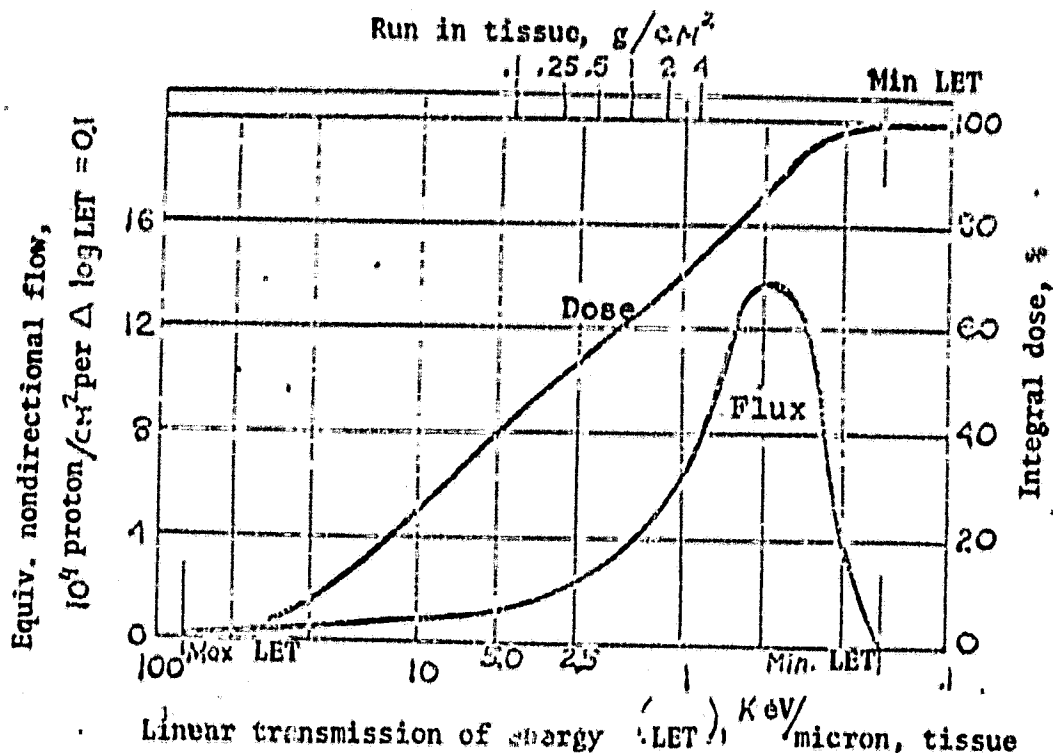


Figure 12. Flux of protons and cumulative doses measured during flight of the Gemini-7 [18].

absolute calibrated plate is about 5% and error in determining effectiveness of measurement in particles of an unknown spectrum is less than 3%. The values of the equivalent irradiation were converted to a tissue dose by multiplying by the coefficient 0.957. In packet #2, the absorbed dose amounted to 424 mrad  $\pm$  9%. Although in packet #1 there was no TLD with  $^7\text{LiF}$ , one can select a number by interpolation among the screened  $^6\text{LiF}$  detectors. The absorbed dose in packet #1, in this way, amounted to 523 mrad  $\pm$  11%. The increase in absorbed dose by 19% in comparison with packet #2 illustrates the effectiveness of screening of the American dosimetric assembly.

### Discussion

The fluence of neutrons in the field of thermal energies was equal to  $3.64 \cdot 10^5$  neutrons/cm<sup>2</sup> (0.228 neutrons/cm<sup>2</sup>s) for 18.5 days of flight of the Kosmos-936. The error of this value is estimated

at  $\pm 20\%$ . This corresponds to a dose of 0.37 mrem. The fluence of neutrons in the field of resonance energies (0.3 eV-1 MeV) was shown to equal  $9.5 \cdot 10^5$  neutrons/cm<sup>2</sup> (0.59 neutrons/cm<sup>2</sup>·s) with error limits from -30% to +50%. This fluence corresponds to approximately 5 mrem. In the field of high energies ( $> 1$  MeV) the best estimate of fluence of neutrons was  $2.1 \cdot 10^6$  neutrons/cm<sup>2</sup> (1.3 neutrons/cm<sup>2</sup>·s). The assumptions made during the calculations can involve an error in this number by a magnitude but the result was obtained by comparison with other measurements with similar conditions [15]. The dose corresponding to the fluence found amounts to about 125 mrem. The full dose due to charged particles plus absorbed dose of gamma radiation was also evaluated. It varied from 424 to 523 mrem for two positions with difference in thickness of protection in all of several g/cm<sup>2</sup>. The errors involved in these numbers are about 10%.

## 6. Nuclear Emulsions.

Monitoring of the proton component on the Kosmos-936 was done using nuclear emulsions of the Ilford G.5 and K.2 types. At first it was intended to measure the LET spectrum of protons in an energy range from 0 to approximately 100 MeV. The method used as was pointed out by Schaefer and Sullivan [19] required using emulsions with varying sensitivity. For this purpose, the above listed types of emulsions were collected in a packet (dimensions of the emulsion 3.8 X 5.1 cm) and placed on all surfaces of the American 25% section and the joint 50% plastic foam cube. The emulsions in plastics are a necessary component in a passive monitoring assembly. At the same time as protons with normal conditions, the etching of the existing plastic detectors are not recorded by them the nuclear emulsions are a well recommended method with high sensitivity and resolution capability for work with single-charge particles. /114

### 6.1. Material and Method.

For recording protons, the G.5 emulsion was selected 25  $\mu$ m and 50  $\mu$ m thick and the K.2 emulsion 100  $\mu$ m thick. The latter are sensitive to protons with an energy of approximately 80 MeV and the former record all charged particles with any energy. Each emulsion is installed on a sublayer made of Melinax with a thickness of 178  $\mu$ m. Usually, before assembly of the emulsions, they are stored in a refrigerator. At the time of assembly they are placed according to type in thickness and are sealed with hot welding in an opaque black polyethylene packet 0.015 cm thick. All this work is done in a dark-room. Each such small packet besides several sheets of plastic is also sealed in a single black bag and placed together comprise a single "orthogonal" detector. The 12 American orthogonal detectors and the 6 Soviet were collected together using [illegible] telephone tape attached to the joint cube and to the 25% American section.

After obtaining the exposed material, the orthogonal detectors were separated from the surface of the cube. They were tested on the appropriate assemblies required after which the small packets with the emulsions were removed and placed again in the refrigerator. In

a dark room, the emulsions were removed and the packets were placed according to number on the orthogonal detector (from 1F-US to 12F-US and from 7F-S to 12F-S); on each emulsion, a disk 3-4 mm in diameter was scratched and in each disk the thickness of each emulsion was measured. Then, each emulsion was separately mounted on a Lucite plate with dimensions 4.5 X 7.6 cm<sup>2</sup> using acral-1 -2 dichloroethane glue (this was done for convenience in rotating the emulsion during processing). Along with the flight emulsions, two reserve packets were also prepared by the same method (1B-US and 2 B-US) for processing. /115

All of the emulsions of the G.5 type with thickness 25 and 50  $\mu$ m were processed in a D-19 developer without preliminary wetting (they were immediately transferred to the heat stage) and the K.2 type emulsion with thickness 100  $\mu$ m were developed in amidol with preliminary wetting in the heating stage. After processing, the emulsions were carefully removed from the Lucite plates and the melinex sub-layer was washed. Then the thickness of each emulsion was measured and two regulation apertures were drilled in each emulsion; then they were packed in light-proof boxes. Then inspection was begun of samples of the K.2 emulsion from the 7 F-US and 11 F-US assemblies in the presence of the ends of the proton tracks. Inasmuch as the K.2 emulsion was less sensitive than the G.5, with the same exposure on them there was considerably lower density of grain apparent and therefore the ends of the proton tracks could easily be detected. However, in view of the long duration of exposure (18.5 days) a very serious problem was the excessive density of tracks so that one had to use an immersion lens with a 100-fold magnification and a 10-fold magnification eyepiece just to scan the ends of the proton tracks. The criteria for selecting the ends of the tracks were the following: the track must intersect one of the surfaces of the emulsion (that is, it must as a whole be within the volume of the emulsion as can occur in a case of protons of emission formed); the track cannot be taken at the beginning of a star (which would exclude these two possibilities that each end of the track is noted on the opposite side in order to be sure that it intersects the surface and does not pass through from a star); in the consideration one must include tracks of all immersion angles. /116

As was pointed out above, the extreme density of tracks required recording with high magnification and moreover, only 25% of the field of vision could be scanned at one time so that one did not lose the ends of the proton tracks. One hardly need say that in the most sensitive G.5 emulsion it was practically impossible to count the grains the tracks even with 1000-fold magnification. This prevented evaluating the LET spectrum of protons with energies higher than approximately 10 MeV (10 MeV approximately corresponds to a value of the LET at which in the G.5 emulsions it is impossible to count the number of grains in a track, that is, the density of grains is so high that the tracks appear to be continuous).

## 6.2. Results.

A count of the ends of the tracks from the K.2 emulsions was done in 7F-US and 11F-US orthogonal packets. In the volume of emulsions

examined, a correction was made for precipitation and a recount was made for the equivalent volume of tissue using the average ratio of retarding capability equal to 2 (in an interval from 0 to 10 MeV the ratio of retarding capabilities of tissue to the proton varies from 1.7 to 2.2). Using the well known values of LET and KQ (coefficient of quality) in the tissue as a function of energy protons, the absorption doses and equivalent doses were found. All of these data are summarized in Table 10.

TABLE 10

/117

Orthogonal Detectors	Total Number of Count- ed Ends of Tracks	Volumetric Density ( $\frac{\text{Particles}}{\text{cm}^3 \text{ tissue}}$ )	Dose (Millirad)	Equivalent Dose (Millirem)
7 F-US	$95 \pm 9.6$	$(2.56 \pm 0.27) \times 10^5$	$44.2 \pm 0.5$	$130.2 \pm 13.7$
II F-US	$59 \pm 6.2$	$(2.87 \pm 0.46) \times 10^5$	$49.6 \pm 0.8$	$145.9 \pm 20.4$

### 6.3. Discussion.

/116

The purpose of this section of the experiment was to evaluate the contribution of protons to radiation during flight of the Kosmos-936. For an evaluation of irradiation by protons in the interval of energy from approximately 10 MeV to approximately 100 MeV we used the G.5 emulsions and a count method for the number of grains depending on the LET. This function can be obtained from the calibrated curve of the relationship of the number of grains to the residual run in a given emulsion for the long end of the tracks and the tabulated data of the relationship of the LET to the residual run of protons in the G.5 emulsion [10]. In the field from 0 to approximately 10 MeV in the tracks of protons in the G.5 emulsion it was very difficult, if not impossible, to count the number of grains. Inasmuch as the K.2 emulsions easily record the ends of the proton tracks and thanks to their lower sensitivity in comparison with G.5 emulsions, they with uniform irradiation form less apparent grains whose differentiation and count of the track ends is much easier. Measurements with the K.2 (0-10 MeV) and with the G.5 (10-100 MeV) components, with addition give the full spectrum of protons from 0 to 100 MeV.

/118

Even preflight it was well known that in the G.5 emulsions the tracks with minimum density of grains ( $g_0 = 19$  grains/100  $\mu\text{m}$  of emulsion) and more probably tracks with 2  $g_0$  and 3  $g_0$  cannot be different due to the excessive density of tracks expected in this long-term flight (3  $g_0$  corresponds, approximately, to 100 MeV protons). However, the irradiation was such that it was practically impossible to count

the grains in the G.5 emulsions with a thickness of 25 or 50  $\mu\text{m}$  and it was very difficult and time consuming to determine the number of track ends in the K.2 emulsions. For this reason, results are obtained only for protons with energies from 0 to 10 MeV.

#### Additional Reports.

Additional reports on the K-206 experiment will be presented later. They will be based on studies being made at the present time. Certain fields of the work being done are described below.

The results of gamma scanning on the Vostok type satellite, on the Kosmos-936, which give a distribution of protection of spacecraft in relation to the container for the K-206 experiment are necessary for analysis of the effect of protection on the fluence of HZE particles. The results of gamma scanning were not obtained. /119

A comparison of the Soviet and American experiments which was the main task of the K-206 will be made later after an exchange of reports.

Studies of the effectiveness, sensitivity and reactions of plastic detectors with accelerated ions of a known energy and charge obtained on the Bevalak in Berkeley are being made. The results of these studies will be used for improving existing calibrated relationships for plastic detectors and treating of results obtained in the K-206 experiment.

In order to considerably improve precision in determining Z and expand the spectrum up to  $Z = 26$  the Lexan part of the assembly will soon be measured. The results obtained from the Lexan will be tied to the results from the layers of cellulose nitrate.

Other improvements in the Z spectrum proposed for the future will be measurement of large values of etched tracks of particles. This assembly was measured with a resolution of 7  $\mu\text{m}$ . It is completely possible to obtain a 5 times larger resolution without a corresponding increase in measurement time. This will be done by scanning with low magnification and measurement with large.

An analysis of data on measurement of neutrons is being done right now. Calibration of thermal neutrons being made at the present time makes it possible to directly calibrate the detectors which were on the Kosmos-936. This will be better than that based on bibliographical data which can be less precise. Also, the coefficient of selfscreening will be measured. Such studies are being done to clarify the question as to whether approximations used when calculating fluences of high energy neutrons can be improved.

# REFERENCES

/120

1. Benton, E.V. and M. M. Collver, "Registration of heavy ions during the flight of Gemini VI, Hlth. Phys., 13, 495-500 (1967).
2. Benton, E.V. and W.D. Nix, "The restricted energy loss criteria for registration of charged particles in plastics", Nucl. Instrum. Meth., 67, 343-347 (1969).
3. Benton, E.V., R. P. Henke and D. D. Peterson, "Plastic nuclear track detector measurement of high-LET radiation on Apollo, Skylab and ASTP space missions", Nucl. Track Detection, 1, 27-32 (1977).
4. Benton, E.V., D.D. Peterson, J.V. Bailey and T. Parnell, "High LET particle exposure of Skylab astronauts", Hlth. Phys., 32, 15-19, (1977).
5. Benton, E.V., D.D. Peterson, A.M. Marennny and V.I. Popov, "HZE particle radiation studies aboard Kosmos-782." (To be published in Hlth. Phys.).
6. Fishman, G.J., "Neutron and proton activation measurements from Skylab," AIAA Paper No. 74-1227, AIAA/AGU Conference on Scientific Experiments of Skylab, Huntsville, Alabama (1974).
7. Fleischer, R.L., P.B. Price and R.L. Walker, "Nuclear tracks in solids", Berkeley, University of California Press (1975).
8. Hewitt, J.E., H.J. Schaefer and J.J. Sullivan, "Radiation exposure during the Biosatellite III primate flight," Hlth. Phys., 23, 460-468 (1972).
9. Jahnert, B., "The response of TLD-700 thermoluminescent dosimeters to protons and alpha-particles," Hlth. Phys., 23, 112-114 (1972).
10. Janni, J.F., "Calculation of energy loss, range, path length, straggling, multiple scattering, and the probability of inelastic nuclear collisions for 0.1- to 1000 MeV protons." AFWL-TR-650150, (1966).
11. Khodai-Joopari, A., "Fission properties of some elements below radium," UCRL-16489.
12. McCormick, G.H., and B.L. Cohen, "Fission and total reaction cross sections for 22 MeV protons on Th-232, U-235 and U-238." Phys. Rev., 96, 722-724 (1954).
13. Merker, M., "The contribution of galactic cosmic rays to the atmospheric neutron maximum dose equivalent as a function of neutron energy and altitude." Hlth. Phys., 25, 524-527 (1973).

/121

14. Pappas, R., E. Techilin and N. Goldstein "A standardized method for making neutron fluence measurements by fission tracks in plastics," JNNRDL-TR-1089.
15. Grist, T. C., M. Furst, D.R. Burnett, J. H. Bau, and C. L. Peacock, Jr., "Spacecraft-produced neutron fluxes on Skylab -- preliminary report." Division of Geological and Planetary Science, California Institute of Technology, Pasadena, California 91125.
16. Roberts, J.H., R.A. Parker, F. J. Congel, J. Kastner and B.G. Oltman, "Environmental neutron measurements with solid state track recorders," Rad. Effects 3, 283-285 (1970).
17. Rogers, D.W.O., M. L. Walsh, B.H. Orr and N. Teekman, "Albedo dosimetric response to monoenergetic neutrons." High. Phys. 33, 251-254 (1977).
18. Schaefer, H.J. and J.J. Sullivan, "Radiation monitoring with nuclear emulsions on project Gemini II. Results on the 14-day mission Gemini VII," NAMI-990, January (1967).
19. Schaefer, H.J. and J.J. Sullivan, "Nuclear emulsion measurements of the astronauts' radiation exposure on the Apollo-Soyuz mission," NAMRL-1228 (1976).
20. Stehn, J.R., M.D. Goldberg, B.A. Magurno and R. Wiener-Chasman, "Neutron cross sections," Vol. III. BNL 325 (1965).
21. Steiner, R.M. and J.A. Jungerman, "Proton induced fission cross sections for U-235, U-238, Th-232, Bi-209 and Au-197 at 100 to 340 MeV," Phys. Rev. 101, 807-813 (1955).
22. Wollenberg, H.A. and A.R. Smith, "Energy and flux determinations of high-energy nucleons [illegible]."

As a result of studies made on K-206 experiment the following can be pointed out:

1. The values of doses measured by the Soviet and American thermoluminescent dosimeters coincide in limits of error for the experiment. Close values of doses were obtained and calculation on the LET spectrum measured by the Soviet nuclear emulsions.

2. The values of absorbed doses of protons with energy less than 10 MeV measured by the Soviet and American specialists using emulsions practically coincide. The equivalent doses vary by 1.65 times which is due to the higher value of the quality factor obtained for the spectrum of protons in the Soviet emulsions ( $QF = 4.9$  in the Soviet NFE and 2.95 in the American NFE). The causes for this disparity must be clarified in subsequent experiments.

3. In the K-206 experiment, close values of fluences were obtained for heavy charged particles measured by the Soviet and American plastic detectors. The cause of divergence in fluences of heavy nuclei was successfully understood in the experiment on the Kosmos-782 AES. The basis for this difference was the different thresholds of recording of the Soviet and American detectors, and the difference in positioning. Moreover, as a result of calibrations, the threshold of recording KNTs was made more precise for large charges. Earlier, in calibration for low energy ions at Dubna, the threshold of recording particles with  $LET_{100}$  amounted to  $196 \frac{\text{KeV}}{\mu\text{m}}$ . According to the results of calibration at Berkeley with high energies, this threshold amounted to  $230 \frac{\text{KeV}}{\mu\text{m}}$  of the charge spectrum.

4. In the K-206 experiment, close values of fluences of neutrons were obtained with energies greater than 1 MeV. Measurements were made by specialists in the USSR and USA using fissionable foils. Later on interest was expressed in obtaining data on spectra of neutrons.

5. Estimated measurements made in the K-206 experiment using the TLS for doses outside the satellite indicated that the size of the dose for flight reaches 20 rads whereas radiation is fairly soft and the dose drops sharply with thickness. There is further interest in a more careful study of the composition of radiation outside the satellite and also the principle of attenuation of this radiation in the protective shield.

/123

6. A calibrated curve of the relationship of LET to the potential of development of the emulsion was obtained for the first time in a broad range of LET values.

7. The first experiments were made in studying fragmentation of iron nuclei in an emulsion. For this purpose at Berkeley the emulsion chambers were irradiated with ions of iron. At the present time, the results are being processed.

5. In the K-206 experiment it was discovered that the shape of the LET spectra obtained using a C-1 spectrometer and nuclear emulsions differ from each other. To discover the cause for this disparity, apparently, it is necessary to conduct ground experiments on beams of charged particles using the C-1 and the NFF as detectors.

In this way the K-206 experiment has made it possible to obtain new information on characteristics of cosmic radiation in the biosatellite orbit, to correctly understand the results of the preceding experiment on the Kosmos-782 AES. Moreover, this experiment from beginning to end was planned and conducted as a joint Soviet-American experiment. The K-206 experiment also posed new questions which must be solved in succeeding Soviet-American experiments on the radiation protection of the K-309 on the 1979 biosatellite. In the design of the K-309 experiment, conclusions of the study on the Kosmos-782 and 936 AES are considered and particular attention will be devoted to the following:

- study of the characteristics of cosmic radiation outside a satellite and also the principle of attenuation of this radiation in the protective shield;

- study of the neutron component (spectra, fluxes);

/124

- study of the characteristics of radiation in high LET-nucleus outputs;

- expansion of the LET range of recorded particles. For this purpose it was proposed that one use new types of plastic detectors of the CR type which make it possible to record low energy protons;

- conduct of ground calibrations of detectors on the USSR and USA accelerators;

- a further study of fragmentation of heavy nuclei as the protective substance.